2009-08-12

Development of Biocompatible Polymer Monoliths for the Analysis of Proteins and Peptides

Yun Li
Brigham Young University - Provo

DEVELOPMENT OF BIOCOMPATIBLE POLYMER MONOLITHS FOR THE ANALYSIS OF PROTEINS AND PEPTIDES

by

Yun Li

A dissertation submitted to the faculty of

Brigham Young University

in partial fulfillment of the requirements for the degree of

Doctor of Philosophy

Department of Chemistry and Biochemistry

Brigham Young University

December 2009

BRIGHAM YOUNG UNIVERSITY

GRADUATE COMMITTEE APPROVAL

of a dissertation submitted by

Yun Li

This dissertation has been read by each member of the following graduate committee and by majority vote has been found to be satisfactory.

Date	Milton L. Lee, Chair
Date	H. Dennis Tolley
Date	Steven R. Goates
Date	Adam T. Woolley
Date	Steven R. Herron

BRIGHAM YOUNG UNIVERSITY

As chair of the candidate's graduate committee, I have read the dissertation of Yun Li in its final form and have found that (1) its format, citation, and bibliographical style are consistent and acceptable and fulfill university and department style requirements; (2) its illustrated materials including figures, tables, and charts are in place; and (3) the final manuscript is satisfactory to the graduate committee and is ready for submission to the university library.

_____ _____

Date

Milton L. Lee
Chair, Graduate Committee

Accepted for the Department

_____

Paul B. Farnsworth
Department Chair

Accepted for the College

_____

Thomas W. Sederberg
Associate Dean, College of Physical and Mathematical Sciences

ABSTRACT

DEVELOPMENT OF BIOCOMPATIBLE POLYMER MONOLITHS FOR THE ANALYSIS OF PROTEINS AND PEPTIDES

Yun Li

Department of Chemistry and Biochemistry

Doctor of Philosophy

Biocompatibility is an important issue for the development of chromatographic stationary phases for the analysis of biomolecules (including proteins and peptides). A biocompatible stationary phase material is a material that resists nonspecific adsorption of biomolecules and does not interact with them in a way that would alter or destroy their structures or biochemical functions.

The monolithic column format is a good alternative to typical spherical particle packed columns for capillary liquid chromatography of biomacromolecules. Several novel anion-exchange polymer monoliths for the analysis of proteins were synthesized for improved biocompatibility. Two novel polymeric monoliths were prepared in a single step by a simple photoinitiated copolymerization of 2-(diethylamino)ethyl methacrylate and polyethylene glycol diacrylate (PEGDA), or copolymerization of 2-(acryloyloxy)ethyl trimethylammonium chloride (AETAC) and PEGDA, in the presence of selected porogens. The resulting monoliths contained functionalities of diethylaminoethyl (DEAE) as a weak

anion exchanger and quaternary amine as a strong anion exchanger, respectively. An alternative weak anion exchange monolith with DEAE functionalities was also synthesized by chemical modification after photoinitiated copolymerization of glycidyl methacrylate (GMA) and PEGDA. The dynamic binding capacities of the three monoliths were comparable or superior to values that have been reported for various other monoliths. Chromatographic performances were also similar to those provided by a modified poly(GMA-co-ethylene glycol dimethacrylate) monolith. Separations of standard proteins were achieved under gradient elution conditions using these monolithic columns. This work represents a successful attempt to prepare functionalized monoliths via direct copolymerization of monomers with desired functionalities. Compared to earlier publications, laborious surface modifications were avoided and the PEGDA crosslinker improved the biocompatibility of the monolithic backbone.

Protein separations by capillary size exclusion chromatography (SEC) require a monolith that is biocompatible, has sufficient pore volume, has the appropriate pore size distribution, and is rigid. Most polymer monoliths have not possessed a biomodal pore-size distribution, i.e., especially with one distribution in the macropore region and the other in the mesopore region. Furthermore, non-specific adsorption of proteins in these stationary phases has persisted as a major unresolved problem. To overcome these difficulties, a porous poly[polyethylene glycol methyl ether acrylate (PEGMEA)-co-PEGDA] monolith which can resist adsorption of both acidic and basic proteins when using an aqueous buffer without any organic solvent additives was developed. Based on this biocompatible monolith, surfactants were introduced as porogens with the hope of significantly increasing the mesopore volume within the polymer. Two types of surfactants were studied, including

poly(ethylene oxide)-poly(propylene oxide)-poly(ethylene oxide) (PEO-PPO-PEO) or PPO-PEO-PPO and Brij. Pore size distributions were examined using a well-defined molecular weight range series of proteins and peptides by inverse size exclusion chromatography, which indicated relatively large volume percentages of mesopores and micropores. The two new monoliths demonstrated different SEC behaviors, low nonspecific adsorption of proteins, and high mechanical rigidity.

High density lipoprotein (HDL) is a heterogeneous class of lipoprotein particles with subspecies that differ in apolipoprotein and lipid composition, size, density, and charge. In this work, I developed a new capillary SEC method for size separation of native HDL particles from plasma using a capillary packed with BioSep-SEC-4000 particles, Three major sizes of HDL particles were separated. Additionally, capillary SEC and capillary strong anion-exchange chromatography of non-delipidated HDL were accomplished using poly(PEGMEA-co-PEGDA) and poly(AETAC-co-PEGDA) monoliths. These new LC methods using packed and monolithic stationary phases provided rapid separation of HDLs and excellent reproducibility.

ACKNOWLEDGMENTS

I am very grateful for the support throughout this project from my advisor, Dr. Milton L. Lee. He has been a great resource for suggestions and encouragement on the project as well as for advice and help for my career path. I am honored that I could have an opportunity to study in his group. What I have learned from him is invaluable to me and my future career development.

I would also like to thank professors in the chemistry department for teaching me fundamentals and experimental skills in analytical chemistry. My graduate committee members, Dr. H. Dennis Tolley, Dr. Steven R. Goates, Dr. Adam T. Woolley, and Dr. Steven R. Herron have provided critical evaluation and useful suggestions in my progress reports during my five-year PhD program. Current and past members of the Lee group are gratefully acknowledged for their helpful discussions and friendship. In particular, I would like to thank Dr. Binghe Gu and Dr. Yansheng Liu for their collaboration and helpful suggestions. I have learned a lot from them about polymer monoliths and practical liquid chromatography techniques. I also thank Dr. Shu-ling Lin and Dr. Xuefei Sun for helpful ideas, deep discussions and friendship. I am indebted to my lab mates, Yuanyuan Li, Miao Wang, Yan Fang, Dan Li, Aaron Nackos, Tai Truong, Jacolin Murray, Xin Chen, Jie Xuan, Kun Liu, Jesse Contreras and other friends in both Dr. Lee's research group and in the department. Their friendship and kind help made me feel part of a large family.

I express my gratitude to people in the department instrument shop, especially Robert Hallock. I give Susan Tachka and Sarah Holstine special thanks for their service

and support. I also appreciate the opportunity and financial support offered by the Department of Chemistry and Biochemistry at Brigham Young University. The financial support from Berkeley HeartLab and National Institutes of Health is also gratefully acknowledged.

Finally, I would like to thank my parents, Kemao Li and Yulan Wu, and my sister, Shujuan Li, for their continuous love and support throughout my years at BYU. Their love and understanding were great impetuses to my Ph.D. study. I owe many thanks to all my tutors and friends with names not mentioned here who paved the way for me during my life.

TABLE OF CONTENTS

LIST OF ABBREVIATIONS xiv

LIST OF TABLES xvii

LIST OF FIGURES xviii

CHAPTER 1 BACKGROUND AND SIGNIFICANCE 1

1.1 Introduction 1

1.2 Biocompatibilty in Chromatography 2

1.2.1 Definitions 2

1.2.2 Protein Adsorption 3

1.2.3 Non-specific Adsorption of Proteins 5

1.2.4 Nondesirable Adsorption in Chromatography 6

1.3 Known Materials That Resist Protein Adsorption 8

1.4 Biocompatible Polymer Monoliths for Bioseparations 9

1.4.1 Polyacrylamide-based Monoliths 10

1.4.2 Polymethacrylate or polyacrylate-based Monoliths 13

1.5 Monoliths for Analysis of Proteomic Samples 18

1.6 Conclusions 20

1.7 Dissertation Overview 21

1.8 References 21

CHAPTER 2 PREPARATION OF POLYMERIC MONOLITHS BY COPOLYMERIZATION OF ACRYLATE MONOMERS WITH AMINE FUNCTIONALITES FOR ANION-EXCHANGE CAPILLARY LIQUID CHROMATOGRAPHY OF PROTEINS 30

2.1 Introduction 30
2.2 Experimental Section 35
2.2.1 Chemicals 35
2.2.2 Polymer Monolith Preparation 36
2.2.3 Capillary Liquid Chromatography 37
2.2.4 Dynamic Binding Capacity and Mass Recovery Measurements 38
2.2.5 Safety Considerations 38
2.3 Results and Discussion 39
2.3.1 Polymer Monolith Preparation 39
2.3.2 Biocompatibility 44
2.3.3 Chromatographic Performance 44
2.3.4 Dynamic Binding Capacity 46
2.3.5 Column Characterization 48
2.3.6 Application 52
2.4 Conclusions 54
2.5 References 56
CHAPTER 3 PREPARATION OF POLYMER MONOLITHS THAT EXHIBIT SIZE EXCLUSION PROPERTIES FOR PROTEINS AND PEPTIDES 59
3.1 Introduction 59
3.2 Experimental Section 65
3.2.1 Chemicals and Reagents 65
3.2.2 Polymer Monolith Preparation 65
3.2.3 Size Exclusion Chromatography 66

3.2.4 Inverse Size-Exclusion Chromatography 68
3.2.5 Safety Considerations 68
3.3 Results and Discussion 68
3.3.1 Effect of Surfactant as Porogen 69
3.3.2 Effect of Monomer Composition and Proportion 73
3.3.3 Morphology of PEG Monoliths 73
3.3.4 Effect of Column Diameter, Column Length and Flow Rate 75
3.3.5 Chromatographic Evaluation 78
3.3.6 Inverse Size Exclusion Chromatography Characterization 81
3.4 Conclusions 84
3.5 References 84
CHAPTER 4 PREPARATION OF POLYMER MONOLITHS WITH TARGET MESOPORE SIZE DISTRIBUTIONS FOR SIZE EXCLUSION CHROMATOGRAPHY OF PROTEINS… 88
4.1 Introduction 88
4.2 Experimental Section 91
4.2.1 Chemicals and Reagents 91
4.2.2 Preparation of Polymer Monoliths 92
4.2.3 Size Exclusion Chromatography 92
4.2.4 Scanning Electron Microscopy 95
4.2.5 Safety Considerations 95
4.3 Results and Discussion 95
4.3.1 Flow Properties of Monolithic Columns 95

4.3.2 Pore Properties of Monolithic Columns 97
4.3.3 ISEC Curves of Monolithic Columns 98
4.3.4 SEC Separation of Proteins 102
4.3.5 Effect of flow rate and column length 103
4.4 Conclusions 103
4.5 References 107
CHAPTER 5 CAPILLARY LIQUID CHROMATOGRAPHY OF HIGH DENSITY LIPOPROTEINS 110
5.1 Introduction 110
5.2 Experimental Section 115
5.2.1 Chemicals and Reagents 115
5.2.2 Column Preparation 116
5.2.3 LC of High Density Liporotein 117
5.3 Results and Discussion 119
5.3.1 SEC Separation Using Packed BioSep-SEC-4000 Columns 119
5.3.2 SEC Separation Using the Monolithic Column 123
5.3.3 Anion-exchange Chromatography of HDL 129
5.4 Conclusions and Perspective 131
5.5 References 131
CHAPTER 6 FUTURE DIRECTIONS 135
6.1 Investigation of New Meso-porogens for Developing Monoliths for Size Exclusion Chromatography (SEC) of Proteins 135
6.2 Further Improvement in Anion-exchange Monolithic Columns 141

6.3 Prepareation of Other Types of Polymer Monoliths Using PEGDA as Crosslinker 142
6.4 Two-dimensional LC of High Density Lipoproteins 144
6.5 References 146

LIST OF ABBREVIATIONS

2D GE	two-dimensional gel electrophoresis
2D LC	two-dimensional liquid chromatography
AAm	acrylamide
AEC	anion exchange chromatography
AETAC	2-(acryloyloxy)ethyl trimethylammonium chloride
AIBN	azobisisobutyronitrile
AMPS	2-acrylamido-2-methyl-1-propanesulfonic acid
APS	ammonium persulphate
BSA	bovine serum albumin
BuMA	butyl methacrylate
CE	capillary electrophoresis
CLC	capillary liquid chromatography
DBC	dynamic binding capacity
DEA	diethylamine
DEAE	diethylaminoethyl
DEAEA	2-(diethylamino)ethyl acrylate
DEAEMA	2-(diethylamino)ethyl methacrylate
DMPA	2-dimethoxy-2-phenyl acetophenone
EDMA	ethylene dimethacrylate
FITC	fluorescein isothiocyanate

GGE	gradient gel electrophoresis
GMA	glycidyl methacrylate
HDL	high density lipoprotein
HEA	2-hydroxyethyl acrylate
HEMA	2-hydroxyethyl methacrylate
HIC	hydrophobic interaction chromatography
HILIC	hydrophilic interaction chromatography
IEC	ion exchange chromatography
ISEC	inverse size exclusion chromatography
LC	liquid chromatography
MBAA	N, N'-methylenebisacrylamide
M-IPG	monolithic immobilized pH gradient
MW	molecular weight
pDMAEMA	poly[2-(dimethylamino)ethyl methacrylate]
PEG	poly(ethylene glycol)
PEGDA	polyethylene glycol diacrylate
PEGMEA	polyethylene glycol methyl ether acrylate
PEI	polyethyleneimine
PEO-PPO-PEO	poly(ethylene oxide)-poly(propylene oxide)-poly(ethylene oxide)
pI	isoelectric point
pMETAC	poly[(2-(methacryloyloxy) ethyl trimethylammonium chloride]
PSDVB	polystyrene divinylbenzene
PVA	poly(vinyl alcohol)

QA	quaternary amine
ROMP	ring-opening metathesis polymerization
RPC	reversed-phase chromatography
RSD	relative standard deviation
SAX	strong anion exchange
SCX	strong cation exchange
SD	standard deviation
SDS	sodium dodecyl sulfate
SEM	scanning electron microscopy
SFR	stable free radical
SPME	solid-phase microextraction
TEMED	tetramethylethylenediamine
THF	tetrahydrofuran
TMSPMA	3-(trimethoxysilyl) propyl methacrylate
WAX	weak anion-exchange

LIST OF TABLES

Table 2.1. Reagent composition of several monoliths used in this study. 40

Table 2.2. Physical properties of several monoliths used in this study..... 41

Table 2.3. Comparison of DBCs of various anion-exchangers..... 47

Table 2.4. Reproducibilities of the new monolithic columns. 51

Table 3.1. Proteins and peptides used in this study..... 67

Table 3.2. Physical characteristics of SEC monoliths..... 70

Table 3.3 Influence of flow rate on resolutions. 77

Table 3.4 Pore volume distribution for M-5. 83

Table 4.1. Proteins and peptides used in this study..... 93

Table 4.2. Efficiency, resolution and flow permeability values of the poly(PEGMEA-co-PEGDA) monoliths..... 99

Table 5.1. Five proteins used in this study. 118

Table 6.1. Physical micelle parameters of some surfactants used for templating polyacrylamide and poly(2-hydroxyethyl methacrylate)..... 138

LIST OF FIGURES

Figure 1.1. Monomers and crosslinkers used in preparing biocompatible monoliths.. 11

Figure 2.1. Reaction scheme and monomers involved in synthesizing the anion-exchange monoliths. 34

Figure 2.2. SEM photographs of (A) DEA modified poly(GMA-co-EDMA); (B) DEA modified poly(GMA-co-PEGDA); (C) poly(DEAEMA-co-PEGDA); (D) poly(AETAC- co-PEGDA). 43

Figure 2.3. Anion-exchange chromatography of standard proteins. 45

Figure 2.4. Breakthrough curves obtained by fontal analysis. 49

Figure 2.5. Backpressure dependency on linear velocity for the AETAC and DEAEMA functionalized monoliths. 53

Figure 2.6. Strong anion-exchange (SAX) chromatography of total protein lysate of *E. coli* DH5α. 55

Figure 3.1. Structural formulas of reagents for synthesizing the monoliths. 64

Figure 3.2. SEC separations on PEG monoliths synthesized with (A) different ratios of copolymer to EE (M-1, M-2 and M-3), and (B) different MWs of copolymer (M-2, M-4, M-5 and M-6). 72

Figure 3.3. SEM images of M-0, M-1, M-2 and M-6 using a magnification of 10 000. 74

Figure 3.4. SEC separations on M-2 with different column i.d.s (A) and lengths (150 μm i.d.) (B).. 76

Figure 3.5. Comparison of resolution obtained for protein mix using (left) a packed column and (right) a monolithic column.. 79
Figure 3.6. Plot of pressure drop against flow rate of mobile phase.. 80
Figure 3.7. SEC calibration curve for M5 monolithic column.. 82
Figure 4.1. SEM images of M0 and M2 monoliths. 100
Figure 4.2. SEC calibration curves for proteins and peptides using an M2 column (23 cm × 150 μm i.d.). A reference sample (M0) polymerized without Brij at a 1-dodecanol/ hexanes ratio of 0.5:0.6 is also included. 101
Figure 4.3. SEC separation of a protein mixture using a poly(PEGMEA-co-PEGDA) monolith.. 104
Figure 4.4. Influence of mobile phase flow rate on SEC resolution.. 105
Figure 4.5. Influence of column length on SEC resolution.. 106
Figure 5.1. Separations of high MW protein standards using BioSep-SEC-4000 particle- packed SEC columns.. 121
Figure 5.2. Separation of HDL using a BioSep-SEC-4000 particle-packed capillary SEC column.. 122
Figure 5.3. Low adsorption of proteins on a PEG monolith. 124
Figure 5.4. Chromatograms of individual proteins.. 126
Figure 5.5. Chromatogram of an HDL standard.. 127
Figure 5.6. Separation of HDL standard using gradient gel electrophoresis. 128
Figure 5.7. Strong anion-exchange chromatography of HDLs.. 130
Figure 6.1. Chemical structures of the proposed surfactants for synthesizing new monoliths..... 140

Figure 6.2. Monomers involved in synthesizing weak anion-exchange monoliths. 143

Figure 6.3. Chemical structures of proposed monomers. 145

CHAPTER 1 BACKGROUND AND SIGNIFICANCE

1.1 Introduction

The term "biocompatible" is typically used in reference to medical devices. It indicates that the material of which the device is constructed does not produce a toxic, injurious, or immunological response in living tissue.[1,2] Many materials have been identified that are compatible with tissue to varying degrees, e.g., titanium (implants), polymethylmethacrylate (contact lenses), ceramics (dental prosthesis), polyurethanes (artificial heart), and pyrolytic carbon (heart valve implants).[3] A good review concerning biocompatibility was recently published.[4]

During the last 20 years, polymer-based monolithic supports have been introduced into separation science,[5,6] as well as into the field of organic catalysis and biocatalysis.[7-11] Major contributions have been made by Svec, Fréchet, and co-workers, who initially developed radical polymerization systems for these purposes.[12] Polymer monolithic media represent uniformly structured matrices with large interpenetrating pores (usually in the low micrometer range), which provide unique advantages such as fast kinetics, high reactivity, and high throughput. Other advantages of monoliths are that they can be created in virtually any form by a simple molding process, and they demonstrate reasonable mechanical strength. All of these advantages qualify the monolith format as excellent for biochemical and medical applications if it possesses the added quality of good biocompatibility. For example, biocompatible, highly porous monolithic scaffolds for use in both cell cultivation and tissue engineering have been prepared from hydrophilic monomers by electron-beam-initiated free-radical polymerization and ring-opening

metathesis polymerization.[13]A novel implantable, wireless, monolithic passive pressure sensor for ophthalmic application was microfabricated using parylene as a biocompatible structural material.[14] A polyamide rate-modulated monolithic drug delivery system with biocompatible and biodegradable properties was recently patented.[15] A monolithic pH-sensitive hydrogel valve for biochemical and medical applications was designed, constructed and tested in a microfluidic device.[16]

The definition of "biocompatible" when used to describe a chromatographic property differs somewhat from its use to describe medical devices. To date, a specific definition of a biocompatible stationary phase for chromatographic applications has not been proposed. In this chapter, I begin with a general description of biocompatibility as it relates to a chromatographic stationary phase. Then, the characteristics and molecular structures of protein-resistant surfaces are explored. Finally, I review the polymeric monoliths which demonstrate negligible non-specific adsorption of proteins in chromatographic separations. Selected applications in liquid chromatography (LC) and microfluidics for protein and peptide separations are described.

1.2 Biocompatibilty in Chromatography

1.2.1 Definitions

The word "biocompatibility" seems to have been mentioned for the first time by Hegyeli and Homsy in the early 1970s.[17,18] Since then, biocompatibility has been redefined several times for biomaterials, and its definition is very contextual.[4,19,20] The most recent definition was given by Williams in 2008: "Biocompatibility refers to the ability of a biomaterial to perform its desired function with respect to a medical therapy, without eliciting any undesirable local or systemic effects in the recipient or beneficiary of that

therapy, but generating the most appropriate beneficial cellular or tissue response in that specific situation, and optimizing the clinically relevant performance of that therapy."[4] And most importantly: "····the sole requirement for biocompatibility in a medical device intended for sustained long-term contact with the tissues of the human body is that the material shall do no harm to those tissues, achieved through chemical and biological inertness."

The concept of biocompatibility can be transferred to chromatographic stationary phases such as monoliths. I define a biocompatible stationary phase material as a material that resists nonspecific adsorption of biomolecules (including proteins and peptides) and does not interact with them in a way that would alter or destroy their structures or biochemical functions. For example, various chromatographic interactions or size exclusion effects should allow high recoveries of proteins and enzymes, and good retention of their enzymatic activities after the chromatographic procedures.[21-23] The biocompatibility of a stationary phase can be achieved through control of surface chemistry and protein adsorption. The closely related term "inertness" reflects the resistance of the stationary phase to protein adsorption and denaturation.[24]

1.2.2 Protein Adsorption

The 20 naturally occurring amino acids found in proteins/peptides vary dramatically in properties of their side-chains (such as polarity and charge).[25] Protein molecules can be characterized by their size (molecular weight) and shape, amino acid composition and sequence, isoelectric point (pI), hydrophobicity, and biological affinity. Differences in these properties can be used as the basis for separation methods applied in purification strategies.[26] However, proteins tend to adsorb nonspecifically to most solid

surfaces due to various hydrophobic domains, charged sites and hydrogen bond donor/acceptor groups. Protein adsorption occurs at different types of interfaces, and protein-surface interactions are important in bioseparations and other biomedical applications.

The adsorption of a protein on a surface is a complex process. Both the kinetics of the adsorption and the structure of the layer of adsorbed protein is important in this process.[27,28] The adsorption process generally involves the following steps: transport towards the interface by diffusion or diffusion/convection, binding to the surface, detachment from the interface, and transport away from the interface.[29-31] When adsorbed at interfaces, proteins may undergo conformational changes or structural rearrangements. A significant conformational change would result in protein denaturation, i.e., the complete loss of activity.

The major types of interactions that are relevant in protein adsorption are: (1) hydrophobic interaction between protein and hydrophobic sites on the surface,[32] (2) electrostatic interaction between charged protein molecules and oppositely charged sites on the surface,[33] (3) hydrogen bonding between protein and hydrogen donor/acceptor,[34] and (4) affinity binding between protein and specific functional groups on the surface.[35] Hydrophobic interaction plays a major role in protein adsorption, and increasing the surface hydrophilicity to some extent is expected to lessen the adsorption. Most polymer surfaces have some hydrophobic characteristics. An adsorbed layer of protein typically contains more ions and water than protein, and the presence of a chaotropic agent not only destabilizes the structure of the protein but also influences its adsorption properties.[36] For example, detergents or chaotropic salts can weaken hydrophobic interactions.[37]

Additionally, most surfaces acquire some charge when exposed to ionic solution. In such cases, electrostatic interaction becomes more important, even dominating protein adsorption kinetics. Even if the overall charge of a protein is zero, i.e., at its isoelectric point, electrostatic interaction between the protein and a surface may still exist, because the charge distribution on the protein surface is not uniform. In most cases, affinity binding contributes to the specific interaction between a protein and immobilized ligand, whereas hydrophobic, electrostatic and hydrogen bonding interactions are nonspecific.

In the above-mentioned protein-surface interactions, the governing factors are determined both by the physical and chemical states of the adsorbing material, protein surface, and solution environment,[38] including the hydrophobicites, electrostatic charges and potentials of the material and protein surface (which can be controlled by varying the pH and ionic strength in the system), and the chemical composition of the material. Other factors that may also influence protein adsorption by surfaces include intermolecular forces between adsorbed molecules, solvent-solvent interactions, strength of functional group bonds, and chemistry, topology and morphology of the solid surface. Additionally, the adsorption of proteins at the liquid-solid interface often exhibits features that are irreversible on experimental time scales. Results are negligible desorption, slow surface diffusion, or surface-induced conformational or orientational changes.[39]

1.2.3 Non-specific Adsorption of Proteins

As the name suggests, specific adsorption indicates adsorption of a target protein to an immobilized ligand or otherwise specially prepared surface due exclusively to biospecific interactions.[40] Non-specific adsorption may be regarded as “foreign,” leading to undesirable properties or reactions.[41,42] Consider a surface that contains specific

functional groups but is inherently "sticky" and permits nonspecific adsorption. Such a surface may lead to excessive protein-surface interaction, resulting in the loss of activity. In addition, a substantial percentage of protein molecules can adsorb on the surface with their active sites inaccessible to target molecules. Finally, a target molecule can also adsorb nonspecifically on the "sticky" surface, thus contributing to the background signal. Therefore, for technologies that involve contact of surfaces with biomolecules, it is fundamentally desirable to maintain inert surfaces and reduce non-specific adsorption of proteins. Examples include: (1) sensitive solid-phase immunoassays that retain selectivity even in the presence of high concentrations of serum proteins,[43] (2) biochemical separations using media that are resistant to biofouling,[44] (3) quantitative optical biosensors for protein characterization,[45] (4) surgically implanted prostheses that are biocompatible,[46] and (5) solid-phase supports for the growth of adherent cells.[47] The mechanisms underlying nonspecific protein adsorption are still not completely understood. Electrostatic interaction and hydrophobic interaction are two main mechanisms involved in non-specific protein adsorption.[48] Of course, a combination of these two effects may occur. Many studies and reviews have focused on properties of surfaces that lead to hydrophobic adsorption of proteins.[49,50]

1.2.4 Nondesirable Adsorption in Chromatography

Size-exclusion (SEC), ion-exchange (IEC), reversed-phase (RPC) and hydrophobic interaction (HIC) chromatography are the most widely employed chromatographic techniques for separation of proteins and peptides.[51] Ideal SEC occurs only when there is no interaction between the analytes and the column matrix. Unfortunately, SEC columns may exhibit some interaction with solutes, resulting in deviation from ideal size-exclusion

behavior, i.e., non-ideal SEC.[52,53] Although these non-ideal, mixed-mode effects may provide increased selectivity, they must be suppressed if predicable solute elution behavior is required. Thus, electrostatic effects (or hydrophobic effects) between analytes and the column matrix can be minimized by adding salt to the mobile phase or changing its pH.

IEC is a very useful chromatographic mode for protein/peptide separations. Although IEC is based on electrostatic interaction between analyte and matrix, the matrix may often exhibit significant hydrophobic characteristics, leading to mixed mode contributions to solute separations.[54] Mixed-mode effects can enhance peptide or protein separation because proteins are polyions with both hydrophobic and hydrophilic surfaces.[55] However, the removal of non-specific hydrophobic interactions may be necessary in order to elute solutes in the specifically desired separation mode. A low polarity organic solvent such as acetonitrile can be added to the mobile phase buffer to suppress hydrophobic interactions between the solute and the ion-exchange matrix.[56] The excellent resolving power of RPC has resulted in it becoming the predominant LC technique for peptide and protein separations (particularly the former) in recent years. Protein denaturation is a common problem in RPC due to the strong hydrophobic interactions. Similarly, HIC of proteins is based on the strength of hydrophobic interactions between proteins and a non-polar stationary phase. However, compared to RPC, the mobile phase conditions utilized are milder, and the relative hydrophobicity and density of the bonded ligands are lower. Additionally, in HIC, the stationary phases and operating conditions are designed to preserve proteins in their native conformations. Thus, proteins in their native states are eluted in order of surface hydrophobicity.[57]

It is important to minimize non-specific interactions in chromatographic separations to (1) obtain predicable solute elution behavior, (2) obtain good recovery of sample mass and bioactivity, and (3) avoid slow adsorption-desorption kinetics that lead to important band broadening. As is well known, denaturation of sample proteins during separation and irreversible attachment to the matrix results in poor recovery.[58] The preservation of native conformation (and bioactivity) is often a primary consideration in method development and may restrict the separation conditions within certain limits.

1.3 Known Materials That Resist Protein Adsorption

Soft gel media, typically crosslinked dextran, cellulose, polyacrylamide, agarose and polysaccharides, have demonstrated low non-specific interactions with peptides and proteins, and have been widely applied in gel electrophoresis and gel permeation chromatography.[59-62] Composite materials, such as highly crosslinked polyacrylamide-polysaccharide, polyacrylamide-dextran, and dextran-agarose composites have been developed to provide more rigid backbones.[63] Other neutral hydrophilic polymers were also investigated and found useful in preventing protein adsorption, such as polyvinyl alcohol,[64] polyethylene oxide,[65] polyvinylpyrrolidinone[66], and a copolymer of polyethylene glycol and polypropylene glycol.[67] All of these polymers are neutral (i.e., no ionic interactions possible) and hydrophilic, and their surfaces share the following structural features: (1) hydrophilic, (2) overall electrically neutral, and (3) hydrogen bond acceptors, but (4) not hydrogen bond donors. Other materials used in gel electrophoresis reported in 1992 by Zewert and Harrington are polyhydroxy methacrylate, polyhydroxy acrylate, polyethylene glycol methacrylate and polyethylene glycol acrylate. Successful electrophoresis of proteins demonstrated the protein compatibility of such polymers.[68]

However, these inert polymers and gels are too soft to be used for LC. Biocompatible hydrogels can be prepared by copolymerization of hydrophilic monomers, or crosslinking of hydrophilic polymers.[69]

1.4 Biocompatible Polymer Monoliths for Bioseparations

Usually, polymer monoliths are prepared by polymerization of monomer solutions, which are composed of monomer, crosslinker, porogen and initiator. They can be initiated either by a redox system, e.g., tetramethylethylenediamine (TEMED) and ammonium persulphate (APS), or by a free radical initiator, e.g., 2-dimethoxy-2-phenyl acetophenone (DMPA) or azobisisobutyronitrile (AIBN). An alternative way to initiate the radical polymerization process is by high energy irradiation. Compared to silica monoliths, polymeric monoliths, in particular, offer the advantage that by choosing the right functional monomer, monoliths for a variety of chromatographic purposes can be designed, such as for improved biocompatibility.

Generally, there are two ways to obtain biocompatible polymer monoliths. One is through surface modification (e.g., grafting) to create a hydrophilic surface within the monolith that resists the adsorption of proteins, including chemical reactions of surface functionalities and grafting of chains of functional polymers. Separation of the monolith synthesis and surface modification processes allows each process to be optimized independently. Neutral hydrophilic polymers such as acrylamide, and poly(ethylene glycol) methacrylate monomers have been used to prepare protein-resistant surfaces on polymer monoliths via surface grafting.[70] Hydrophilic-grafted monoliths seem well-suited for use as inert enzyme-immobilization matrices for flow-through enzymatic microreactors. The other more direct way to form biocompatible polymer monoliths is by direct

copolymerization of hydrophilic monomers, leading to the formation of hydrophilic network structures. Most commonly used monomers are hydrophilic methacrylamides and methacrylates, as shown in Figure 1.1. The chemistry of a monolith is largely controlled by choice of the monomers used in its preparation. Polymerization of vinyl monomers is most frequently initiated via radical initiators (peroxides, azo-compounds). Radicals are generated by heating, by the use of a redox initiator or a photoinitiator.

1.4.1 Polyacrylamide-based Monoliths

Acrylamide (AAm) is a moderately hydrophilic co-monomer which imparts some hydrophilicity in monolithic materials. It is typically polymerized with a crosslinker to build some rigidity into the skeletal structure of the polymer. The most common cross-linker is N, N'-methylenebisacrylamide (MBAA). Continuous rods made from a crosslinked polyAAm were initially the first monolithic materials for chromatography purposes,[71,72] and they were based on solvent-swollen poly(acrylic acid-co-MBAA). Despite the lack of a permanent pore structure, this material was used in the separation of proteins by an ion-exchange mechanism. A more rigid poly(AAm-co-MBAA) monolith was prepared by copolymerization of the hydrophilic monomers in the presence of a porogenic solvent for potential use in separation of biological polymers, solid-phase extraction, or for immobilization of proteins.[73] A new monolithic immobilized pH gradient (M-IPG) was achieved using poly(AAm-co-MBAA) monolith.[74] Compared with poly(methacrylate ester) based M-IPG, the hydrophilicity of the new material was improved, and the adsorption of proteins was avoided. A rigid, porous poly(AAm-co-butyl methacrylate-co-MBAA) monolith containing up to 15% butyl methacrylate (BuMA) units was prepared by direct polymerization and used as a separation medium

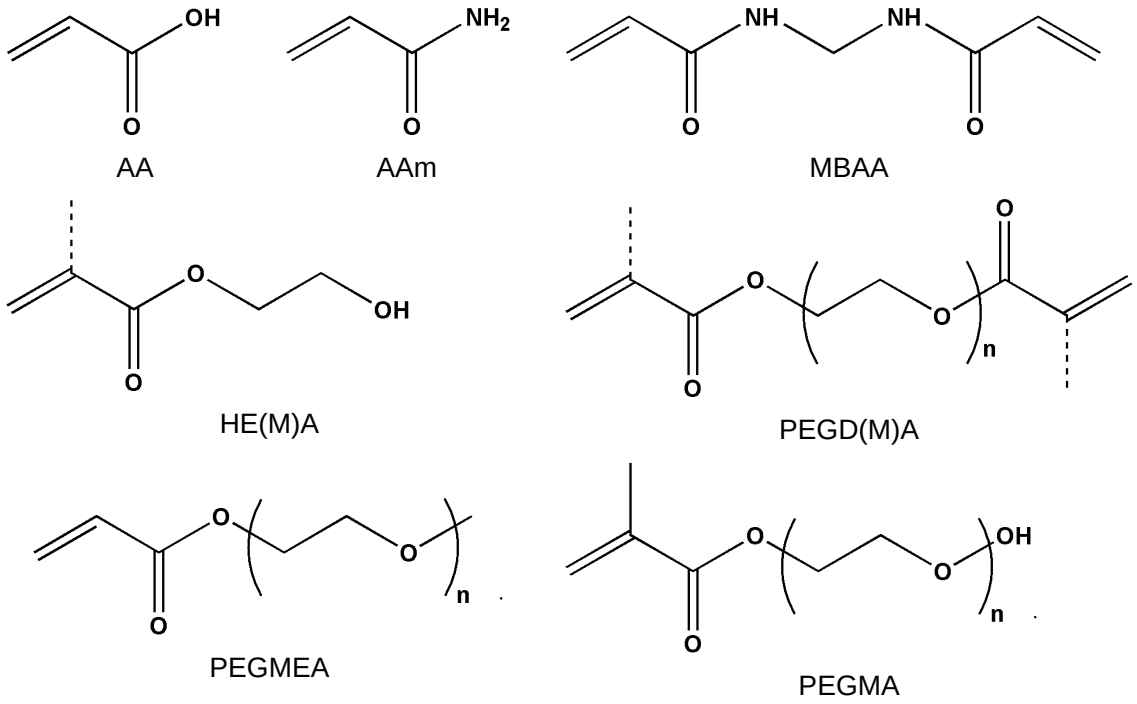

Figure 1.1. Monomers and crosslinkers used in preparing biocompatible monoliths.

for rapid HIC of proteins.[75] Palm and Novotny[76] developed a porous polymer monolithic trypsin microreactor for fast peptide mass mapping, which offered high flow permeability as well as biocompatibility. The monolith was prepared by polymerization of AAm, *N*-acryloxysuccinimide and MBAA in an electrolyte buffer with PEG as molecular template. Incorporation of AAm and MBAA certainly helped to improve the biocompatibility. The material did not irreversibly bind proteins and, thus, did not foul easily, so that it could be reused for the analysis of human plasma without loss of efficiency. A continuous bed matrix from a monomer solution (piperazine diacrylamide and methacrylamide) containing allyl glycidyl ether and 2-hydroxyethyl methacrylate (HEMA) was derivatized with C18 ligands for RPC of proteins and peptides.[77] Furthermore, additional dimethyldiallylammonium chloride could be added to the monomers to create charged ligands for reversed-phase electrochromatography of proteins.[78] Highly crosslinked rigid polyAAm can serve as a platform for the preparation of specific separation media for chromatographic modes such as HIC and affinity chromatography of proteins, both of which require biocompatible surfaces endowed with ligands or functionalities.

Additionally, due to their hydrophilicity in chromatographic behavior, polyAAm-based monoliths were successfully used in hydrophilic-phase electrochromatography of neutral (oligo)saccharides.[79, 80] However, the main use of the AAm networks has been in electroseparation methods, mainly for SDS-PAGE in slightly crosslinked gels, and electrochromatography of small molecules in highly crosslinked gels.[81-83] The fundamental polymerization procedure and its kinetics in AAm porous systems have been extensively discussed.[84-86] PolyAAm-based supermacroporous

monolithic cryogel beds can be prepared by radical cryogenic copolymerization under freezing-temperature conditions.[87] Recently, semi-interpenetrating polymer networks using biocompatible polyurethane and AAm were synthesized from different isocyanate -terminated polyurethane prepolymers derived from polytetramethylene ether glycol. Compared to a pure polyAAm network, the mechanical and thermal properties were enhanced due to higher crosslinking density imparted by the hard segments.[88] However, the resulting structure was not suitable for chromatographic applications.

1.4.2 Polymethacrylate or polyacrylate-based Monoliths

Polymethacrylate-based materials comprise the largest and most examined class of monolithic sorbents. The main advantage of current macroporous methacrylate-based monoliths is their suitability for separation of large molecules, such as proteins and polynucleotides, as well as large particles such as viruses.[89] Excellent reviews were recently published that summarize the preparation and the application of polymethacrylate-based monolithic columns for separation, purification and analysis of low and high molecular mass compounds in micro- and large-scale LC formats.[90, 91]

PolyHEMA is a known biocompatible material used in the production of contact lenses.[92] 2-Hydroxyethyl acrylate (HEA) is also a biocompatible monomer, which can be introduced into the monolith backbone in order to increase its biocompatibility. For example, increasing the HEA monomer content in the comonomer mixture (up to 18 vol%) in the preparation of the hydrophilic poly(HEA-co-diethylene glycol dimethacrylate) monolith by radiation-induced polymerization resulted in monoliths with increased hydrophilic character.[93,94] However, further increase of HEA monomer content transformed the monolith into a soft gel. The resulting monoliths were tested as

chromatographic columns, and were found suitable for separation of nucleic acids and amino acids. An important advantage of separation using this copolymer monolith is that it is environmentally friendly, since water instead of organic solvent can be used.

As mentioned above, weakly hydrophobic monolithic microcolumns are suitable for separation of proteins in the HIC mode. Neither poly(BuMA-co-glycerol dimethacrylate) nor poly(BuMA-co-butanediol dimethacrylate) was useful for HIC of proteins due to the significant hydrophobicities of the monoliths. To achieve the desired hydrophilicity of the stationary phase, HEMA was added to the polymerization mixture with the intention of decreasing retention in dilute aqueous buffers to a level useful for HIC.[95] The resulting poly(BuMA-co-HEMA-co-butanediol dimethacrylate) monolith was used for the separation of a protein mixture consisting of myoglobin, ribonuclease A and lysozyme under linear gradient conditions and at a flow rate of 2.5 μL/min. The functionalized monolith by direct copolymerization of ethylene dimethacrylate (EDMA), HEMA, and 2-vinyl-4,4-dimethylazlactone was used to prepare microreactors for immobilization of trypsin and assay of enzymatic activity.[96-98] As a result of their high digestion rate, these reactors could be easily coupled in-line with liquid chromatography or electrochromatography to enable the separation of digested proteins. A highly porous (up to 80% pore volume) open-cellular monolithic polymer was prepared from HEMA and MBAA (or EDMA) using a high internal phase emulsion. This property may be particularly valuable in chromatographic applications involving biomolecules such as proteins.[99]

PEG is a neutral, non-toxic polymer that has an affinity for water, which helps to create a microenvironment conducive for protein stabilization and improved biomolecular

interactions.[100] Oligoethylene glycol is the most common functional group used to resist non-specific adsorption of proteins and other biological materials. This protein-resistant characteristic is probably caused by a steric stabilization effect or low van der Waals interaction with proteins.[101,102]

Poly(glycidyl methacrylate-co-EDMA) is one of the most prevalent copolymer systems, since the epoxy groups can be easily modified with functionalities for specific interactions, such as hydrophobic, ion exchange, affinity and reversed phase separations. Additionally, the remaining epoxy groups can be hydrolyzed into diol functionalities to increase the hydrophilicity of the monolith. However, even if the epoxy groups are blocked, there is not sufficient hydrophilicity to minimize non-specific protein adsorption in an aqueous mobile phase without an organic additive. Recently, Krenkova et al. grafted a poly(glycidyl methacrylate-co-EDMA) monolith with PEGMA in order to eliminate non-specific adsorption of proteins and peptides before reacting with azlactone functionalities for enzyme immobilization.[103] Surface-modified macroporous poly(BuMA-co-EDMA) monoliths that resist adsorption of proteins can be prepared using either single- or two-step photografting of a series of hydrophilic monomers,[70,104] such as AAm, HEMA, vinyl pyrrolidinone, and PEGMA. Photografted layers of PEGMA reduced protein adsorption to less than 2% relative to unmodified surfaces. The sequential two-step photografting process consisted of (1) formation of covalently bound surface photoinitiator sites followed by (2) surface-localized graft polymer. Monomer concentration and irradiation time during photografting were found to be the most important parameters for optimization of the two-step process. Surface modification using a two-step sequential photografting technique leads to a substantial increase in surface hydrophilicity and a

large reduction in protein adsorption. This photografting technique should allow monoliths to be used for a variety of bioanalytical applications that require minimal nonspecific adsorption of biomolecules. Hydrophilic photografting should also be useful for creating nonfouling surfaces in applications such as mixers, valves, and filters.

Oligo(ethylene glycol) dimethacrylates with different lengths of PEG bridging moieties between methacrylate units have been used to copolymerize with BuMA for RPC of proteins. However, the hydrophilic crosslinkers do not significantly change the retention behavior of the column since the hydrophobicity of the stationary phase originates mainly from the butyl groups in the monomer and the hydrocarbon polymer backbone.[105] However, three PEG molecules (PEG-methacrylate, -diacrylate and -dimethacrylate) could be incorporated into galactose-based polyacrylate hydrogels to reduce non-specific protein binding.[106]

Recently, PEG-acrylates and PEG-diacrylates containing three or more moieties in the PEG chains were used to synthesize monoliths with improved biocompatibility. The monomers polyethylene glycol methyl ether acrylate (PEGMEA) and polyethylene glycol diacrylate (PEGDA) were copolymerized for a porous monolith that resists adsorption of both acidic and basic proteins when using an aqueous buffer without any organic solvent additives.[107] Clean fluorescent images obtained after flushing PEGDA-based monoliths loaded with fluorescein isothiocyanate (FITC)-labeled BSA were demonstrated to show negligible nonspecific adsorption of proteins. Based on these results, SEC monoliths with various molecular weight separation ranges for proteins or peptides were prepared.[108,109] These monoliths are expected to be useful for biological sample preparation and

purification, such as removal of nonprotein contaminants (e.g. DNA and viruses), protein aggregate removal, the study of biological interactions, and protein folding.

An strong cation-exchange column that possesses negligible non-specific interactions (i.e., hydrophobic interactions) was prepared from copolymerization of vinylsulfonic acid and the biocompatible crosslinker, PEGDA.[110] Excellent peak shapes for peptides and proteins were obtained without addition of acetonitrile in the eluent. The reduced hydrophobicity of the stationary phase originates mainly from the low hydrocarbon content of the functional monomer and the PEG units in the biocompatible crosslinker. The hydrophobicities of the monoliths were compared under RPC conditions, yielding capacity factors of almost zero for a poly(PEGDA) monolith and 4.4 for a poly(EDMA) monolith. EDMA is the most widely used crosslinker used for synthesizing polymethacrylate-based monoliths. When EDMA was replaced by PEGDA, the new poly (GMA-co-PEGDA) monolith provided better resolution between conalbumin and ovalbumin, largely due to the reduced tailing of the conalbumin peak.[111] High recovery of proteins could be obtained on the monoliths incorporating PEGDA as crosslinker. Additionally, two novel polymeric monoliths for anion exchange capillary LC of proteins were prepared in a single step by a simple photoinitiated copolymerization of two amine-containing monomers with the biocompatible crosslinker, PEGDA, in the presence of selected porogens. A poly(HEMA-co-PEGDA) monolith was incorporated in an electric field gradient focusing micofluidic device to reduce the bandwidths of focused proteins in the channel. The focused protein bands were symmetrical due to negligible interaction between the monolith and proteins.[112] A poly(methacrylic acid-EDMA) monolith was shown to be biocompatible when used for in-tube solid-phase microextraction (SPME) of

several antibiotics and angiotensin II receptor antagonists.[113,114] The SPME columns could be reused without loss of extraction efficiency since they did not foul easily.

Recently, Courtois et al. proposed the utilization of PEG as a constituent of the porogen solution to obtain a more biocompatible monolithic support.[115] The idea was to produce a monolithic support with large protein-compatible pores characterized by a protein-friendly surface, which would not cause unfolding or denaturation of the separated proteins. The authors used 1.5–20 kDa PEGs dissolved in 2-methoxyethanol and a series of co-porogens as a porogen system.

1.5 Monoliths for Analysis of Proteomic Samples

Proteomics is the study of how information coded in a cell is expressed and regulated at the protein level to achieve the function of an organism.[116] Among the goals of proteomics are the following: the identification of all the proteins in a given cell, tissue or organisms; determination of how these proteins interact; and, finally, to understand the mechanism of the function of these proteins. An ultimate result of proteomics is the understanding of complex biological systems, which can lead to new diagnostics and therapy. The first step toward this end is the identification of all proteins in a given system by protein mapping or profiling. Typically, this is considered the discovery phase of proteomics and involves the comparison of different states of a cell or tissue, such as diseased vs. normal, mature vs. immature, or drug-treated vs. non-treated. Traditionally, this profiling has been accomplished by two-dimensional gel electrophoresis.[117-119] Although two-dimensional polyacrylamide gel electrophoresis has successfully resolved proteomes, it is labor-intensive, time-consuming, and, at best, semi-quantitative.

One of the bottlenecks for proteomics research is the sample throughput. Sample separation is time-consuming, often taking several hours per sample. Development of stationary phases for LC has taken place for more than 35 years, however, the field has not come to saturation, since the need for columns for high-speed and high-resolution LC is enormous, especially in proteomics. "All separations in chromatography would benefit from high resolution, high column capacity, fast separations and low back pressure." [120] The use of monolithic columns for separations in proteomics provides a simple approach to achieve these goals, mostly due to enhanced mass transfer, high column efficiency and easy preparation and functionalization.[121]

Another important aspect of future development is the miniaturization of instrumentation, including the separation column. There are many publications describing miniaturized chips and their use for separation of proteins and peptides. Large monolithic columns are desirable for preparative-scale separations. However, due to the small sample volumes and low concentrations encountered in proteomics analysis, capillary monolithic columns for use in nano-LC have recently grown in interest.[122] Nano-LC using flow rates of 200-300 nL/min to separate peptides in 75-100 μm i.d. columns dominates the field. The capillary format also provides two other advantages: first, immobilization of the monolith at the capillary wall eliminates the necessity of preparing a tiny retaining frit; second, direct on-line coupling of capillary LC to mass spectrometry becomes easier.[123] Certainly, enhancements in separation techniques must be followed by improvements in the filed of mass spectrometry, enabling it to keep pace with fast-developing separation technology.

1.6 Conclusions

The concept of "biocompatibility" was applied successfully to chromatographic stationary phases. A biocompatible stationary phase material should be able to resist nonspecific adsorption of biomolecules and preserve their bioactivities. The characteristics of a biocompatible material that resist protein adsorption were also summarized. Generally, there are two methods to obtain a biocompatible stationary phase: surface modification of a suitable polymer and direct copolymerization of hydrophilic monomers. The two main classes of biocompatible monoliths were reviewed, including polyacrylamide-based and polymethacrylate (or polyacrylate)-based polymer monoliths. Integration of PEG into the polymethacrylate or polyacrylate monolith network proved beneficial in the reduction of non-specific protein interaction.

Two of the most significant advantages of monoliths are easy fabrication and abundance of chemistry. However, the surface modification approach, which is the most complex, is the most widely used. Recent introduction of surface-reactive monomers or biocompatible monomers could simplify this process. It is anticipated that in addition to developing more convenient and effective surface modification techniques for monolith fabrication from conventional commodity polymers, the use of functional monomers with inherent properties suitable for specific chromatographic applications, including improved biocompatibility, will receive more attention in the future. Additionally, development of new monoliths with improved biocompatibility and built-in functionalities would introduce new tools for selective sample cleanup and enrichment, and therefore enable researchers to dig deeper into the proteome.

1.7 Dissertation Overview

Chapters 2 to 4 describe my research on the development of biocompatible polymer monoliths for protein and peptide analysis. Chapter 2 describes the development of a series of novel anion-exchange monoliths for high-resolution separation of proteins, in which PEGDA was incorporated in the monolithic backbone to improve its resistance to protein adsorption. This chapter also demonstrates a new AEC method for analysis of whole cell lysates of proteins using these monoliths. Chapters 3 and 4 report developments of biocompatible monolithic stationary phases for capillary SEC separations of proteins and peptides. This work represents a breakthrough in SEC monolith synthesis. Surfactants were introduced as porogens with the hope of significantly increasing the mesopore volume within the polymer. Two types of surfactants were studied, including poly(ethylene oxide)-poly(propylene oxide)-poly(ethylene oxide) (PEO-PPO-PEO) and PPO-PEO-PPO (Chapter 3), and Brij (Chapter 4). Chapter 5 presents the analysis of HDL using a capillary packed with BioSep-SEC-4000 particles, as well as capillaries containing poly(PEGMEA- co-PEGDA) and poly(AETAC-co-PEGDA) monoliths. Chapter 6 presents proposed future directions in monolith development for protein and peptide separations.

1.8 References

1. Baguneid, M. S.; Seifalian A. M.; Salacinski H. J.; Murray, D.; Hamilton, G.; Walker, M. G. *Br. J. Surg.* **2006,** *93*, 282-290.
2. Mahashabde, A.; Kay, M. F.; Glazer, B.; Zhang, J. U.S. Patent 7,005,138, **2006**.
3. Williams, D. F. *J. Med. Eng. Tech.* 1977, *1*, 195-198. Bertoluzza, A.; Monti, P.; Arciola, C. R.; Pizzoferrato, A. *Clin. Mater.* 1991, *8*, 165-169. Fischer, H.; Karaca, F.;

Marx, R. *J. Biomed. Mater. Res.* 2002*, 61,* 153-158. Kolff, W. J.; Akutsu, T.; Dreyer, B.; Norton, H. *Trans. Am. Soc. Artif. Intern. Organs*, 1959, *5*, 298-300. Ryder J. K.; Cao, H. *J. Heart Valve Dis.* 1996, *5*, S79-S85, S86-S96.

4. Williams, D. F. *Biomaterials* **2008**, *29*, 2941-2953.
5. Svec, F.; Fréchet, J. M. J. *Science* **1996**, *273*, 205-211.
6. Svec, F.; Fréchet, J. M. J. *Anal. Chem.* **1992**, *54*, 820-822. Wang, Q. C.; Svec, F.; Fréchet, J. M. J. *Anal. Chem.* **1993**, *65*, 2243-2248. Fréchet, J. M. J.; Svec, F. U.S. patent 5,334,310, **1994**.
7. Goemann, A.; Deverell, J. A.; Munting, K. F.; Jones, R. C.; Rodemann, T.; Canty, A. J.; Smith, J. A.; Guijt, R. M. *Tetrahedron*, **2009**, *65*, 1450-1454.
8. Canty, A. J.; Deverell, J. A.; Gomann, A.; Guijt, R. M.; Rodemann, T.; Smith, J. A. *Aust. J. Chem.* **2008**, *61*, 630-633.
9. Kunz, U.; Kirschning, A.; Wen, H. L.; Solodenko, W.; Cecilia, R.; Kappe, C. O.; Turek, T. *Catalysis Today* **2005**, *105*, 318-324.
10. Jin, S.; Venkataraman, D.; DiSalvo, F. J.; Peters, E. C.; Svec, F.; Fréchet, J. M. J. Book of Abstracts, 219th ACS National Meeting, San Francisco, CA, March 26-30, **2000**.
11. Petro, M.; Svec, F.; Fréchet, J. M. J. *Biotechnol. Bioeng.* **1996**, *49*, 355-363.
12. Svec, F.; Jelinkova, M.; Votavova, E. *Angew. Makromol. Chem.* **1991**, *188*, 167-176.
13. Löber, A.; Verch, A.; Schlemmer, B.; Höfer, S.; Frerich, B.; Buchmeiser, M. R. **2008**, *47*, 9138-9147.
14. Chen, P-J.; Rodger, D. C.; Saati, S.; Humayun, M. S.; Tai, Y-C. *J. Microelectromech. S.* **2008**, *17*, 1342-1351.

15. Kolawole, O. A.; Pillay, V.; Choonara, Y. E. PCT Int. Appl. **2008**, 56 pp.
16. Ayala, V. C.; Michalzik, M.; Harling, S.; Menzel, H.; Guarnieri, F. A.; Büttgenbach, S. *J. Phys.: Conf. Ser.* **2007**, *90*, 012025, 6 pp.
17. Hegyeli, R. J. *J. Biomed. Mater. Res.* **1971**, *5*, 1-17.
18. Homsy C. A. *J. Biomed. Mater. Res.* **1970**, *4*, 351-356.
19. Williams, D. F. *Definitions in Biomaterials: Progress in Biomedical Engineering*, Amsterdam: Elsevier, 1987.
20. Williams, D. F. *Med. Device Technol.* **2003**, 14, 10-3.
21. Schafer, W. A.; Carr, P. W. *J. Chromatogr.* **1991**, *587*, 149-160.
22. Clausen, A. M.; Carr, P. W. *Anal. Chem.* **1998**, *70*, 378-385.
23. He, H.; Yu, Q.; Feng, Y.; Da, S. *J. Liq. Chrom. Rel. Technol.* **2009**, *32*, 468-482.
24. Chapman, R. G.; Ostuni, E.; Liang, M. N.; Meluleni, G.; Kim, E.; Yan, L.; Pier, G.; Warren, H. S.; Whitesides, G. M. *Langmuir*, **2001**, *17*, 1225-1233.
25. Nelson, D. L.; Cox, M. M. *Lehninger Principles of Biochemistry*, 4th ed.; W. H. Freeman and Company: New York, 2004.
26. Guo, D.; Mant, C. T.; Taneja, A. K.; Parker, J. M. R.; Hodges, R. S *J. Chromatogr.* **1986**, *359*, 499-517.
27. Ramsden, J. J. *Q. Rev. Biophys.*, **1994**, *27*, 41-105.
28. Lin, Y. S.; Hlady, V. *Colloids and Surfaces, B. Biointerfaces*, **1994**, *2*, 481-491.
29. Malmsten, M. In *Protein Architecture: Interfacing Molecular Assemblies and Immobilization Biotechnology*; Lvov, Y., Möhwald, H., Eds.; Marcel Dekker: New York, 2000, 1-23.
30. Norde, W. In *Physical Chemistry of Biological Interfaces*; Baszkin, A., Norde, W.,

Eds.; Marcel Dekker: New York, 2000, 115-135.

31. Ramsden, J. J. *J. Mol. Recognit.* **1997**, *10*, 109-120.
32. Chen, W. -Y.; Wu, C. -F.; Liu, C.-C. *J. Colloid Interface Sci.***1996,** *180,* 135-143.
33. Sharma, S.; Agarwal, G. P. *Anal. Biochem.* **2001**, *288*, 126-140.
34. Yoon, J. -Y.; Kim, J. H.; Kim, W. -S. *Colloids Surf. B* **1998**, *12*, 15-22.
35. Beeskow, T. C.; Kusharyoto, W.; Anspach, F. B.; Kroner, K. H.; Deckwer, W. -D. *J. Chromatogr. A* **1995**, *715*, 49-65.
36. Henderson, M. A. *Surf. Sci. Rep.* **2002**, *46*, 1–308.
37. Farrah, S. R.; Shah, D. O.; Ingram, L. O. *Proc. Natl. Acad. Sci.* **1981**, *78*, 1229-1232.
38. Israelachvili, J. *Intermolecular and Surface Forces*, 2nd ed.; Academic Press: London, 1992.
39. Ratner, B. D. In *Principles of Regenerative Medicine*; Atala, A., Lanza, R., Thomson, J. A., Nerem, R., Eds.; Academic Press: New York, 2008, 734-742.
40. Roque, A. C. A.; Lowe, C. R. In *Affinity chromatography, Methods and Protocols*; Zachariou, M. 2nd Eds.; Humana Press: New York 2008, 1-23.
41. Ratner, B. D. *J. Biomed. Mater. Res.* **1993**, *27*, 837-850.
42. Ratner, B. D. *J. Control. Release.* **2002**, *78*, 211-218.
43. Jenkins, S. H.; Heinerman, W. R.; Halsall, H. B. *Anal. Biochem.* **1988**, *168*, 292-297.
44. Kessler, G. H.; Lund, D. B. *Fouling and Cleaning in Food Processing*; Prien Chiemsee: Federal Republic of Germany 1989.
45. Cross, G. H.; Reeves, A. A.; Brand, S.; Popplewell, J. F.; Peel, L. L.; Swann, M. J.; Freeman, N. J. *Biosens. Bioelectron.* **2003**, *19*, 383-390.
46. Baier, R. E.; Meyer, A. E.; Natiella, J. R.; Natiella, R. R.; Carter, J. M. *J. Biomed.*

Mater. Res. **1984**, *18*, 337-355.

47. Schakenraad, J. M.; Busscher, H. J. *J. Colloids Surf.* **1989**, *42*, 331-339.
48. Habash, M.; Reid, G. *J. Clin. Pharmacol.* **1999**, *39*, 887-898.
49. Andrade, J. D.; Hlady, V. *Adv. Poly. Sci.* **1986**, *79*, 1-63.
50. Sadana, A. *Chem. Rev.* **1992**, *92*, 1799-1818.
51. Mant, C. T.; Hodges, R. S. *High-performance Liquid Chromatography of Peptides and Proteins: Separation, Analysis, and Conformation*; CRC Press: Boca Raton, Florida, 1991.
52. Kopaciewicz, W.; Regnier, F. E. *Anal. Biochem.* **1982**, *126*, 8-16.
53. Mouat, M. F.; Manchester, K. L. *J. Liq. Chrom. Rel. Technol.* **1997**, *20*, 143-153.
54. Floyd, T. R.; Cicero, S. E.; Fazio, S. D.; Raglion, T. V.; Hsu, S-H.; Winkle, S. A.; Hartwick, R. A. *Anal. Biochem.* **1986**, *154*, 570-577.
55. Majors, R. E.; Lees, A.; Burkhardt, M. *LC GC* North America, Jan 1, 2009
56. Burke, T. W. L.; Mant, C. T.; Black, J. A.; Hodges, R. S. *J. Chromatogr.* **1989**, *476*, 377-389
57. Osthoff, G.; Louw, A. I.; Visser, L. *Anal. Biochem.* **1987**, *164*, 315-319.
58. Snyder, L. R.; Kirkland, J. J.; Glajch, J. L. *Practical LC method development*, 2nd Ed., Wiley-Interscience publication, JOHN WILEY & SONS, New York, 1997.
59. Hjerten, S.; Mosbach, R. *Anal. Biochem.* **1962**, *3*, 109-118.
60. Porath, J.; Flodin, P. *Nature*, **1959**, *183*, 1657-1659.
61. Hjerten, S. *Arch. Biochem. Biophys.*, **1962**, *99*, 466-475.
62. Eriksson, K. -O. In *Biochromatgraphy*: *Theory and Practice*; Vijayalakshmi, M. A., Eds.; CRC Press: Boca Raton, FL , 2002, 9-23.

63. Porath, J. *J. Protein Chem.* **1997**, *16*, 463-468.

64. Clarke, N. J., Tomlinson, A. J., Schomburg, G., Naylor, S. *Anal. Chem.* **1997**, *69*, 2786-2792.

65. Preisler, J., Yeung, E. S. *Anal. Chem.* **1996**, *68*, 2885-2889.

66. McCormick, R. *Anal. Chem.* **1988**, *60*, 2322-2328.

67. Zhao, Z., Malik, A., Lee, M. L. *Anal. Chem.* **1993**, *65,* 2747-2752.

68. Zewert, T., Harrington, M. *Electrophoresis* **1992**, *13*, 817-824, 824-831.

69. Schacht, E. H. *J. Phys: Conf. Ser.* **2004**, *3*, 22-28.

70. Stachowiak, T. B., Svec, F., Fréchet, J. M. J. *Chem. Mater.* **2006**, 18, 5950-5957.

71. Hjertén, S., Liao, J., Zhang, R. *J. Chromatogr*. **1989**, *473*, 273-275.

72. Hjertén, S., Li, Y.; Liao, J.; Mohammad, J.; Nakazato, K.; Pettersson, G. *Nature* **1992**, *356*, 810-811.

73. Xie S., Svec, F., Fréchet, J. M. J. *J. Polym. Sci. Polym. Chem* **1997**, *35*, 1013-1021.

74. Zhu, G.; Zhang, W.; Zhang, L.; Liang, Z.; Zhang, Y. *Sci. China, Ser. B Chem.* **2007**, *50*, 526-529.

75. Xie, S.; Svec, F.; Fréchet, J. M. J. *J. Chromatogr. A* **1997**, *775,* 65-72.

76. Palm, A. K., Novotny, M. V. *Rapid Commun. Mass Spectrom.* **2004**, *18*, 1374-1382.

77. Liao, J.; Li, Y.; Hjertén, S. *Anal. Biochem.* **1996**, *234*, 27-30.

78. Ericson, C.; Hjertén, S. *Anal. Chem.* **1999**, *71*, 1621-1627.

79. Que, A. H.; Novotny, M. V. *Anal. Chem.* **2002,** *74*, 5184-5191.

80. Guryča, V.; Mechref, Y.; Palm, A. K.; Michálek, J.; Pacáková, V.; Novotný, M. V. *J. Biochem. Biophys. Methods* **2007**, *70*, 3-13.

81. Hoegger, D.; Freitag, R. *J. Chromatogr. A* **2001**, *914*, 211-222.

82. Palm, A.; Novotny, M. V. *Anal. Chem.* **1997**, *69*, 4499-4507.

83. Tegeler, T. J.; Mechref, Y.; Boraas, K.; Reilly, J. P.; Novotny, M. V. *Anal. Chem.* **2004**, *76*, 6698-6706.

84. Sayil, C.; Okay, O. *Polymer* **2001**, *42*, 7639-7652.

85. Durmaz, S.; Okay, O. *Polymer* **2000**, *41*, 5729-5735.

86. Okay, O. *Prog. Polym. Sci.* **2000**, *25*, 711-719.

87. Yao, K.; Shen, S.; Yun, J.; Wang, L.; He, X.; Yu, X. *Chem. Eng. Sci.* **2006**, *61*, 6701-6708.

88. Merlin, D. L.; Sivasankar, B. *Eur. Polym. J.* **2009**, *45*, 165-170.

89. Peterka, M.; Glover, D.; Kramberger, P.; Banjac, M.; Podgornik, A.; Barut, M.; Štrancar, A. *Bioprocess. J.* **2005**, *March/April*, 1-6.

90. Vlakh, E. G.; Tennikova, T. B. *J. Sep. Sci.* **2007**, *30*, 2801-2813.

91. Vlakh, E. G.; Tennikova, T. B. *J. Chromatogr. A* **2009**, *1216*, 2637-2650.

92. Nicolson, P. C.; Vogt, J. *Biomaterials* **2001**, *22*, 3273-3283.

93. Beiler, B.; Vincze, A.; Svec, F.; Sáfráry, A. *Polymer* **2007**, *48*, 3033-3040.

94. Beiler, B.; Sáfrány, A. *Radiat. Phys. Chem.* **2007**, *76*, 1351–1354

95. Hemström, P.; Nordborg, A.; Svec, F.; Fréchet, J. M. J. Irgum, K. *J. Sep. Sci.* **2006**, *29*, 25-32.

96. Peterson, D. S.; Rohr, T.; Svec, F.; Fréchet, J. M. J. *Anal. Chem.* **2003**, *75*, 5328-5335.

97. Peterson, D. S.; Rohr, T.; Svec, F.; Fréchet, J. M. J. *J. Proteome. Res.* **2002**, *1*, 563-568.

98. Peterson, D. S.; Rohr, T.; Svec, F.; Fréchet, J. M. J. *Anal. Chem.***2002**, *74*,

4081-4088.

99. Kovačič, S.; Sÿtefanec, D.; Krajnc, P. *Macromolecules* **2007**, *40,* 8056-8060.

100. Harris, J. M.; Zalipsky, S. *Poly(ethylene glycol): Chemistry and Biological Applications*, ACS Symposium Series 680; American Chemical Society: Washington, D.C., 1997.

101. Jeon, S. J.; Andrade, J. D. *J. Colloid Interface Sci.* **1991**, *142*, 159-166.

102. Jeon, S. I.; Lee, J. H.; Andrade, J. D., DeGennes, P. G. *J. Colloid Interface Sci.* **1991**, *142*, 149-158.

103. Krenkova, J.; Lacher N. A.; Svec, F. *Anal. Chem.* **2009**, *81*, 2004-2012.

104. Stachowiak, T. B.; Svec, F.; Fréchet, J. M. J. In *Proceedings of Micro Total Analysis Systems 2006*, Kitamori, T., Fujita, H.; Hasebe, S., Eds.; Society for Chemistry and Micro-Nano Systems: Tokyo, Japan, 2006, 227-229.

105. Nordborg, A.; Svec, F.; Fréchet, J. M. J. ; Irgum, K. *J. Sep. Sci.* **2005**, *28*, 2401-2406.

106. Charles, P. T.; Stubbs V. R.; Soto, C. M.; Martin, B. D.; White, B. J.; Taitt, C. R. *Sensors* **2009**, *9*, 645-655.

107. Gu, B.; Armenta, J. M.; Lee, M. L. *J. Chromatogr. A* **2005**, *1079*, 382-391.

108. Li. Y.; Tolley, H. D.; Lee, M. L. *Anal. Chem.* **2009**, *81*, 4406–4413.

109. Gu, B.; Li, Y.; Lee, M. L. *Anal. Chem.* **2007**, *79*, 5848-5855.

110. Li, Y.; Gu, B.; Tolley, H. D.; Lee, M. L. *J. Chromatogr. A* **2009**, *1216*, 5525–5532.

111. Li, Y.; Lee, M. L. in preparation.

112. Sun, X.; Farnsworth, P. B.; Woolley, A. T.; Tolley, H. D.; Warnick, K. F.; Lee, M. L. *Anal. Chem.* **2008**, *80*, 451-460.

113. Nie, J.; Zhang, M.; Fan, Y.; Wen, Y.; Xiang, B.; Feng, Y. *J. Chromatogr. B* **2005**, *828*, 62-69.

114. Wen, Y.; Wang, Y.; Feng, Y. *Talanta* **2006**, *70*, 153-159.

115. Courtois, J.; Byström, E.; Irgum, K. *Polymer* **2006**, *47*, 2603-2611.

116. Manabe, T. *Electrophoresis* **2000**, *21*, 1116-1122.

117. O'Farrell, P. H. *J. Biol. Chem.* **1975**, *250*, 4007-4021.

118. Gorg, A.; Postel, W.; Gunther, S. *Electrophoresis* **1988**, *9*, 531-546.

119. Hancock, W. S.; Wu, S. L.; Shieh, P. *Proteomics* **2002**, *2*, 352-359.

120. Gray, M. J.; Slonecker, P. J.; Dennis, G.; Shalliker, R. A. *J. Chromatogr. A* **2005**, *1096*, 92-100.

121. Tanaka, N.; Kobayashi, H.; Ishizuka, N. Minakuchi, H.; Nakanishi, K.; Hosoya, K.; Ikegami, T. *J. Chromatogr. A* **2002**, *965*, 35-49.

122. Barroso, B.; Lubda, D.; Bischoff, R. *J. Proteome Res.* **2003**, *2*, 633-642.

123. Tomer, K. B.; Moseley, M. A.; Deterding, L. J.; Parker, C. E. *Mass spectrom. Rev.* **1994**, *13*, 431-457.

CHAPTER 2 PREPARATION OF POLYMERIC MONOLITHS BY COPOLYMERIZATION OF ACRYLATE MONOMERS WITH AMINE FUNCTIONALITES FOR ANION-EXCHANGE CAPILLARY LIQUID CHROMATOGRAPHY OF PROTEINS

2.1 Introduction

Anion exchange chromatography (AEC) is often used for analyzing proteins because it is typically performed under neutral or slightly basic pH conditions where proteins remain in their native states.[1-3] The technique is based on the reversible binding of negatively charged functional groups on biomolecules to positively charged groups in the stationary phase and their subsequent displacement by either increasing the ionic strength or pH of the mobile phase. Commonly used anion exchangers are functionalized with amines.[4-6] Typically, weak anion exchangers contain diethylaminoethyl (DEAE) or polyethyleneimine (PEI) functionalities, while strong anion exchangers are quaternary amines. As for stationary phase support materials, silica and organic polymers have replaced polysaccharides (such as cellulose, agarose and dextran) because of their excellent mechanical stabilities.[7,8] Additionally, polymers, such as highly cross-linked polystyrene divinylbenzene (PSDVB), are popular because they have a wider pH stability range than silica, while possessing comparable mechanical stability if highly crosslinked.[8,9]

Monolithic stationary phases have grown in interest because of their characteristic enhanced mass transfer and simple preparation. Polymeric monoliths, in particular, offer the advantage that by choosing the right functional monomer, monoliths for various chromatographic applications can be designed, such as reversed-phase and affinity chromatography.[10,11] DEAE, which is used to prepare weak anion-exchangers (WAX), was

introduced into a monolithic stationary phase after thermally initiated polymerization of a rod of poly(glycidyl methacrylate-co-ethylene glycol dimethacrylate) (GMA-co-EDMA) by reaction of the epoxy groups on the rod with diethylamine (DEA).[12,13] Similarly, a PEI modified weak anion-exchanger was also prepared based on a poly(GMA-co-EDMA) monolith.[14] In another report, WAX functionalities were introduced into poly(GMA) chains grafted onto a porous-fiber membrane by radiation-induced graft polymerization and subsequent functionalization.[15] Based on poly(GMA-co-DVB) monoliths, DEAE or quaternary ammonium functionalities were introduced to provide WAX or strong anion-exchange (SAX) stationary phases for the separation of oligonucleotides, or oligonucleotides and nucleosides, respectively.[16,17] Acetonitrile was added to the mobile phase to suppress the hydrophobic interaction mainly from divinylbenzene. By this surface modification approach, only a single functionality could be introduced. Additionally, when conducting the *in situ* reaction, in order to achieve maximum surface coverage and high reproducibility, special care had to be taken with respect to compatibility of the solvent adsorbed on the matrix surface, reaction temperature, and reaction time. In another approach, an SAX stationary phase was prepared by coating a porous poly(butyl methacrylate-co-ethylene dimethacrylate -co-2-acrylamido-2-methyl-1-propanesulfonic acid) (BMA-co-EDMA-co-AMPS) monolith by electrostatic attachment of quaternary amine (QA)-functionalized latex particles for the separation of saccharides.[18] However, pore size and flow permeability were decreased after coating with a layer of latex particles.

Surface grafting is another effective approach for introducing ionizable groups onto the surface of monoliths, which also involves two main steps, matrix formation and functionality attachment. For example, anion exchange polymer chains of poly[2-

(dimethylamino)ethyl methacrylate] (pDMAEMA) and poly[(2-(methacryloyloxy) ethyl trimethylammonium chloride] (pMETAC) have been grafted onto macroporous polyacrylamide gels by free-radical polymerization. These monoliths achieved protein binding capacities of up to 6-12 mg/mL, but no separation was demonstrated.[19] The ionizable monomers AMPS and METAC were also grafted onto macroporous polymer monoliths for fabricating electroosmotic pumps.[20] Surface grafting can introduce multiple functionalities onto a single monolith. However, this approach usually suffers from low grafting efficiency, swelling of grafted polymer and, therefore, reduced permeability of the final monolith.[21]

Direct copolymerization of functional monomers undoubtedly provides the simplest approach for preparation of functionalized monoliths. Using this technique, Gu et al. designed and synthesized a series of strong cation-exchange (SCX) monoliths by incorporating different sulfonic acid-functionalized monomers with decreasing hydrophobicity.[22,23] High-performance separations of peptides and proteins were achieved using these columns. A poly(AMPS-co-PEGDA) monolith exhibited a dynamic binding capacity (DBC) that exceeded 150 μequiv/mL of peptides or 300 mg/mL of proteins, which were much higher than for an AMPS grafted poly(GMA-co-EDMA) monolith.[24] However, the preparation of such monoliths using direct copolymerization of functional monomers is not always successful because of difficulties experienced in finding a porogen system that dissolves all of the monomers while enabling the formation of monoliths with desired pore structure. Despite advances in the theoretical understanding of polymerization processes,[25,26] the selection of porogens still remains largely empirical.

Minimal nonspecific interaction between analytes and stationary phase is very desirable in order to keep proteins in their native states and to allow reversible adsorption.[27,28] Polyethylene glycol (PEG) is a hydrophilic, biocompatible polymer. Surface-bound PEG can resist the non-specific adsorption of proteins and other biological species,[29] which has been achieved by incorporating PEG monomers into polymer networks by graft polymerization,[30] or by attaching PEG chains directly to polymer surfaces by various coupling reactions.[31] Recently, reaction of PEG functionalized monomers, such as polyethylene glycol methyl ether acrylate (PEGMEA) and polyethylene glycol diacrylate (PEGDA) yielded monoliths that demonstrated negligible non-specific adsorption of proteins.[32] Krenkova et al. reported the grafting of poly(GMA-co-EDMA) monolith with poly(ethylene glycol) methacrylate before attaching reactive azlactone functionalities for enzyme immobilization in order to minimize non-specific adsorption of proteins and peptides.[33]

Based on previous work in Dr Lee's laboratory,[22,23] the design of successful functionalized monoliths has followed two main strategies: (1) incorporation of monomers that simultaneously provide functionalities with high selectivity, and (2) application of a biocompatible crosslinker (PEGDA) that forms monoliths with decreased non-specific adsorption. In this paper, two functional monomers containing anion-exchange functionalities, 2-(diethylamino)ethyl methacrylate (DEAEMA) and 2-(acryloyloxy)ethyl trimethylammonium chloride (AETAC) were utilized, as shown in Figure 2.1. Two novel anion-exchange polymeric monoliths were prepared by direct copolymerization of DEAEMA and PEGDA, and copolymerization of AETAC and PEGDA. The resulting monoliths contained DEAE (a WAX group) and QA (a SAX group), respectively. Both

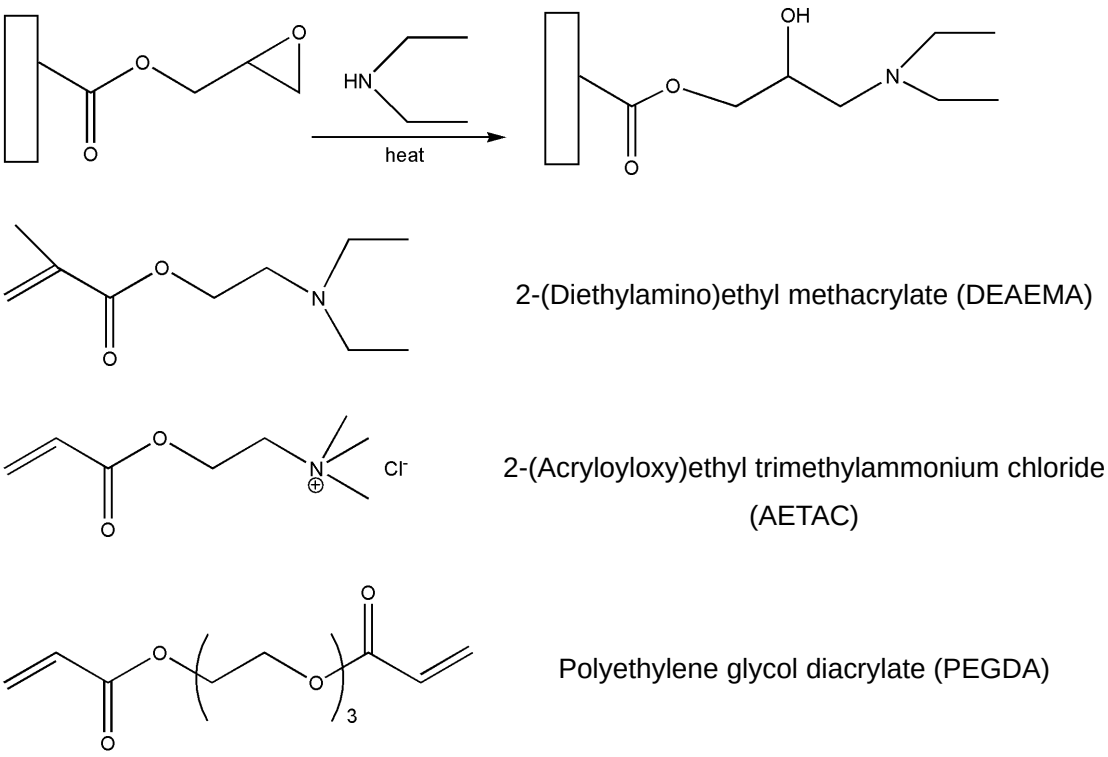

Figure 2.1. Reaction scheme and monomers involved in synthesizing the anion-exchange monoliths.

demonstrated comparable chromatographic properties and did not require additional surface functionalization. An alternative WAX monolith was also obtained by copolymerization of GMA and PEGDA (replacing EDMA) and subsequent functionalization. These anion-exchange monolithic columns were prepared in a capillary format using 75 μm i.d. capillaries by photoinitiated polymerization and then were evaluated for LC separation of standard proteins.

2.2 Experimental Section

2.2.1 Chemicals

2,2-Dimethoxy-2-phenylacetophenone (DMPA, 99%), 2,2'-azobisisobutyronitrile (AIBN, 98%), 3-(trimethoxysilyl)propyl methacrylate (TMSPMA, 98%), PEGDA (Mn ~258), EDMA (98%), GMA (> 97%), DEAEMA (99%), and AETAC (80 wt. % solution in water) were purchased from Sigma-Aldrich (Milwaukee, WI). DEA (99+ %) was obtained from Acros Organics (Morris Plains, NJ). All of the monomers were used without further purification. Porogenic solvents, cyclohexanol, methanol, ethyl ether, and hexanes, and chemicals for use in mobile phases were LC grade. Buffer solutions were prepared with deionized water from a Millipore water purifier (Billerica, MA) and filtered through a 0.22-μm membrane filter.

Proteins, myoglobin (MYO) from equine skeletal muscle, conalbumin (CON) from chicken egg white, ovalbumin (OVA), bovine serum albumin (BSA), and soybean trypsin inhibitor (STI) were purchased from Sigma-Aldrich. The total protein from lysate of the host *Escherichia. coli* DH5α was obtained as described previously.[34]

2.2.2 Polymer Monolith Preparation

First, a fused silica capillary with UV-transparent fluorinated hydrocarbon polymer (75 μm i.d., 375 μm o.d., Polymicro Technologies, Phoenix, AZ) was silanized using TMSPMA in order to anchor the polymer monolith on the capillary wall as previously described.[23] In this study, PEGDA was chosen as the only crosslinker because of its effectiveness in reducing non-specific adsorption of proteins on the monolith. Then the polymer precursor was prepared by mixing monomer, crosslinker, porogens, and initiator (see Table 2.1 for reagent compositions). The mixture was ultrasonicated for ~20 s considering the volatility of ethyl ether. Subsequently, the reaction mixture was introduced into the silanized capillary by capillary action, and irradiated using a UV curing system as previously reported.[22] After polymerization was complete, the monolithic column was connected to an LC pump and extensively flushed with methanol to remove the porogenic solvents and unreacted reagents. As mentioned in the introduction, DEAE functionalities could be introduced after polymerization of the rod of poly(GMA-co-PEGDA) by reaction of the epoxy groups with DEA. Typically, DEA was pumped through the column to completely "wet" the polymer first, and then the column was sealed at both ends by a closed loop filled with DEA, and heated at 55˚C for 12 h in an oven. Residual epoxy groups were blocked by washing the column with 1.0 M Tris buffer, pH 8.0. After preparation, both ends of the monolithic column were placed in water to keep the monolith wet. For reference, a DEA modified poly(GMA-co-EDMA) monolith was also prepared.

Monolithic columns were characterized by scanning electron microscopy (SEM, FEI Philips XL30 ESEM FEG, Hillsboro, OR). SEM images of the monolith inside the capillary provided information on the pore structure, i.e., approximate globule and pore

sizes. Monomer conversion is an important measurement used to evaluate polymerization efficiency. To measure monomer conversion, a bulk monolith was prepared under the same polymerization conditions as used to prepare the same monolith in a capillary except that the bulk monolith was prepared in a mold.[23] The monolith formed was Soxhlet extracted with methanol overnight, and then dried under vacuum at ~60˚C for 5 h. Monomer conversion was calculated by comparing the weight of polymer monolith to the weight of the total monomers.

2.2.3 Capillary Liquid Chromatography

Chromatographic separations were carried out using a system previously described.[22] It consisted of two syringe pumps (ISCO model 100 DM, ISCO, Lincoln, NE), a static mixer, a Valco splitting tee, and a Valco sample injector with an internal 60-nL loop (Valco, Houston, TX). The mobile phases in the two pumps were 10 mM Tris buffer, pH 7.6 (buffer A), and sodium chloride plus buffer A (buffer B), respectively. The splitter had a 33-cm fused-silica capillary (30 μm i.d., 375 μm o.d.) connected to its third outlet to provide a ~1:1000 split ratio between the analytical column and waste. Flow rates were measured at the exits of the column and the splitter capillary using empty Hamilton syringes (Hamilton, Reno, NV). Both pumps were operated in the constant flow mode to deliver the desired gradient program, and they were set to deliver solvents at a constant flow rate in the range of 70-200 nL/min. Standard proteins dissolved in buffer A were used for testing these monolithic columns. On-line UV detection at 214 nm was used. The chromatographic conditions are given in the figure captions.

To investigate the permeability of these monolithic columns, pressure drop measurements were made at room temperature (~23˚C) using pure water as the permeating

fluid at flow rates ranging from 50 to 200 nL/min. Each column pressure was obtained by subtracting the system pressure from the measured value on the read-out display.

2.2.4 Dynamic Binding Capacity and Mass Recovery Measurements

Dynamic binding capacity (DBC) is one of the most important properties of an ion-exchange column, which determines the resolution, column loadability, and gradient elution strength. The DBC was examined via open-loop frontal analysis.[35] Specifically, the monolithic column was first equilibrated with buffer A, and then a solution of 3.0 mg/mL BSA in buffer A that had been preloaded in a sample loop (~3 m long, 320 μm i.d.) was pumped through the monolithic column (~10 cm long, 75 μm i.d.) at a flow rate of 150 nL/min. One end of the sample loop was connected to the pump and the other end was connected to the column using a True ZDV Union (Upchurch Scientific, Oak Harbor, WA). The volume of protein solution needed to saturate the column was measured by a breakthrough curve which could be recorded directly by monitoring the UV absorbance. Protein mass recovery was determined by a direct comparison of the protein peak areas obtained with and without the analytical column as described previously.[36]

2.2.5 Safety Considerations

The GMA, DEAEMA and AETAC monomers, and the PEGDA and EDMA crosslinkers may act as sensitizers. Additionally, DEA is a severe eye and respiratory tract irritant. Relative MSDS information about these reagents should be consulted and special care should be taken for handling these reagents. Caution must be taken (such as wearing glasses and gloves) during polymerization steps, since high power UV radiation can cause severe burns to skin and eyes.

2.3 Results and Discussion

2.3.1 Polymer Monolith Preparation

Various monomers (DEAEMA, AETAC and GMA) containing anion-exchange groups or reactive groups were selected for co-polymerization with the biocompatible crosslinker, PEGDA. Usually, good solvents serve as microporogens to provide high surface area, while poor solvents act like macroporogens to provide good bulk flow properties. Whether a solvent is good or poor mostly depends on its relative polarity compared to the polymer. Polymerization conditions optimized for one system cannot be transferred directly to another since different monomers with different polarities are involved.

The reference monolith poly(GMA-co-EDMA) reported by Svec et al. was chosen as a starting point.[12,13] This monolith was prepared in a mixture of cyclohexanol (microporogen) and dodecanol (macroporogen) by thermally initiated polymerization. The ratio of monomer to crosslinker was fixed at 3:2 (Table 2.1). When replacing EDMA with PEGDA as crosslinker, methanol was selected as the macroporogen instead of dodecanol since it was proven efficient for the formation of macroporous throughpores in a poly(PEGDA) monolith. As a result, the new poly(GMA-co-PEGDA) monolith could be formed in 10 min using photoinitiated polymerization instead of thermally initiated polymerization. Compared to the poly(GMA-co-EDMA) monolith (Figure 2.2A), an SEM image of the modified poly(GMA-co-PEGDA) monolith inside a capillary (Figure 2.2B) showed a similar porous structure and somewhat larger globule (~2 μm) and pore sizes (~3 μm), Ethyl ether was found to be another effective porogen for synthesizing monoliths from PEG-based monomers. With optimized combination of methanol and ethyl ether as

Table 2.1. Reagent composition of several monoliths used in this study.

Monolith	Reagent composition							UV Time (min)
	DMPA (g)	Monomer (g)	PEGDA (g)	Cyclo-hexanol (g)	Methanol (g)	Ethyl Ether (g)	Hex-anes (g)	
GMA[a]	0.01[a]	0.48	0.32[a]	1.1	0.10[a]	/	/	/[a]
GMA	0.008	0.48	0.32	1.1	0.1	/	/	10
DEAEMA	0.008	0.48	0.32	/	/	/	0.4	10
AETAC	0.0008	0.4	0.48	/	0.9	0.9	/	5

[a] Poly(GMA-co-EDMA) was prepared as a reference material; 0.01 g AIBN was used as initiator, 0.10 g dodecanol was used as co-porogen, and 22 h heat exposure was applied[12,13].

Table 2.2. Physical properties of several monoliths used in this study.

Monolith	Physical properties[b]				
	DBC (mg/mL)	Recovery (%)	Monomer convsn (wt%)	Permeability ($\times 10^{-14} m^{2}$)	Porosity (%)
GMA[a]	36±2	89±2	-	1.1±0.1	63
GMA	32±3	102±3	83±3	1.9±0.1	69
DEAEMA	24±2	98±3	48±2	6.2±0.2	82
AETAC	56±4	100±2	100±4	1.0±0.2	59

[a]As described in Table 2.1. [b]The physical properties are reported as mean±standard deviation and caculations were based on 95% confidence level, n = 3.

porogens, a poly(AETAC-co-PEGDA) monolith was formed as shown in Figure 2.2D. However, in this polymerization system, methanol was a microporogen, while ethyl ether was a macroporogen. Absence of ethylether or excess methanol led to a glassy, transparent structure. A favorable mass ratio (i.e., 2:3) of AETAC to PEGDA was found for this monolithic column. This polymerization reaction was so fast that only 0.0008 g (~0.03 wt. %) DMPA was enough for initiating the reaction.

Unfortunately, neither methanol nor ethyl ether, nor other combinations of common solvents were successful in producing flow-through poly(DEAEMA-co-PEGDA) monoliths. A flow-through monolith was finally formed using a single porogen, hexanes. There are two possible reasons for this result. One is that most polar solvents cannot be used because they are such good microporogens that poor flow-through monoliths are produced even in the presence of a macroporogen. The second reason is that unreacted monomers can serve in part as microporogens since they are relatively good solvents for the polymer compared to the macroporogen. The application of a single macroporogen was also in agreement with the SEM image of poly(DEAEMA-co-PEGDA) (see Figure 2.2C), which demonstrated large globule (~3.6 μm) and pore sizes (~5 μm) and, consequently, much higher permeability (Table 2.2).

From these images, it can be immediately seen that poly(GMA-co-PEGDA) and poly(DEAEMA-co-PEGDA) have structures that are similar to poly(GMA-co-EDMA) reported earlier, i.e., clusters of congregated irregular micro-globules with voids between them (pores). However, the morphology of the poly(AETAC-co-PEGDA) monolith was very different from the others, but quite similar to the SCX poly(vinylsulfonic acid-co-PEGDA) monolith synthesized previously,[23] i.e., a labyrinth of tortuous cavities of

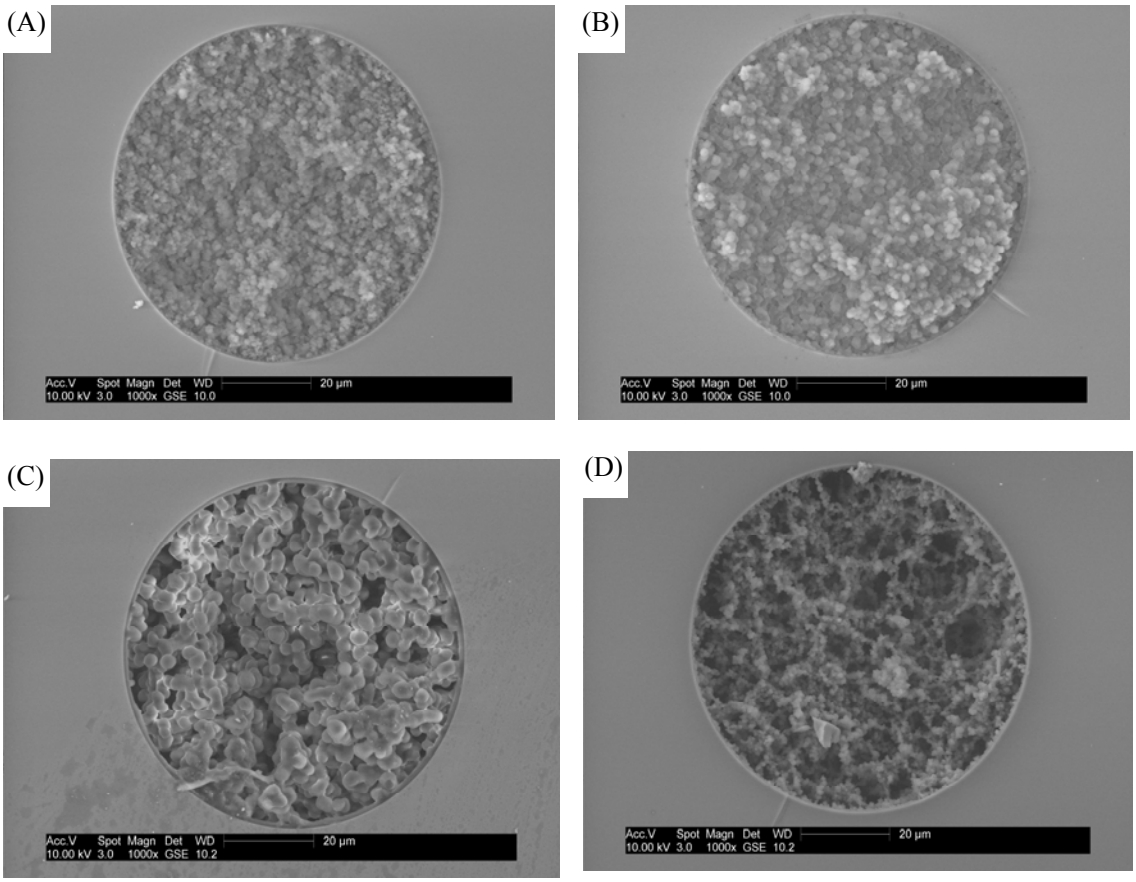

Figure 2.2. SEM photographs of (A) DEA modified poly(GMA-co-EDMA); (B) DEA modified poly(GMA-co-PEGDA); (C) poly(DEAEMA-co-PEGDA); (D) poly(AETAC-co-PEGDA).

different sizes formed by aggregated chains of particles.

2.3.2 Biocompatibility

In two previous papers, clean fluorescence images obtained after flushing PEGDA-based monoliths with fluorescein isothiocyanate (FITC)-labeled BSA were demonstrated to show negligible nonspecific adsorption of proteins.[32] Furthermore, the hydrophobicities of the monoliths were compared under reversed-phase chromatography conditions, yielding retention factors of almost zero for the poly(PEGDA) monolith and 4.4 for the poly(EDMA) monolith.[23] To further evaluate non-specific protein adsorption, protein mass recoveries were examined. A recovery of more than 98% of protein STI was obtained using monoliths incorporating PEGDA as crosslinker, compared to a recovery of 89% when using modified poly(GMA-co-EDMA) (Table 2.2). These tests indicate that polymer monoliths that incorporate PEGDA as crosslinker are more biocompatible.

2.3.3 Chromatographic Performance

The anion-exchange monoliths reported in this study demonstrated efficient separations of proteins of varying molecular weights and pI values. The modified poly(GMA-co-PEGDA) monolith was able to separate OVA, BSA, and STI, which differ by as little as ~0.1 pI value (Figure 2.3A). In isoelectric focusing (IEF), conalbumin separates into 3 major components with pI values of 6.2, 6.6 and 7.2, representing different metalloforms (diferric, monoferric and ion-free, respectively). Similarly, the WAX poly(DEAEMA-co-PEGDA) monolith showed similar separation of conalbumin (Figure 2.3B), which indicates its potential for separating protein isoforms or variants. Compared to other monoliths, faster separation of standard proteins was achieved using the poly(DEAEMA-co-PEGDA) monolith due to a much lower back pressure (data not

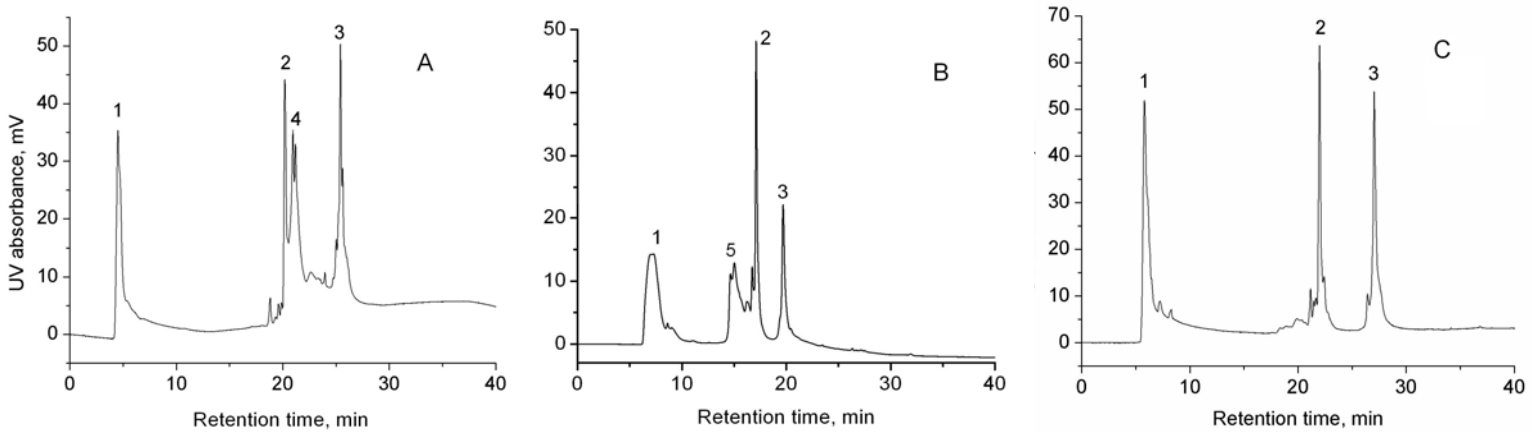

Figure 2.3. Anion-exchange chromatography of standard proteins. Conditions: (A) 75 µm i.d. × 13 cm DEA modified poly(GMA-co-PEGDA), (B) 75 µm i.d. × 16 cm poly(DEAEMA-co-PEGDA), and (C) 75 µm i.d. × 17 cm poly(AETAC-co-PEGDA) monolithic columns; (A) 20 min linear gradient from 0 to 1.0 M NaCl (50 mM/min) in buffer A, (B) 30 min linear gradient from 0 to 0.5 M NaCl (17 mM/min) in buffer A, and (C) 30 min linear gradient from 0 to 1.0 M NaCl (33 mM/min) in buffer A; UV detection at 214 nm; Peak identifications: 1. MYO, 2. OVA, 3. STI, 4. BSA, 5. CON.

shown). The SAX poly(AETAC-co-PEGDA) monolith also demonstrated good separation of standard proteins, MYO, OVA and STI (Figure 2.3C). Both poly(GMA-co-PEGDA) and poly(AETAC-co-PEGDA) afforded higher retention and resolution compared to poly(DEAEMA-co-PEGDA) even under stronger elution strength, which was presumably due to their higher binding capacities for proteins. Furthermore, poly(AETAC-co-PEGDA) provided better protein separations due to a higher peak capacity of 58 compared to peak capacities of 34 and 36 for poly(DEAEMA-co-PEGDA) and poly(GMA-co-PEGDA), respectively.

2.3.4 Dynamic Binding Capacity

Using frontal analysis, the DBC values for the two WAX poly(GMA-co-PEGDA) and poly(DEAEMA-co-PEGDA) monoliths, and one SAX poly(AETAC-co-PEGDA) monolith were measured as 32±3, 24±2 and 56±4 mg/mL of column volume, respectively. These data are comparable or superior to the DBC values that have been reported for various monoliths (Table 2.3). The DBC of the modified poly(GMA-co-EDMA) monolith developed by Svec et al. was 35 mg/mL.[12] Hahn et al. reported BSA binding capacities in the range of 20-30 mg/mL on CIM-DEAE disks from BIA Separations, which were presumably fabricated from ~1 μm diameter particles.[37] My results are also much higher than the DBC of 14 mg/mL reported for a PEI modified weak ion-exchanger based on a poly(GMA-co-EDMA) monolith,[14] or 6-12 mg/mL that was reported for pDMAEMA-grafted pAAm cryogels.[19] For SAX monoliths, Iberer et al. reported a BSA DBC of ~30 mg/mL for a BIA CIM-QA Disk and ~40 mg/mL for a Bio-Rad UNO-Q monolith,[38] which are lower than the value of 56±4 mg/mL for poly(AETAC-co-PEGDA).

Table 2.3. Comparison of DBCs of various anion-exchangers.

WAX media	Data source	DBC (mg/mL)	SAX media	Data source	DBC (mg/mL)
DEAE-GMA-PEGDA	This work	32±3	AETAC-PEGDA	This work	56±4
DEAEMA-PEGDA	This work	24±2	BIA CIM-QA	[38]	30
DEAE-GMA-EDMA	[12]	35	Bio-Rad UNO-Q	[38]	40
BIA CIM-DEAE	[37]	20-30	TSK-Gel Q-5PW-HR	[40]	42
PEI-GMA-EDMA	[14]	14	Q Sepharose FF	[40]	54
DMAEMA-pAAm cryogels	[19]	6-12	Q HyperD 20	[40]	85
Toyopearl DEAE 650M, MacroPrep DEAE	[39]	20, 16			
DEAE Sepharose FF, DEAE Ceramic HyperD 20	[39]	59, 76			

The DBC values of 24±2 and 32±3 mg/mL for the WAX monoliths in this work are superior to those measured for some commercial anion-exchange resins (e.g., 20 mg/mL and 16 mg/mL for Toyopearl DEAE 650M and MacroPrep DEAE Support, respectively), but lower than 59 mg/mL and 76 mg/mL for DEAE Sepharose FF and DEAE Ceramic HyperD 20, respectively.[39] The DBC value of 56±4 mg/mL for the SAX monolith is superior to 42 mg/mL and 54 mg/mL for TSK-Gel Q-5PW-HR and Q Sepharose FF, respectively, but lower than 85 mg/mL for Q HyperD 20.[40] The lower values could be due to less solid phase in the column. For particulate chromatographic media, the total mass of solid is approximately 2~3 times that of a highly porous monolith.[41] The good DBCs of these monoliths are attributed, in part, to their high-through pore structures that afford good pore accessibility by proteins. A high incorporation of functional monomer could also contribute to high DBC.

The sharpness of the breakthrough curve is indicative of the efficiency of mass transfer within the pores of the separation media. As shown in Figure 2.4, all three new anion-exchange monolithic columns achieved very steep breakthrough slopes (b, c, and d) and, hence, highly efficient binding of proteins that provides efficient peaks and high resolution. This is attributed to decreased non-specific interaction of proteins with the monolith backbone when using PEGDA as crosslinker.

2.3.5 Column Characterization

Run-to-run and column-to-column reproducibilities of the three new monoliths were investigated (Table 2.4). For three consecutive runs, the percent relative standard deviations (RSD%) of the retention times of OVA and STI were less than 1.4%, 1.2%, and 2.0% for the modified poly(GMA-co-PEGDA), poly(DEAEMA-co-PEGDA) and

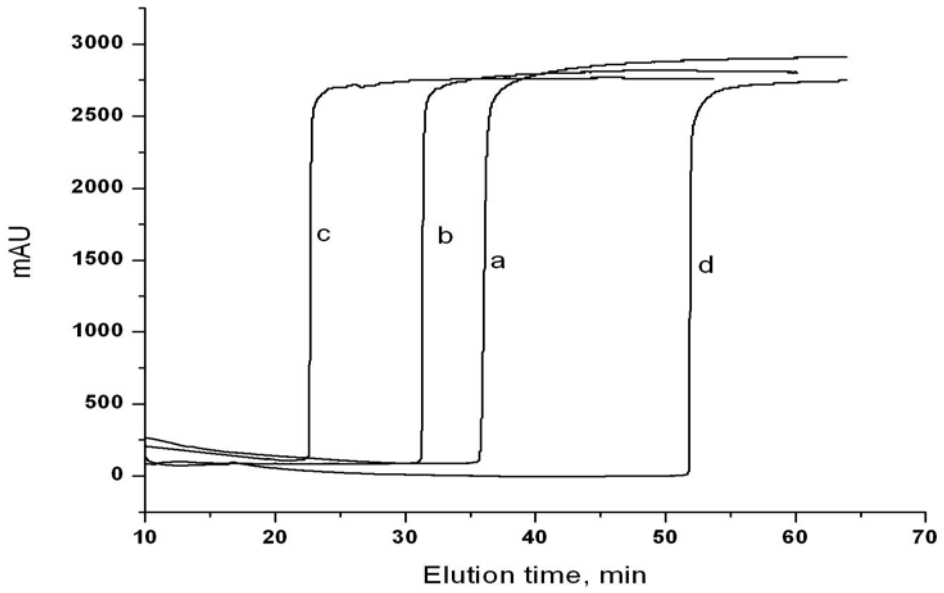

Figure 2.4. Breakthrough curves obtained by fontal analysis. Conditions: 75 μm i.d. × 10 cm (a) DEA modified poly(GMA-co-EDMA), (b) DEA modified poly(GMA-co-PEGDA), (c) poly(DEAEMA-co-PEGDA), and (d) poly(AETAC-co-PEGDA) monolithic columns, 3.0 mg/mL BSA in buffer A as loading phase; 0.15 μL/min; UV detection at 214 nm.

poly(AETAC-co-PEGDA) monoliths, respectively, which indicates that reproducible separations can be achieved using these monolithic capillary columns. Column-to-column reproducibility measurements gave retention time RSD% values (n = 3) ranging from 1.7 to 3.8%. Additionally, these monolithic capillary columns were stable during continuous use for at least two months with constant back pressure. Of course, this is dependent on good attachment of the monolith to the capillary wall and keeping the monolith filled with buffer solution.

Permeability represents the ease or difficulty of mobile phase flow through a chromatographic column. Pure water was pumped through the monoliths to measure their permeabilities since only aqueous buffers were used as mobile phases in this work. Good linearity between pressure drop and flow rate clearly demonstrated that the monoliths were mechanically stable at pressures up to 3000 psi. Calculated permeabilities according to Darcy's Law are listed in Table 2.2.[42] The permeability of the poly(GMA-co-EDMA) monolith was 1.1×10^{-14} m^2, which is in good agreement with a commercial CIM DEAE disk monolithic column from BIA Separations.[43] The poly(GMA-co-PEGDA) monolith, and especially the poly(DEAEMA-co-PEGDA) monolith, gave even higher permeabilities due to larger globule and pore sizes. A ~5 fold increase in permeability makes fast separations using the poly(DEAEMA-co-PEGDA) monolith possible. In addition, since these three monoliths share similar pore structures, their permeabilities did increase with increase in globule and pore sizes (Figure 2.2). Furthermore, as shown in Figure 2.5, a linear dependency of flow rate on back pressure for poly(AETAC-co-PEGDA) and poly(DEAEMA-co-PEGDA) monoliths was also achieved using different pH aqueous Tris buffers (pH = 7.0, 8.0 and 9.0), which reveals minimal swelling of these

Table 2.4. Reproducibilities of the new monolithic columns.[a]

Reproducibilities	Run-to-run (RSD% of retention time)		Column-to-column (RSD% of retention time)	
	OVA	STI	OVA	STI
Poly(GMA-co-PEGDA)	0.9	1.4	2.0	2.9
Poly(DEAEMA-co-PEGDA)	0.3	1.2	1.7	2.3
Poly(AETAC-co-PEGDA)	2.0	0.9	3.8	3.0

[a] For LC conditions, see Figure 2.3.

functional monoliths in aqueous buffers within this pH range. Increasing the pH from 7.0 to 9.0 increased the permeability of these functional monoliths. This observation is consistent with reported data and is probably a consequence of the lower association of anion-exchange groups.[44] The monomer conversions of these monoliths were relatively high, except for poly(DEAEMA-co-PEGDA) which gave 48% monomer conversion (Table 2.2). This is likely due to poor copolymerization resulting from unfavorable monomer reactivity ratio. Such a low monomer conversion may be responsible for its relatively low DBC (24±2 mg/mL), and probably its high permeability.

Using inverse size-exclusion chromatography (ISEC), total porosities were estimated from retention volumes of an unretained molecular tracer (uracil, MW = 112 g/mol) and the geometrical volumes of the columns.[45] The porosity does not seem to be directly related to permeability. A high porosity combined with relatively large volumetric through-pore fraction yields monolithic columns with high permeability. Unfortunately, the PEGDA-based monoliths usually crack or deform during drying, which likely changes the original pore structure. Because of this, mercury intrusion porosimetry was abandoned for investigating the pore properties in this work.

2.3.6 Application

SAX chromatography of the total protein fraction from a lysate of the host E. coli DH5α was achieved using a poly(AETAC-co-PEGDA) monolith (Figure 2.6). Although these peaks were not identified, the separation power of the monolithic column was demonstrated. Of course, only acidic proteins could be separated using this column. The baseline drift was mostly due to the presence of a large amount of cellular material other than proteins in the sample, such as RNA and DNA.

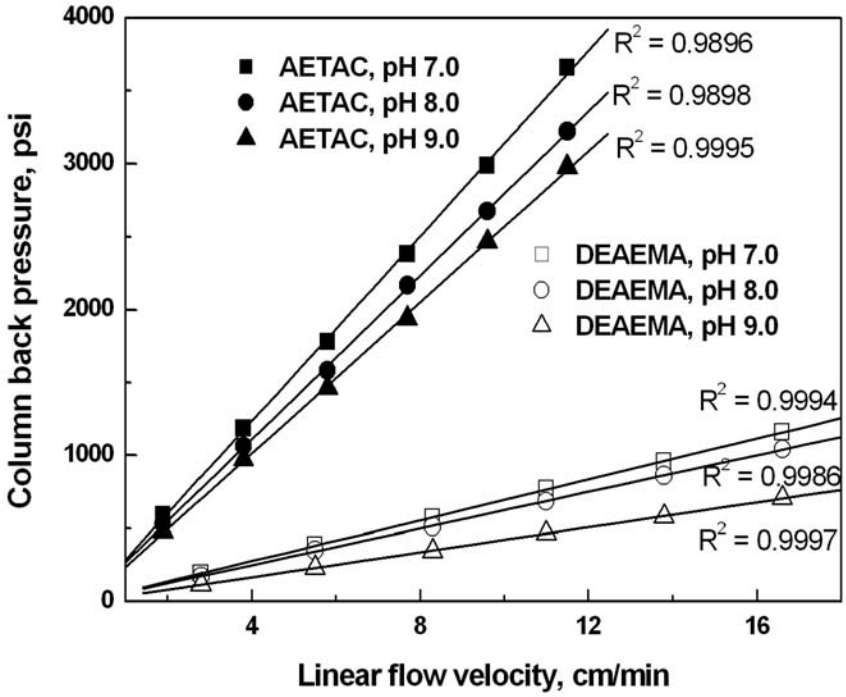

Figure 2.5. Backpressure dependency on linear velocity for the AETAC and DEAEMA functionalized monoliths. Conditions: 15 cm × 75 μm i.d. monolithic columns; 20 mM Tris buffer with pH 7.0, 8.0 and 9.0. Only one measurement for each column was made.

2.4 Conclusions

Two porous monolithic columns were prepared by direct copolymerization of functional monomers with a biocompatible crosslinker, PEGDA, in 75 μm i.d. capillaries in the presence of suitable porogens. They were then evaluated as stationary phases in anion-exchange capillary LC of proteins. The resulting poly(DEAEMA-co-PEGDA) and poly(AETAC-co-PEGDA) monoliths contain DEAE and QA functionalities that are required for WAX and SAX chromatography, respectively. Even without additional surface functionalization, these monoliths produced comparable chromatographic efficiencies and resolution for standard proteins compared to most anion-exchange monoliths reported previously. Compared to the more common poly(GMA-co-EDMA) monolith, the poly(GMA-co-PEGDA) and poly(DEAEMA-co-PEGDA) monoliths were synthesized faster by photoinitiated polymerization (10 min), provided comparable DBC, demonstrated faster kinetic adsorption of proteins, and provided higher permeability. The SAX poly(AETAC-co-PEGDA) monolith provided partial separation of a complex protein mixture, mostly due to its superior binding capacity and separation efficiency.

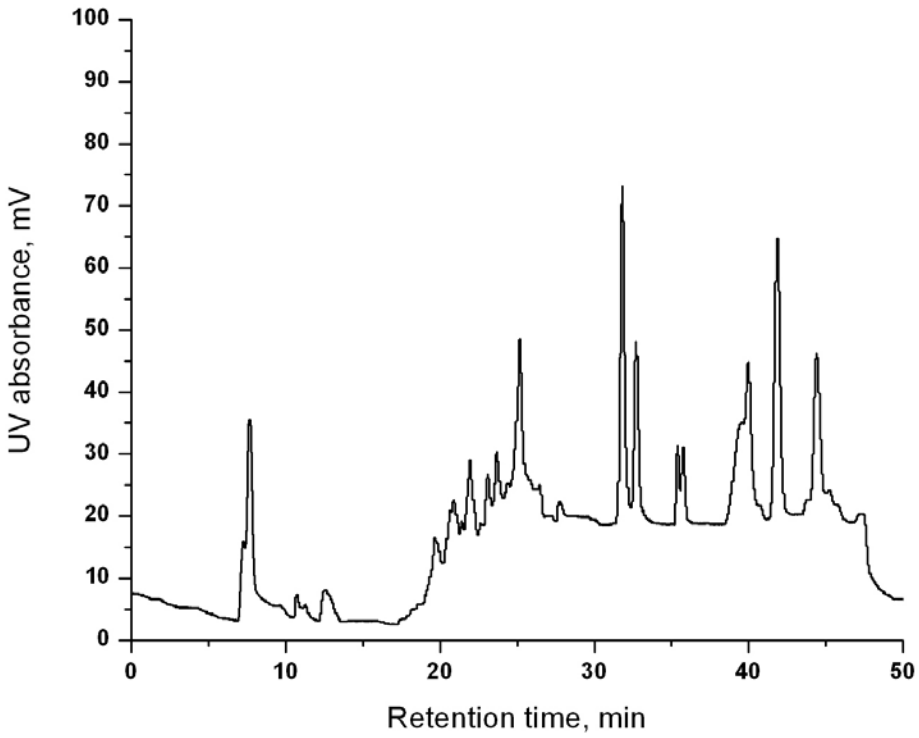

Figure 2.6. Strong anion-exchange (SAX) chromatography of total protein lysate of *E. coli* DH5α. Conditions: 75 μm i.d. × 18 cm poly(AETAC-co-PEGDA) monolithic column; buffer A was 20 mM Tris (pH 7.6) and buffer B was buffer A plus 0.5 M NaCl, linear AB gradient from 2 to 98% B in 30 min, and held for 5 min; 100 nL/min flow rate; 1.0 mg/mL analyte concentration; UV detection at 214 nm.

2.5 References

1. Henry, M. P. In *LC of Macromolecules: A Practical Approach*; Oliver, R. W. A., Ed.; IRL Press at Oxford University Press: Oxford, 1989; pp 91-125.
2. Stanton, P. In *LC of Peptides and Proteins: Methods and Protocols*; Aguilar, M. -I., Ed.; Humana Press: Totowa, NJ, 2004; pp 23-43.
3. Chang, S. H.; Noel, R.; Regnier, F. E. *Anal. Chem.* **1976**, *48*, 1839-1845.
4. Horvath, J.; Boschetti, E.; Guerrier, L.; Cooke, N. *J. Chromatogr. A* **1994**, *679*, 11-12.
5. Boschetti, E. *J. Chromatogr. A* **1994**, *658*, 207-236.
6. Josić, D.; Reusch, J. *J. Chromatogr.* **1992**, *590*, 59-76.
7. Alpert, A. J.; Regnier, F. E. *J. Chromatogr.* **1979**, *185*, 375-392.
8. Rounds, M. A.; Rounds, W. D.; Regnier, F. E. *J. Chromatogr.* **1987**, *397*, 25-38.
9. Marlin, N. D.; Smith, N. W. *Anal. Bioanal. Chem.* **2005**, *382*, 493-497.
10. Premstaller, A.; Oberacher, H.; Huber, C. G. *Anal. Chem.* **2000**, *72*, 4386-4393.
11. Armenta, J. M.; Gu, B.; Humble, P. H.; Thulin, C. D.; Lee, M. L. *J. Chromatogr. A* 2005, 1097, 171-178.
12. Svec, F.; Fréchet, J. M. J. *Biotechnol. Bioeng.* **1995**, *48*, 476-480.
13. Sykora, D.; Svec, F.; Fréchet, J. M. J. *J. Chromatogr. A* **1999**, *852*, 297-304.
14. Wang, M.; Xu, J.; Zhou, X.; Tan, T. *J. Chromatogr. A* **2007**, *1147*, 24-29.
15. Koguma, I.; Sugita, K.; Saito, K.; Sugo, T. *Biotechnol. Prog.* **2000**, *16*, 456-461.
16. Bisjak, C. P.; Bakry, R.; Huck, C. W.; Bonn, G. K. *Chromatographia* **2005**, *62*, S31-S36.

17. Wieder, W.; Bisjak, C. P.; Bakry, R.; Huck, C. W.; Bonn, G. K. *J. Sep. Sci.* **2006**, *29*, 2478-2484.

18. Hilder, E. F.; Svec, F.; Fréchet, J. M. J. *J. Chromatogr. A* **2004**, *1053*, 101-106.

19. Savina, I. N.; Galaev, I. Y.; Mattiasson, B. *J. Mol. Recognit.* **2006**, *19*, 313-321.

20. Tripp, J. A.; Svec, F.; Fréchet, J. M. J.; Zeng, S.; Mikkelsen, J. C.; Santiago, J. G. *Sens. Actuators, B* **2004**, *99*, 66-73.

21. Frankovič, V.; Podgornik, A.; Krajnc, N. L.; Smrekar, F.; Krajnc, P.; Štrancar, A. *J. Chromatogr. A* **2008**, *1207*, 84-93.

22. Gu, B.; Chen, Z.; Thulin, C. D.; Lee, M. L. *Anal. Chem.* **2006**, *78*, 3509-3518.

23. Gu, B.; Li, Y.; Lee, M. L. *Anal. Chem.* **2007**, *79*, 5848-5855.

24. Viklund, C.; Svec, F.; Fréchet, J. M. J.; Irgum, K. *Biotechnol. Prog.* **1997**, *13*, 597-600.

25. Okay, O. *Progr. Polym. Sci.* **2000**, *25*, 711-779.

26. Courtois, J.; Byström, E.; Irgum, K. *Polymer*, **2006**, *47*, 2603-2611.

27. Calmon, C. *React. Polym.* **1982**, *1*, 3-19.

28. Andrade, J. D.; Hlady, V. *Adv. Polym. Sci.* **1986**, *79*, 1-63.

29. Harris, J. M.; Zalipsky, S. *Poly(ethylene glycol): Chemistry and Biological Applications*, ACS Symposium Series 680; American Chemical Society: Washington, D.C., 1997.

30. Su, Y. H.; Gomboltz, W. R. *Polym. Prep.* **1987**, *28*, 292-294.

31. Lee, S. W.; Laibinis, P. E. *Biomaterials* **1998**, *19*, 1669-1675.

32. Gu, B.; Armenta, J. M. Lee, M. L. *J. Chromatogr. A* **2005**, *1079*, 382-391.

33. Krenkova, J.; Lacher, N. A.; Svec, F. *Anal. Chem.* **2009**, *81*, 2004-2012.

34. Lee, P. S.; Lee, K. H. *Biotechnol. Bioeng.* **2003**, *84*, 801-814.

35. Jacobson, J.; Frenz, J.; Horváth, C. *J. Chromatogr.* **1984**, *316*, 53-68.

36. Yang, Y.; Harrison, K.; Kindsvater, J. *J. Chromatogr. A* **1996**, *723*, 1-10.

37. Hahn, R.; Panzer, M.; Hansen, E.; Mollerup, J.; Jungbauer, A. *Sep. Sci. Technol.* **2002**, *37*, 1545-1565.

38. Iberer, G.; Hahn, R. Jungbauer, A. *LC GC* **1999**, *17*, 998-1005.

39. Staby, A.; Jensen, R. H.; Bensch, M.; Hubbuch, J.; Dünweber, D. L.; Krarup, J.; Nielsen, J.; Lund, M.; Kidal, S.; Hansen, T. B.; Jensen, I. H. *J. Chromatogr. A* 2007, 1164, 82-94.

40. Staby, A.; Jensen, I. H.; Mollerup, I. *J. Chromatogr. A* **2000,** *897*, 99-111.

41. Leinweber, F. C.; Tallarek, U. *J. Chromatogr. A* **2003**, *1006*, 207-228.

42. Darcy, H. In *Physical Hydrology*; Freeze, R. A.; Back, W., Ed.; Hutchinson Ross: Stroudsburg, PA, 1983.

43. Mihelič, I.; Nemec, D.; Podgornik, A.; Koloini, T. *J. Chromatogr. A* **2005**, *1065*, 59-67.

44. Kontturi, K.; Mafé, S.; Manzanares, J. A.; Svarfvar, B. L.; Viinikka, P. *Macromolecules* **1996**, *29*, 5740-5746.

45. Al-Bokari, M.; Cherrak, D.; Guiochon, G. *J. Chromatogr. A* **2002**, *975*, 275-284.

CHAPTER 3 PREPARATION OF POLYMER MONOLITHS THAT EXHIBIT SIZE EXCLUSION PROPERTIES FOR PROTEINS AND PEPTIDES

3.1 Introduction

Size exclusion chromatography (SEC), also known as gel filtration chromatography, has long been one of the most widely used techniques for the separation and purification of biological macromolecules, especially proteins.[1-3] The separation is based exclusively on the hydrodynamic sizes of the molecules. Consequently, an ideal size-exclusion medium for protein (or peptide) separation should have no interaction with the analytes, and it must have sufficient pore volume and pore size distribution to resolve the molecular weight range of proteins (or peptides).[4] A soft gel medium (typically polyacrylamide, dextran or agarose) has conventionally been used at low pressure. To be applicable in high-performance liquid chromatography (HPLC), additional stationary phase requirements of rigidity and stability must be met. In this respect, columns packed with hydrophilic bonded silica or highly crosslinked polymeric particles are typically used for SEC separation of proteins or peptides in aqueous solution.[5,6] Commercially available SEC columns from analytical to preparative scale typically have pore sizes ranging from 120 to 500 Å.[7] Even capillary SEC was demonstrated in the early years of microcolumn separations.[8,9] Compared to conventional SEC, capillary SEC offers several advantages, such as low eluent consumption, ease of interfacing with a mass spectrometer, and ability to prepare long columns. In addition, they have achieved more efficient separations than conventional columns after optimization.[10] However, care must be taken to minimize dead

volume in the capillary LC system, since the capillary column bed is only a few microliters in total volume.[11]

A monolithic column structure would be advantageous as an SEC stationary phase in view of its ease of preparation and low cost, as well as good stability.[12,13] To be suitable for the SEC of biopolymers, such as proteins, it must also be biocompatible, rigid, and have sufficient mesopore volume (i.e., pore diameters ranging from 2 to 50 nm). Although monoliths have been applied successfully in various chromatographic separation modes for proteins, such as reversed phase (RPC), ion exchange (IEC) and affinity chromatography,[14-16] no reports have described their use in aqueous SEC of proteins, mostly because of problems with non-specific adsorption of proteins and difficulty experienced in the synthesis of monoliths having a bimodal pore-size distribution, with one pore size in the macropore region (> 50 nm) and the other in the mesopore region (2-50 nm).

Generally, monoliths can be divided into two categories: silica and organic polymer. Silica monoliths are prepared by a sol-gel process with subsequent dissolution-precipitation, resulting in a bimodal pore structure, i.e., with macropores that provide mobile phase flow through the monolith and mesopores that provide chromatographic retention.[17,18] Inverse SEC experiments using polystyrene standards have confirmed the existence of a relatively large volume of mesopores (10-12%) with a proper size range for SEC.[19,20] However, the high degree of non-specific interactions between silanol groups and proteins limits its application for SEC separation of proteins. Organic polymer monoliths are prepared by in situ polymerization of monomers and crosslinkers in the presence of porogens and initiators. Using conventional one-step free-radical polymerization,

macopores and micropores (< 2 nm) are typically produced in the case of a binary or ternary porogenic mixture of poor and good solvents, respectively; however, few mesopores are observed.[21-23] Hence, the resulting polymer monoliths provide almost no separation in the size exclusion mode due to the absence of mesopores. Although great effort has been made to produce mesopores by systematically varying the composition of the polymerization mixture, resultant monoliths have not been able to provide efficient and selective SEC separation.[24]

Recently, attempts have been made to utilize new polymerization methods to synthesize polymer monoliths for SEC. A porous poly(styrene-co-divinylbenzene) (PSDVB) polymer prepared by stable free radical (SFR) mediated polymerization demonstrated marginal separation of a mixture of three polystyrene standards with MWs of 3 200 000, 210 500, and 580.[25] However, the inherent hydrophobic character of this hydrocarbon-based polymer prevents its use for SEC separation of proteins. In another report, a poly(cyclooctene)-based monolithic column was synthesized for SEC by ring-opening metathesis polymerization (ROMP).[26] The chromatograms of polystyrene standards in the range of MWs from 2 600 to 3 280 000 indicated insufficient mesopore volume. Furthermore, it was also too hydrophobic to be applied directly for aqueous SEC of proteins. Aoki et al. synthesized a poly(glycerol dimethacrylate)-based polymer monolith via viscoelastic phase separation that was induced by monodisperse ultra high MW poly(styrene) as a porogen.[27] Although BET and Hg intrusion measurements demonstrated a sharp bimodal pore distribution for the crushed monolith, the paper did not report the SEC performance of the monolith. While surface modifications of silica, polystyrene, and polycyclooctene-based monoliths could render them somewhat

hydrophilic,[28-30] it would be very challenging to mask the silanol or hydrophobic groups completely via on-column reactions so that they could effectively resist non-specific adsorption of proteins.

We recently reported the synthesis of a biocompatible monolithic material by polymerizing two PEG-based monomers in the presence of ethyl ether and methanol using one-step free radial polymerization.[31] The PEG monolith provided SEC separation of several peptides because of its 10.9% micropore volume; however, no separation of proteins was observed due to a minimal mesopore volume. Further attempts to create mesopores by optimizing some key parameters, such as the composition of the porogenic system and ratio of monomer to crosslinker, were not successful. Therefore, I have spent considerable time and effort searching for new methods to create mesopores within polymeric monoliths.

Surfactants were introduced some years ago as porogens to create small pores of defined size within a polymeric hydrogel or a polymer.[32-34] Using this approach, polymerization is conducted in the presence of high concentrations of specific macromolecules or surfactants, and then pores are generated by removing the porogenic reagents from the polymer. Differences in protein mobilities between gels prepared with sodium dodecyl sulfate (SDS) and their normal gel counterparts were observed in a manner consistent with the creation of approximately 5 nm pores.[32] These hydrogels demonstrated a network of internal pores that could be size selected independently of polymer and crosslinker concentrations.[33] Non-ionic surfactants with relatively large MWs were used to generate 6.7-10.8 nm pore sizes in the polymer matrix.[34]

Inverse size exclusion chromatography (ISEC) uses SEC measurements to characterize the pore structures of porous materials when the probe sizes are known.[35] In order to provide reliable results, there should be no adsorption of the probe compounds on the stationary phase, since pure size exclusion data are required. For silica or PSDVB-based matrices, a series of polystyrenes in tetrahydrofuran (THF) as mobile phase have been used for characterization.[19,20,36] Dextrans in NaCl-phosphate buffer have also been used to investigate pore size distribution of a set of cation-exchange adsorbents based on methacrylate, dextran-silica and agarose.[37] My PEG monolith can resist adsorption of proteins and peptides even when using an aqueous buffer without any organic solvent additives.[31] Thus, it is possible, in principle to use proteins and peptides as probe compounds and an aqueous solution as mobile phase for ISEC characterization of the PEG monoliths. I would expect to obtain a pore size distribution which corresponds to the chromatographic distribution of macromolecules in the SEC mode.

The objective of this study was to prepare monoliths for SEC separation of proteins (or peptides). Two main strategies were considered: first, poly(ethylene glycol) methyl ether acrylate (PEGMEA) and poly(ethylene glycol) diacrylate (PEGDA) (structures shown in Figure 3.1) were used as monomer and crosslinker, respectively, for a biocompatible stationary phase; second, non-ionic surfactants poly(propylene oxide)-block- poly(ethylene oxide)-block- poly(propylene oxide) (PPO-PEO-PPO, abbreviated as PEP) or PEO-PPO-PEO (abbreviated as EPE) were introduced as porogens to create a considerable portion of mesopores for size exclusion of proteins. These tri-block copolymers contained different lengths of PPO and PEO blocks, which yielded different MWs and slightly different polarities.[38] SEC monolithic columns were prepared in fused

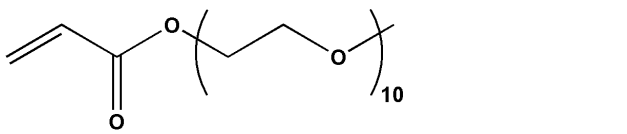

Poly(ethylene glycol) methyl ether acrylate

(PEGMEA, Mn 454)

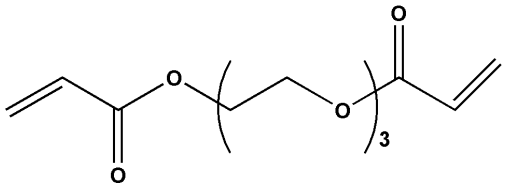

Poly(ethylene glycol) diacrylate

(PEGDA, Mn 258)

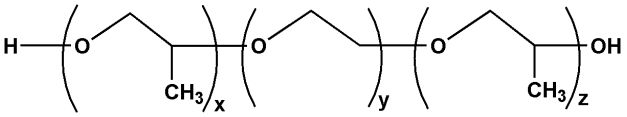

Poly(propylene oxide)-poly(ethylene oxide)-poly(propylene oxide)

(PPO-PEO-PPO) (PEP)

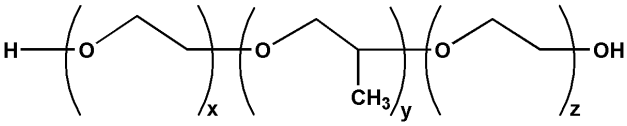

Poly(ethylene oxide)-poly(propylene oxide)-poly(ethylene oxide)

(PEO-PPO-PEO) (EPE)

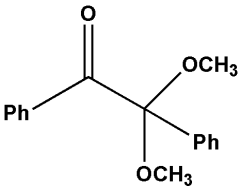

2,2-Dimethoxy-2-phenylacetophenone

(DMPA)

Figure 3.1. Structural formulas of reagents for synthesizing the monoliths.

silica capillary columns by photoinitiated polymerization and then evaluated for SEC separation of proteins and peptides.

3.2 Experimental Section

3.2.1 Chemicals and Reagents

PEGDA (Mn ~258), 3-(trimethoxysilyl)propyl methacrylate (TMSPMA, 98%), PEP (Mn ~2 700, 3 300) and EPE (Mn ~4 400, 5 800), and LC water (CHROMASOLV®) were purchased from Sigma-Aldrich (Milwaukee, WI). Anhydrous ethyl ether was obtained from Fisher Scientific (Fair Lawn, NJ). All of the monomers were used without further purification. Phosphate buffer solutions were prepared with LC water and filtered through a 0.22-μm membrane filter. Table 3.1 gives a list of the proteins and peptides used in the experiments. All proteins and peptides were purchased from Sigma-Aldrich, except lactate dehydrogenase (Calbiochem, San Diego, CA).

3.2.2 Polymer Monolith Preparation

First, fused silica capillaries clad with UV-transparent fluorinated hydrocarbon polymer (Polymicro Technologies, Phoenix, AZ) were silanized using TMSPMA in order to anchor the polymer monolith to the capillary wall as described previously.[39] Then the polymerization mixture for monolith M-1 (see Table 3.2) was prepared by dissolving 0.006 g DMPA in 2.0 g solution (0.3 wt. %) containing 0.15 g PEGMEA, 0.45 g PEGDA, and 1.4 g total porogen (0.6 g PEP and 0.8 g ethyl ether). Other monoliths (i.e., M-2 to M-8) were prepared by varying the ratios of total monomer/total porogen, or PEGMEA/PEGDA, or copolymer/PEP (EPE). Each reagent mixture was ultrasonicated for ~40 s considering the volatility of ethyl ether. Subsequently, the reaction mixture was introduced into the

silanized capillary by capillary action, and irradiated for 10 min using a UV curing system previously described.[31]

Monolithic columns were characterized by scanning electron microscopy (SEM, FEI Philips XL30 ESEM FEG, Hillsboro, OR). The morphologies of the monoliths were observed from the SEM images.

3.2.3 Size Exclusion Chromatography

After polymerization, the monolithic columns were connected to an LC pump and extensively washed with methanol to remove the porogenic solvents and unreacted reagents. The columns were equilibrated first with water and then with buffer. An Eksigent Nano 2D LC system (Dublin, CA) was used to conduct all chromatographic experiments with a K-2600 UV detector (Sonntek, Upper Saddle River, NJ). The detection cell was a 3-nL ULT-UZ-N10 from LC Packings (Sunnyvale, CA). The column was connected to the detection cell using a zero dead volume P-720 Union (Upchurch, Oak Harbor, WA), and the detection wavelength was 214 nm. The LC system for experiments consisted of two pumps and a six-port electronic valve as injector, controlled by the Eksigent v2.08 software. Standard proteins dissolved in buffer were used to evaluate the monolithic columns. The chromatographic conditions are given in the figure captions. In addition, a packed capillary (57 cm × 150 μm i.d.) was prepared and investigated for comparison. The packing material was removed from a commercial BioSep-SEC-4000 guard column purchased from Phenomenex (Torrance, CA). The specifications of the packing material were listed as: hydrophilic bonded silica, 5 μm particle size, 500 Å pore size, 15 000-2 000 000 Daltons exclusion range for native proteins.

Table 3.1. Proteins and peptides used in this study.

Proteins and peptides	Abbreviation	MW (Daltons)[a]	p*I*[b]	Diameter (nm)[c]	Source[a]
Thyroglobulin	TG	670 000	4.6	~15.7	Porcine thyroid gland
Catalase	CAT	250 000	6.7	~10.9	Bovine liver
Lactate dehydrogenase	LDH	143 000	8.5	~8.9	Rabbit muscle
Albumin	BSA	66 000	4.9	~6.7	Bovine serum
Ovalbumin	OVA	44 000	4.7	~5.8	Chicken egg white
Trypsin inhibitor	STI	20 100	4.5	~4.3	Soybean
Aprotinin	AP	6 500	10.5	~2.8	Bovine lung
β-Calcitonin Gene Related Peptide	βCGRP	3 793	---	---	Synthetic
Angiotensin I	ANG I	1 296	7.8	---	Synthetic
Leucine enkephalin	LE	555	5.9	---	---
Uracil	U	112	---	---	---

[a]As specified by suppliers. [b]From Ref. 28 and 43. [c]Based on the Stokes' radius calculated from log (Rs) = 0.369 log (MW) - 0.254.[44]

To investigate the permeability and rigidity of these monolithic columns, pressure drop measurements were made at room temperature (~23˚C) using pure water as the permeating fluid at flow rates ranging from 50 to 300 nL/min.

3.2.4 Inverse Size-Exclusion Chromatography

ISEC was carried out using the same LC instrument as described in section 3.2.3. ISEC experiments were performed with aqueous buffer as solvent. Protein and peptide standards with molecular weights of 555, 1 296, 3 793, 6 512, 20 100, 44 000, 68 000, 143 000 to 670 000 (listed in Table 3.1) were used as probe molecules and they were dissolved in 20 mM phosphate, pH 7.0. Uracil was used to determine the total accessible porosity of the column. Experiments were carried out with a flow rate of 100 nL/min and a sample injection volume of 60 nL. All experiments were repeated in triplicate and the mean values of the retention data were reported.

3.2.5 Safety Considerations

The PEGMEA and PEGDA monomers may act as sensitizers. Ethyl ether is extremely flammable. Relative MSDS information for these reagents should be consulted, and precautions should be taken for handling them. Additionally, caution must be taken (i.e., wearing glasses and gloves), since high power UV radiation can cause severe burns to skin and eyes.

3.3 Results and Discussion

The porosity of a polymeric monolith is primarily dictated by the nature and amount of porogenic solvent employed. The composition and proportion of monomers in the polymerization mixture are two other important parameters that influence porosity. In this study, I mainly investigated the influence of the surfactant as a porogenic solvent on

the SEC properties of the monolith, since the separation is directly influenced by the monolith porosity. The separation of BSA and TG was chosen as a model pair for investigation, which represents an order of magnitude difference in MWs (i.e., 66 000 and 670 000, corresponding to hydrodynamic sizes of 6.7 nm and 15.7 nm).

Generally, polymeric monoliths are designed to maximize the flow-through pore volume to increase column permeability, at the expense of mesopore volume. Polymeric monoliths that contain a considerable mesopore volume typically do not contain sufficient macropores to allow acceptable flow under low back pressure. To avoid high back pressure, a compromise was sought between good permeability and relatively large mesopore volume.

3.3.1 Effect of Surfactant as Porogen

Based on a previous PEG monolith M-0,[31] a total monomer/total porogen weight ratio of 60:140 and a PEGMEA/PEGDA weight ratio of 15:45 were initially selected. Methanol was replaced with a tri-block copolymer PEP (or EPE). The compositions in Table 3.2 were selected on the basis of experience gained in preliminary experiments. Photoinitiated polymerizations are typically carried out at room temperature; therefore, solvents with low boiling points, such as ethyl ether and methanol, can safely be used even in unsealed capillaries. Thermally initiated radical polymerizations are typically allowed to proceed for 6-24 h, whereas our photo-polymerizations were completed in only 10 min.

When ethyl ether was used as the only porogen for polymerization, a pure white monolith was obtained, suggesting that light was scattered by the large pores created with this formulation. In contrast, a monolith created using PEP or EPE as the only porogen provided opaque gels, suggesting that the gel was comprised of small, closed pores which

Table 3.2. Physical characteristics of SEC monoliths

Monolith	Reagent composition				Performance		
	Total monomer / total porogen	PEGMEA /PEGDA	Copolymer /ethyl ether	Copolymer Mn	Resolution[c] mean±SD	Efficiency[d] (plates/m) mean±SD	Permeability[e] ($\times 10^{-15}$ m^2) mean±SD
M-0	60/140	15/45	30/110	MeOH	na	na	14.6±0.5
M-1	60/140	15/45	60/80	2700[a]	0.52±0.02	39 100±900	5.8±0.4
M-2	60/140	15/45	70/70	2700[a]	0.61±0.03	48 900±1200	5.4±0.3
M-3	60/140	15/45	80/60	2700[a]	0.62±0.04	50 400±1400	3.9±0.2
M-4	60/140	15/45	70/70	3300[a]	0.53±0.02	43 000±1300	4.5±0.2
M-5	60/140	15/45	70/70	4400[b]	0.84±0.03	40 900±1000	4.0±0.2
M-6	60/140	15/45	70/70	5800[b]	0.73±0.01	22 500±700	3.5±0.1
M-7	60/140	36/24	70/70	4400[b]	0.64±0.02	48 400±1300	4.2±0.2
M-8	40/160	24/16	80/80	4400[b]	0.41±0.02	20 000±800	11.3±0.5

[a] PEP. [b]EPE. [c]As described in Figure 3.2. [d]Measured for uracil in an aqueous mobile phase at a flow rate of 0.1 µL/min. [e]Calculated according to Darcy's law.[45] [c,d,e]Calculations were based on 95% confidence level, n = 3. All ratios are weight ratios.

prevented flow. The combination of ethyl ether and PEP yielded a porous monolith that allowed constant flow. Monoliths prepared in 5-cm long UV transparent capillaries were used to study the relationship of pressure drop with the percent PEP in the porogenic system. The flow resistance of the monolith was found to increase with an increase in ratio of PEP to ethyl ether, which also indirectly confirms that ethyl ether produces large pores and the tri-block copolymer produces small pores. As seen in Figure 3.2A and Table 3.2, when increasing the PEP to EE ratio from 60:80 to 70:70 to 80:60 (M-1, M-2 and M-3), the resolution between BSA and TG increased, accompanied with a decrease in permeability. This is due to an increase in either mesopore volume or separation efficiency, or both.

Given that considerable differences in the pore structure can be obtained by varying the amount of copolymer, I were also interested in knowing if varying the molecular weight would have a similar effect. To examine this, tri-block copolymers with Mn values of 2 700, 3 300, 4 400, and 5 800 were combined with ethyl ether as porogens (see Table 3.2 and Figure 3.2B). The weight ratios of other reagents in the polymerization mixture were kept the same. As the molecular weight of the copolymer increased, the permeability and column efficiency of the monolith decreased. The resolution did not follow any trend since both large mesopore volume (related to low permeability, to some extent) and good column efficiency are needed for high resolution. For example, compared to M-5, the resolution of M-6 was lower due to the decreased plate numbers even though the mesopore volume was higher. Conversely, SEC columns of high plate numbers may not necessarily provide good resolution unless the mesopore volume is sufficient. According to these experiments, EPE 4 400 and an equivalent ratio of EPE to EE afford the best resolution.

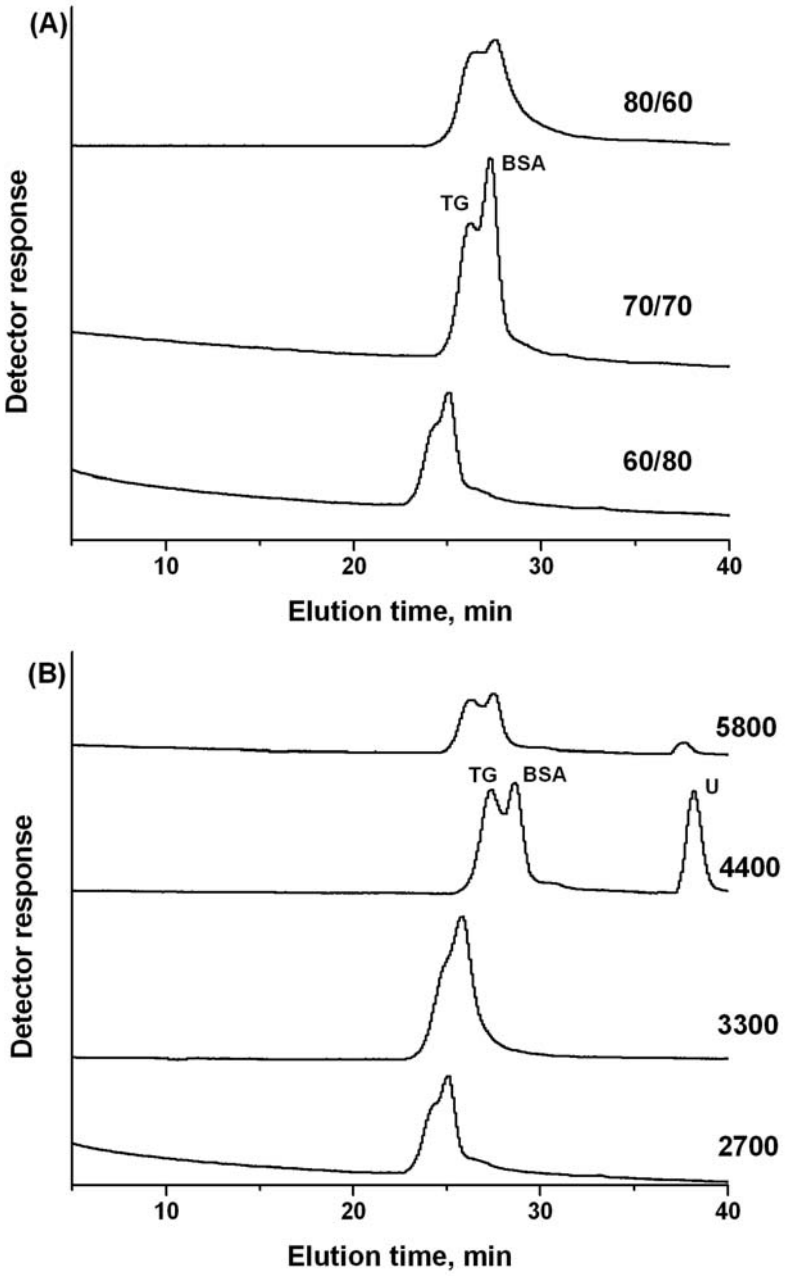

Figure 3.2. SEC separations on PEG monoliths synthesized with (A) different ratios of copolymer to EE (M-1, M-2 and M-3), and (B) different MWs of copolymer (M-2, M-4, M-5 and M-6). Conditions: 18 cm × 150 μm i.d. monolithic columns; 20 mM phosphate containing 0.15 M NaCl, 0.1 μL/min; 60 nL injection volume; UV detection at 214 nm.

3.3.2 Effect of Monomer Composition and Proportion

Decreasing the proportion of crosslinker (PEGDA) in the monomer mixture resulted in slightly increased efficiency and permeability but decreased resolution due to decreased mesopore volume (see M-7). Consequently, a high crosslinker/monomer ratio (3:1) is preferred for both better resolution and greater rigidity. This is consistent with reports that a high proportion of crosslinker in the monomer mixture decreases the average pore size by early formation of highly cross-linked globules with a reduced tendency to coalesce.[40] The experimental results imply that, in this case, the pore-size distribution is also controlled by limitations in swelling of cross-linked nuclei.

Decreasing the total monomer to total porogen ratio was a straightforward approach to increase the permeability (see M-8); however, the resolution was decreased mainly due to decreased column efficiency resulting from a decrease in the monolith homogeneity.

3.3.3 Morphology of PEG Monoliths

Figure 3.3 shows SEM images of M-0, M-1, M-2 and M-6 PEG monoliths prepared with various amounts and MWs of copolymers (see Table 3.2). In M-0, it appears that globules are clumped together, however, individual globules are clearly visible. In M-1 and M-2, the globules are more fused together and only a few individual globules can be seen in the photograph. In M-6, the globules are completely merged together and there is no evidence of individual globules. According to these observations, as the amount or MW of the tri-block copolymer increased, the morphology of the PEG monolith was transformed from an aggregated globule form to complete merging of fused globules. The fused-globule morphology was found to be less permeable than the aggregated-globule

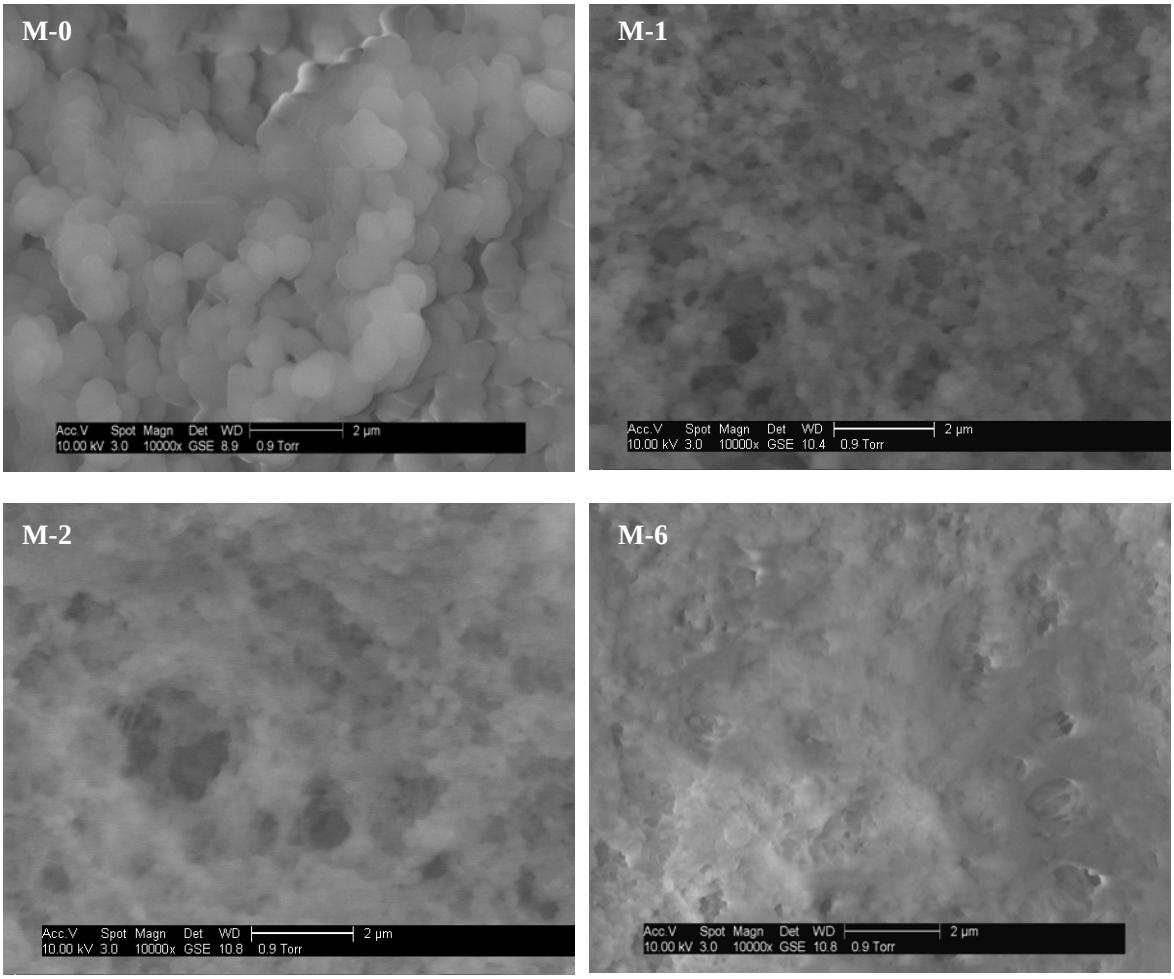

Figure 3.3. SEM images of M-0, M-1, M-2 and M-6 using a magnification of 10 000.

structure. Unfortunately, the PEGDA-based monoliths usually crack or deform during drying that likely change the original pore structure. Because of this, mercury intrusion porosimetry and BET measurements cannot be used for investigating the pore properties of these monoliths.

3.3.4 Effect of Column Diameter, Column Length and Flow Rate

As shown in Figure 3.4A, the 150-μm i.d. column provides better resolution than the 75-μm i.d. column, probably due to increased mesopore volume. However, further increase to 250-μm i.d. led to decreased resolution. There are two possible reasons for this result: first, the pore size distribution changed, since the pore structure had some dependence on the i.d. of the monolithic column;[41] and second, the monolithic matrix in the large diameter column may be less uniform. Free-radical polymerization used for the preparation of porous polymer monoliths is an exothermic process that creates heat. This appears to be a problem in the preparation of larger diameter monolithic columns, since accurate control of the polymerization temperature is more problematic.[42] Inefficient heat dissipation and low light penetration inside the capillary lead to monoliths with heterogeneity in their pore structures and significantly reduced performance.

The resolving power of SEC separations increases with column length due to increased separation efficiency; however, longer columns also lead to longer separation times at a given pressure (Figure 3.4B). The resolution between TG and BSA increased from 0.50, 0.70 to 0.81 when the column length increased from 17 cm, 33 cm to 45 cm. This almost follows the proportional relationship between resolution and square foot of column length. I studied the effect of flow rate on the resolution of proteins and peptides using a 150-μm i.d., 45-cm-long column. As shown in Table 3.3, the resolution between

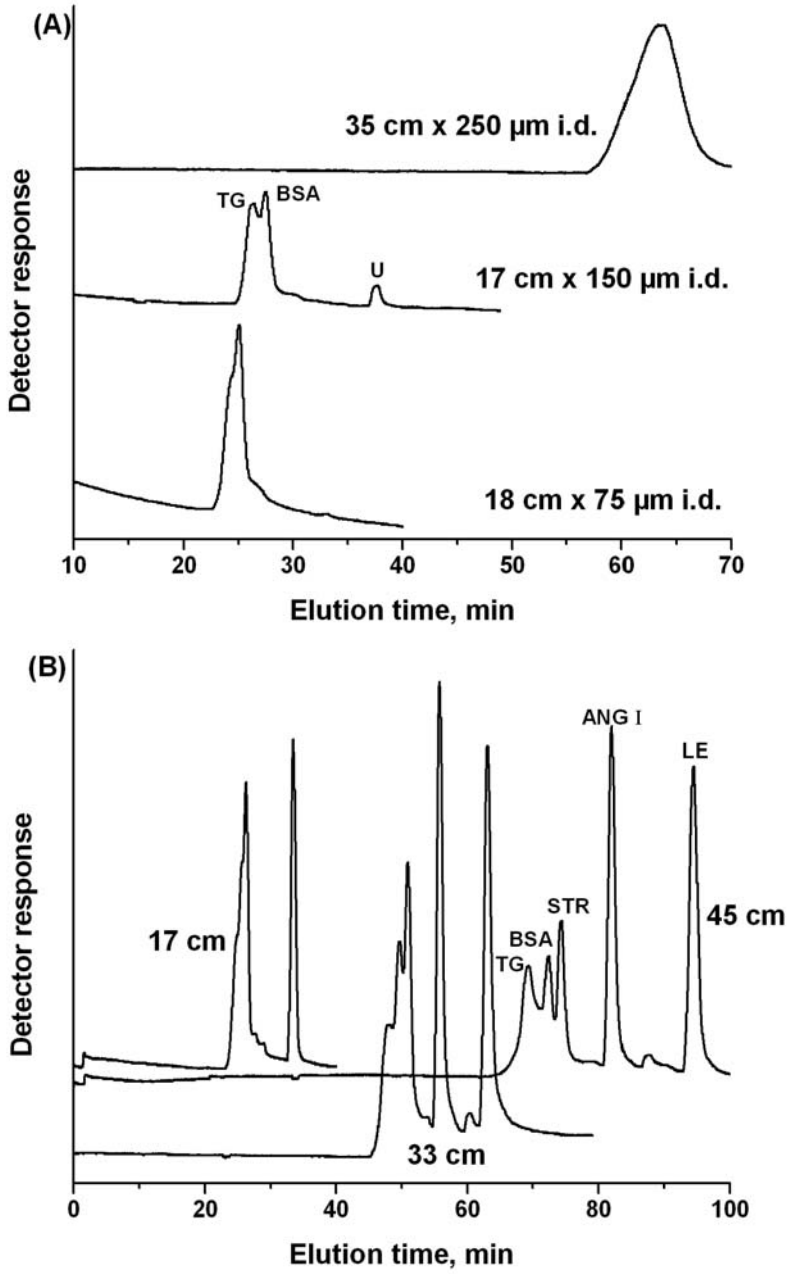

Figure 3.4. SEC separations on M-2 with different column i.d.s (A) and lengths (150 µm i.d.) (B). Conditions as in Figure 3.1. Peak identifications: 1 TG, 2 BSA, 3 STR, 4 βCGRP, and 5 LE.

Table 3.3 Influence of flow rate on resolutions.

Flow rate (nL/min)	Resolution between two successive peaks[a] mean±SD					Efficiency* (N/m)[b] mean±SD	
	TG/BSA	BSA/STR	STR/ANG I	ANG I/LE	LE/U	BSA	LE
100	0.72±0.02	0.82±0.03	2.29±0.06	3.23±0.07	---	18900 ±600	26900 ±700
60	0.80±0.02	0.96±0.04	2.43±0.06	3.50±0.07	1.10±0.03	34100 ±800	29300 ±700

*Condition: 45 cm × 150 μm i.d. M-2 monolith; other conditions as in Figure 3.2.

[a,b]Calculations were based on 95% confidence level, n = 3.

small molecules (peptides) increased by less than 8% as flow rate decreased from 100 to 60 nL/min, because the increased contribution of axial diffusion on efficiency counteracted the more favorable mass transfer, leading to almost constant column efficiency. This was not true for larger molecules, such as BSA, since considerably lower diffusion had much less effect at low flow rate, producing an increase in separation efficiency. The resolution between proteins, especially BSA and STR, increased by as much as 17% as flow rates decreased.

3.3.5 Chromatographic Evaluation

Compared to columns packed with spherical materials with well-defined 15 000-2000 000 exclusion range, my monolithic column demonstrated a broader MW application range from 112 to 670 000, but less resolution for the range from 66 000 to 670 000 (Figure 3.5). Besides proteins, my monolithic column can also separate peptides. If the peptides are loaded on the packed column, it is expected that the peptides would be coeluted out without any separation and after the proteins due to a limited exclusion range for proteins. The main drawbacks of the monolithic column were the relatively low resolution achieved in this range and the extremely long time necessary to carry out the separation. This is due to much lower mesopore volume in this range and high back pressure of the monolith.

The column porosity is determined by the interstitial volume between the particles in a packed column and the volume of the through-pores (macropores) in a monolithic column. Generally, polymer monolithic columns possess much higher macropore volume and lower mesopore volume compared to packed columns, which makes them less suitable for SEC.[24] The synthetic methods described in this work led to increased mesopore volume and a relatively broad pore size distribution, corresponding to the size range of proteins and

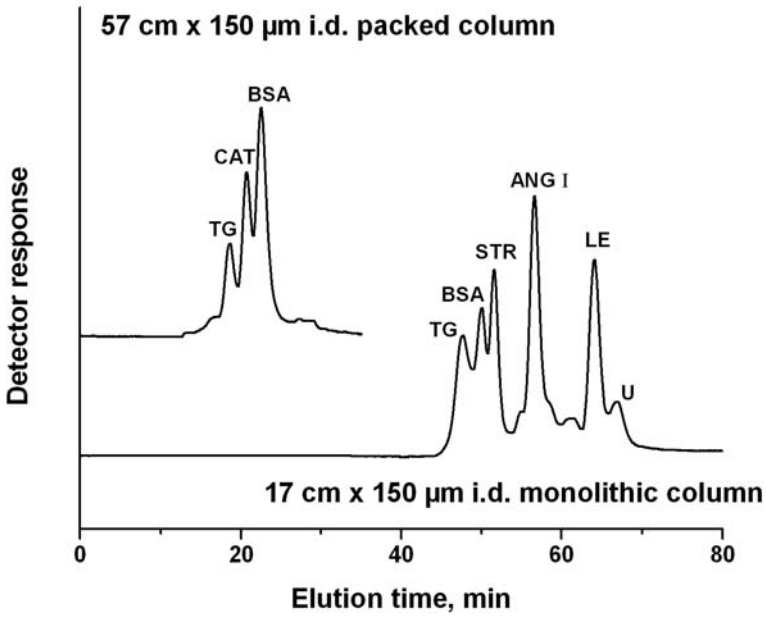

Figure 3.5. Comparison of resolution obtained for protein mix using (top) a packed column and (bottom) a monolithic column. Conditions: 57 cm × 150 µm i. d. BioSep-SEC-4000 particles packed column, 10 mM phosphate containing 0.10 M NaCl, pH 7.0, 0.3 µL /min; and 17 cm × 150 µm i. d. M-5 monolithic column, 10 mM phosphate + 0.15 M NaCl, pH 7.0, 0.06 µL/min; 60 nL injection volume; UV detection at 214 nm.

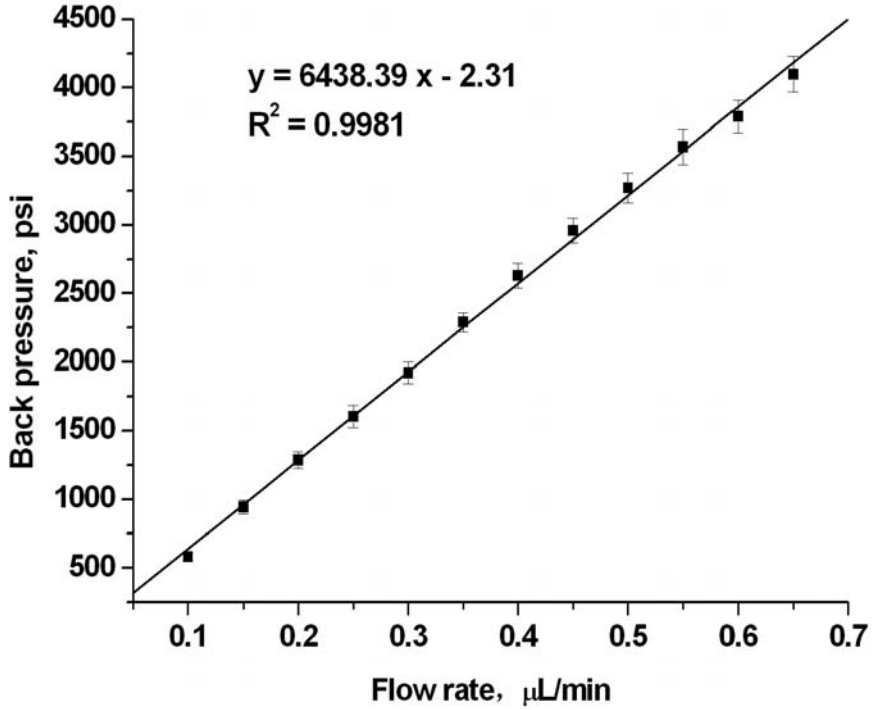

Figure 3.6. Plot of pressure drop against flow rate of mobile phase. Conditions: 18 cm × 150 μm i.d. monolith column (M5); water. Three measurements were made.

peptides. Hence, the resultant monolithic columns could be used for SEC. However, they demonstrated relatively high flow resistance due to their reduced macroporosity. Decreasing the flow rate significantly improved the resolution of larger molecules, however, this led to longer analysis time. To further characterize the SEC monolith, the flow rate dependence on applied pressure was monitored. Good linearity between pressure drop and flow rate clearly demonstrated that the monoliths were mechanically stable at pressures up to 4 000 psi (see Figure 3.6). In this regime, the monoliths are incompressible and, therefore, behave reproducibly.

3.3.6 Inverse Size Exclusion Chromatography Characterization

ISEC was carried out using a set of protein and peptide standards with widely varying but well-defined sizes to determine the mesopore distribution (Table 3.1). This examination is analogous to molecular mass calibration in SEC. It provides an alternative to mercury intrusion porosimetry or nitrogen-adsorption measurements for the determination of pore size distribution. With ISEC, the total porosity (69.0%) was calculated from the retention volumes of a small molecule (uracil, MW = 112 g/mol) and the geometrical volumes of the columns. Similarly, the fractional volume of the pores in a certain range was obtained from the pore volume interval. As shown in Table 3.4, a micropore porosity of 11.9% and a mesopore porosity of 8.5% in the range from 2.8 to 15.7 nm could be responsible for the size separation of peptides and proteins, respectively. The porosity contributed from pores larger than 15.7 nm was 48.6%. The additional mesopore volume fraction in the range of 15.7 ~ 50 nm is unknown because of the absence of larger probe molecules. In a plot of log MW versus elution volume (Figure 3.7), generally, the steeper the line, the worse the separation. For example, the large slope of the segment

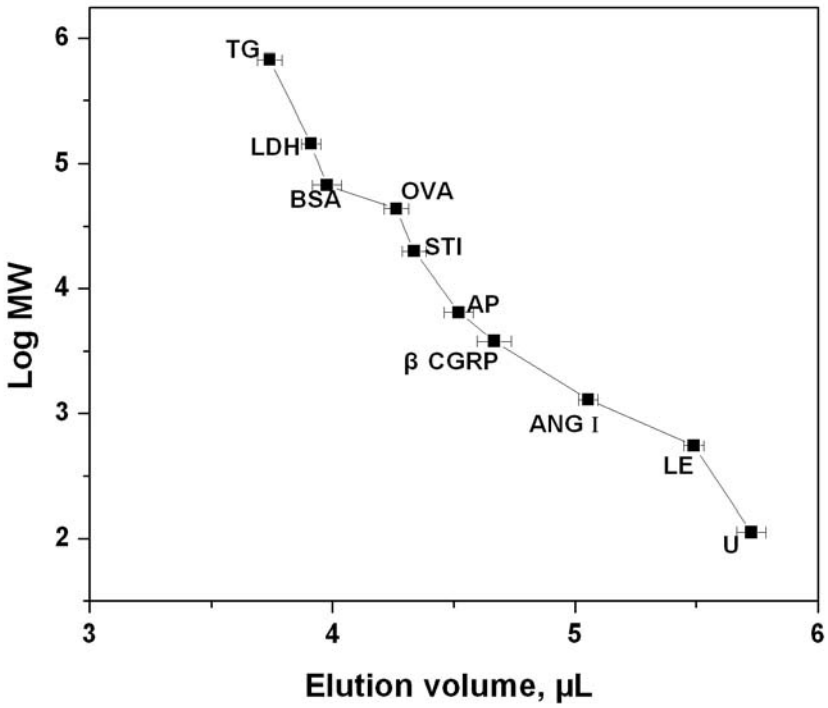

Figure 3.7. SEC calibration curve for M5 monolithic column. Conditions: 30 cm × 150 µm i.d. monolithic column (M5); 20 mM phosphate (pH 7.0) containing 0.15 M NaCl, 0.1 µL/min; analytes, protein and peptide standards in Table 3.1; 60 nL injection volume; UV detection at 214 nm. Three measurements were made.

Table 3.4 Pore volume distribution for M-5.

	Pore range	Pore volume fraction mean±SD[a]
Micropore	< 2 nm	11.9±0.2%
Mesopore	2.8 ~ 15.7 nm	8.5±0.2%
	15.7 ~ 50 nm	unknown
Macropore	> 50 nm	~ 48.6±0.7%

[a]Calculations were based on 95% confidence level, n = 3.

between TG and BSA indicates a lower fractional mesopore volume in this range and, hence, poorer SEC separation.

3.4 Conclusions

I have presented the first promising results showing the possibility of developing polymeric monolithic columns for SEC separation of proteins and peptides. The monolith was prepared in a single step by simple copolymerization of mixtures of PEGMEA and PEGDA in the presence of mixtures of ethyl ether and PEP or EPE having various molecular weights as porogenic solvents. The porous properties of the monolithic columns can easily be controlled through changes in the amount or molecular weight of the surfactant. Separations of several proteins and peptides were achieved with efficiencies of up to 40 900 plates/m. ISEC data using protein and peptide analytes as probes demonstrated a reasonable pore size distribution. SEC separation in the range between 66 000 and 670 000 should be improved by discovering more effective surfactants as porogens. A significant challenge is to improve protein resolution, while at the same time reducing flow resistance and, hence, analysis time. To achieve this, new meso-porogenic solvents or methods must be explored.

3.5 References

1. Unger, K. K. *Trends Anal. Chem.* **1983**, *2*, 271-274.
2. Regnier, F. E. *Anal. Chem.* **1983**, *55*, 1298A-1299A, 1301A-1302A, 1305A-1306A.
3. Yau, W. W.; Kirkland, J. J.; Bly, D. D. *Modern Size-Exclusion Liquid Chromatography*; Wiley-Interscience: New York, 1979.

4. Malawer, E. G. In *Handbook of Size Exclusion Chromatography*; Wu, C-S., Ed.; Chromatographic Science Series, Vol. 69; Marcel Dekker: New York, 1995; Chapter 1.
5. Opiteck, G. J.; Jorgenson, J. W.; Anderegg, R. J. *Anal. Chem.***1997**, *69*, 2283-2291.
6. Cavanagh, J; Thompson, R.; Bobay, B.; Benson, L. M.; Naylor, S. *Biochemistry* **2002**, *41,* 7859-7865**.**
7. Barth, H. G. *LC- GC* Europe **2003**, *23*, 2-6.
8. Cortes, H. J.; Pfeiffer, C. D. *Anal. Chem.* **1993**, *65*, 1476-1480.
9. Prokai, L.; Aaserud, D. J.; Simonsick, W. J., Jr. *J. Chromatogr. A* **1999**, *835*, 121-126.
10. Kennedy, R. T.; Jorgenson, J. W. *J. Microcolumn Sep.* **1990**, *2*, 120-126.
11. Chirica, G.; Lachmann, J.; Chan, J. *Anal. Chem.* **2006**, *78*, 5362-5368.
12. Švec, F.; Tennikova, T. B.; Deyl, Z. *Monolithic Materials: Preparation, Properties, and Applications*, Journal of Chromatography Library, Vol. 67; Elsevier: Amsterdam, 2003.
13. Premstaller, A.; Oberacher, H.; Huber, C. G. *Anal. Chem.* **2000**, *72*, 4386-4393.
14. Wang, F.; Dong, J.; Ye, M.; Jiang, X.; Wu, R.; Zou, H. *J. Proteome Res.* **2008**, *7*, 306–310.
15. Švec, F.; Fréchet, J. M. *Anal. Chem.* **1992**, *64*, 820-822.
16. Lowe, C. R.; Lowe, A. R.; Gupta, G. J. *Biochem. Biophys. Meth.* **2001**, *49*, 561-574.
17. Nakanishi, K. *J. Porous Mater.* **1997**, *4*, 67-112.
18. Nakanishi, K.; Shikata, H.; Ishizuka, N.; Koheiya, N.; Soga, N. *J. High Resol. Chromatgr*. **2000**, *23*, 106-110.
19. Al-Bokari, M.; Cherrak, D.; Guiochon, G. *J. Chromatogr. A* **2002**, *975*, 275-284.

20. Lubda, D.; Lindner, W.; Quaglia, M.; von Hohenesche, C. du F.; Unger, K. K. *J. Chromatogr, A* **2005**, *1083*, 14-22.

21. Svec, F.; Fréchet, J. M. J. *Chem. Mater.* **1995**, *7*, 707-715.

22. Petro, M.; Svec, F.; Gitsov, I.; Fréchet, J. M. J. *Anal. Chem.* **1996**, *68*, 315-321.

23. Eeltink, S.; Herrero-Martinez, J. M.; Rozing, G. P.; Schoenmakers, P. J.; Kok. W. T. *Anal. Chem.* **2005**, *77*, 7342-7347.

24. Urban, J.; Jandera, P.; Schoenmakers, P. *J. Chromatogr. A* **2007**, *1150*, 279-289.

25. Viklund, C.; Nordström, A.; Irgum, K. *Macromolecules* **2001**, *34*, 4361-4369.

26. Lubbad, S.; Buchmeiser, M. R. *Macromol. Rapid Commun.* **2002**, *23*, 617-621.

27. Aoki, H.; Kubo, T.; Ikegami, T.; Tanaka, N.; Hosoya, K.; Tokuda, D.; Ishizuka, N. *J. Chromatogr. A* **2006**, *1119*, 66-79.

28. Sharma, S.; Popat, K. C.; Desai, T. A. *Langmuir* **2002**, 18, 8728-8731.

29. Yang, Y.; Regnier, F. E. *J. Chromatogr.* **1991**, 544, 233-247.

30. Buchmeiser, M. R.; Seeber, G.; Mupa, M.; Bonn, G. K. *Chem. Mater.* **1999**, *11*, 1533-1540.

31. Gu, B.; Armenta, J. M. Lee, M. L. *J. Chromatogr. A* **2005**, *1079*, 382-391.

32. Rill, R. L.; Locke, B. R.; Liu, Y.; Dharia, J.; Van Winkle, D. H. *Electrophoresis* **1996**, *17*, 1304-1312.

33. Patterson, B. C.; Van Winkle, D. H.; Chakrapani, M.; Locke, B. R.; Rill, R. L. Book of Abstracts, 218th ACS National Meeting, New Orleans, Aug. 22-26, 1999.

34. Jang, J.; Bae, J. *Chem. Commun.* **2005**, *9*, 1200-1202.

35. Gorbunov, A. A.; Solovyova, L. Y.; Pasechnik, V. A. *J. Chromatogr.* **1988**, *448*, 307-332.

36. Ousalem, M.; Zhu, X.; Hradil, J. *J. Chromatogr. A* **2000**, *903*, 13-19.

37. DePhillips, P.; Lenhoff, A. M. *J. Chromatogr. A* **2000**, *883*, 39-54.

38. Chu, B.; Zhou, Z. *Physical Chemistry of Poly(oxyalkylene) Block Copolymer Surfactants.* In: *Non-ionic Surfactants: Polyoxyalkylene Block Copolymers*, Nace V. M., Ed.; Vol. 60; Marcel Dekker: New York, 1996.

39. Gu, B.; Li, Y.; Lee, M. L. *Anal. Chem.* **2007**, *79*, 5848-5855.

40. Viklund, C.; Švec, F.; Fréchet, J. M. J.; Irgum, U. *Chem. Mater.* **1996**, *8*, 744-750.

41. Gu, C.; Lin, L.; Chem, X.; Jia, J.; Ren, J.; Fang, N. *J. Chromatogr. A* **2007**, *1170*, 15-22.

42. Peters, E. C.; Svec, F.; Fréchet, J. M. J. *Chem. Mater.* **1997**, *9*, 1898-1902.

43. Stout, R. W.; DeStefano, J. J. *J. Chromatogr.* **1985**, *326*, 63-78.

44. Uversky, V. N. *Biochemistry* **1993**, *32*, 13288-13298.

45. Darcy, H. In: *Physical Hydrology*; Freeze, R. A.; Back, W., Ed.; Hutchinson Ross: Stroudsburg, PA, 1983.

CHAPTER 4 PREPARATION OF POLYMER MONOLITHS WITH TARGET MESOPORE SIZE DISTRIBUTIONS FOR SIZE EXCLUSION CHROMATOGRAPHY OF PROTEINS

4.1 Introduction

Monoliths, which comprise a new generation of stationary phases for liquid chromatography (LC), consist of a continuous, porous material that can be synthesized *in situ* in a chromatographic column.[1,2] The monolithic column format is a good alternative to typical spherical particle packed columns for capillary LC in view of ease of preparation and low back pressure, combined with continually improving performance.[3,4] Polymer-based monoliths, in particular, have covered all popular biomolecule separation modes, including size exclusion,[5] ion-exchange,[6,7] affinity,[8] reversed-phase,[9] hydrophobic interaction (HIC)[10] and hydrophilic interaction chromatography (HILIC) [11], as a result of the availability of a wide variety of functional monomers and easily achievable biocompatibility. For example, the epoxide groups on a macroporous poly(glycidyl methacrylate-co-ethylene dimethacrylate) monolith can be coupled with various functional groups for particular bioapplications;[12,13] the incorporation of poly(ethylene glycol diacrylate) (PEGDA) into the monolith backbone increases its biocompatibility.[5,6] Such surface compatibilization is of particular importance in various bioapplications, since it reduces or even prevents nonspecific surface adsorption.

Porosity represents an important structural feature of monolithic material. It may be used to vary important material properties, such as density, mechanical strength, and refractive index. Additionally, porosity may be used to enhance transport processes as well as molecular recognition, which are related to the essential parameters of chromatographic

columns, such as permeability, efficiency, selctivity and retention.[14-18] Three types of pores have been involved in monolithic structures, macropores (>50 nm), mesopores (2-50 nm) and micropores (< 2 nm). Macropores serve as flow-through pores that enable superior transport properties, allowing access to micropores or mesopores. The average size of these throughpores usually controls the column permeability.[14,15] Also relevant to column permeability are tortuosity and constriction of channels formed by these throughpores and their connectivity. Mesopores (diffusional pores) provide the needed surface area for molecular recognition sites, which are important for chromatographic retention. The structure of the mesopore network significantly affects the mass transfer kinetics and, hence, column efficiency.[16] It also controls the phase ratio in the column and may influence the retention ability of the monolith.[17] Additionally, mesopores are also important for size exclusion of larger protein molecules.[6] In contrast, the presence of micropores in a monolith is not favorable for chromatographic performance as the adsorption energy in micropores is high and the mass transfer kinetics through micropores are slow.[18]

Monoliths can be divided into two main categories based on their chemical compositions: inorganic oxides and organic polymer-based monoliths. Silica monoliths prepared by the sol-gel process exhibit a distinct bimodal pore volume distribution with macropores and mesopores.[19,20] However, micropores are rare in silica-based monoliths. One of the important advantages of silica monoliths is the possibility to control and optimize separately the dimensions of the macropores and the porons (i.e., globules of porous silica).[21] In contrast, organic polymer monoliths are now primarily prepared using free radical polymerization, initiated thermally or through ultraviolet light. Generally, the microstructures of such materials are characterized by a comparably broad distribution of

micro- and macropores, which are generated by means of solvent-induced phase separation. However, most polymer monoliths have few mesopores in their pore size distribution, which provides almost no separation in SEC.[22-24] Actually, for most polymeric monoliths, mesopores are suppressed to obtain a adequate flow through the monoliths.

The pore size distribution of a monolith is extremely important and should be designed properly to fit each type of application. SEC requires the monolith to have the right mesopore pore size distribution and large pore volume to achieve high separation selectivity and resolution. This is different from interactive LC, in which the separation performance is mainly dependent on the surface area and surface properties of the stationary phase material. Of course, for high column efficiency, the monolithic material for SEC should be uniform as in interactive LC. SEC is typically conducted using large columns connected in series because large pore volume is desirable for high resolution and accurate molecular weight (MW) measurements.[25] However, long analysis time accompanied with significant solvent consumption are disadvantages of this approach. In recent years, there has been increasing interest in developing high-speed SEC using a single column with small dimensions.[26] Small diameter SEC columns would enable the preparation of long columns for improved column efficiency. For this reason, the monolithic capillary column format would be a good alternative to typical spherical particle packed columns for SEC due to ease in preparation and low back pressure. The use of a temperature gradient during the polymerization process could even possibly yield polymer monoliths with porosity gradients, however, no successful study of producing SEC monoliths in this manner has been reported.[27]

I have recently reported the preparation of porous poly(polyethylene glycol methyl ether acrylate-co-polyethylene glycol diacrylate) [poly(PEGMEA-co-PEGDA)] monoliths that exhibit size exclusion properties. The polymerization process includes mono- and divinylic monomers as well as a porogenic solvent containing a high MW copolymer and a conventional free radical polymerization initiator.[5] The pore size distributions of these monolithic polymers differ fundamentally from the typical pore size distribution of poly(PEGMEA-co-PEGDA) monoliths prepared without the high MW copolymer in the polymerization mixture.[28] In contrast to these "classical" monoliths using low MW organic liquids as porogens, the pore size distribution for the SEC material is more appropriate for separating proteins and peptides by SEC. I attribute this porosity mainly to the use of a high MW copolymer as porogen. Despite these promising characteristics, my initial use of high MW porogenic solvents led to porous polymers with relatively high flow impedance, which limits their usefulness for fast analysis. At this point, the discovery of new mesoporogens producing monoliths with low back pressure is key to preparation of materials with the desired properties.

Brij is another polyoxyethylene surfactant that has been used in developing polyacrylamide media with appropriate pore size distributions for improved globular protein separation.[29] In this chapter, I report a poly(PEGMEA-co-PEGDA) monolith with higher permeability, suitable for SEC of proteins by using Brij 58 P as the mesoporogen.

4.2 Experimental Section

4.2.1 Chemicals and Reagents

2,2-Dimethoxy-2-phenylacetophenone (DMPA, 99%), PEGMEA (Mn ~454), PEGDA (Mn ~258), 3-(trimethoxysilyl)propyl methacrylate (TMSPMA, 98%), Brij® 30

(Mn ~362), Brij® 56 (Mn ~683), Brij® 58 P (Mn ~1124), Brij® 700 (Mn ~4670), 1-dodecanol, hexanes and LC water (CHROMASOLV®) were purchased from Sigma-Aldrich (Milwaukee, WI). All of the monomers were used without further purification. Phosphate buffer solutions were prepared with LC water and filtered through a 0.22-μm membrane filter. Table 4.1 gives a list of the proteins and peptides used in the experiments. All proteins and peptides were purchased from Sigma-Aldrich.

4.2.2 Preparation of Polymer Monoliths

Fused silica capillaries clad with UV-transparent fluorinated hydrocarbon polymer (Polymicro Technologies, Phoenix, AZ) were silanized using TMSPMA in order to anchor the polymer monolith to the capillary wall as described previously.[6] The polymer precursors were prepared by dissolving DMPA in a solution containing PEGMEA and PEGDA (1:3 weight ratio) and porogen, consisting of a ternary mixture of varying amounts of Brij, 1-dodecanol and hexanes. For example, the polymer precursor corresponding to M2 in Table 4.2 contained 0.006 g DMPA, 0.15 g PEGMEA, 0.45 g PEGDA, and 1.4 g total porogen (0.5 g 1-dodecanol, 0.6 g hexanes and 0.3 g Brij 58 P). After sonication for ~10 min, the polymer precursor was heated for several min at 50 ^{o}C until a clear solution was observed. Subsequently, the reaction mixture was introduced into the silanized capillary by vacuum, and irradiated for 6 min using a PRX 1000-20 Exposure Unit (TAMARACK Scientific, Corona, CA).

4.2.3 Size Exclusion Chromatography

After polymerizations were completed, the monolithic columns were connected to an LC pump and extensively washed with methanol to remove porogenic solvents and unreacted reagents. During flushing, the monolithic columns were placed in a stirred water

Table 4.1. Proteins and peptides used in this study.

Proteins and peptides	Abbreviation	MW (Daltons)[a]	p*I*[b]	Diameter (nm)[c]	Source[a]
Thyroglobulin	TG	670 000	4.6	~15.7	Porcine thyroid gland
Catalase	CAT	250 000	6.7	~10.9	Bovine liver
Albumin	BSA	66 000	4.9	~6.7	Bovine serum
Trypsin inhibitor	STI	20 100	4.5	~4.3	Soybean
Leucine enkephalin	LE	555	5.9	---	---
Uracil	U	112	---	---	---

[a]As specified by suppliers. [b]From Ref. 28 and 30. [c]Based on the Stokes' radius calculated from log (Rs) = 0.369 log (MW) – 0.254.[31]

bath (~50 ^{o}C) in order to increase the solubility of Brij in the eluent. The columns were then equilibrated first with water and then with buffer. An Eksigent Nano 2D LC system (Dublin, CA) was used to conduct all chromatographic experiments with a K-2600 UV detector (Sonntek, Upper Saddle River, NJ). The detection cell was a 3-nL ULT-UZ-N10 from LC Packings (Sunnyvale, CA). The column was connected to the detection cell using a zero dead volume P-720 Union (Upchurch, Oak Harbor, WA). Standard proteins or peptides dissolved in 20 mM phosphate (pH 7.0) were used to evaluate the monolithic columns. The solutions were injected through a six-port electronic valve as injector with a 1 μL capillary injection loop, and injection timing was controlled by switching the valve. Ultraviolet absorbance detection was carried out at 214 nm, and the detector signal was recorded using Eksigent v2.08 software. Furthermore, SEC calibration curves were determined for the monoliths using the protein and peptide standards listed in Table 4.1, and 20 mM phosphate buffer containing 0.15 M NaCl as mobile phase. All SEC experiments were carried out at room temperature (~23 ^{o}C) and the chromatographic conditions are given in the figure captions.

To investigate the permeability and rigidity of these monolithic columns, pressure drop measurements were made at room temperature (~23 ^{o}C) using pure water as the permeating fluid at flow rates ranging from 50 to 300 nL/min. Additionally, the total porosity, of the monolithic stationary phase, defined as $\varepsilon_T = V_M/V_C$, was determined from inverse size-exclusion chromatography data. V_M is the elution volume of uracil (a small non-retained, totally permeating compound; M_r = 112 g/mol) and V_C is the geometrical volume of an empty cylindrical column. Thyroglobulin (TG) with a molecular weight of 670 000 was the largest protein used in this study. The porosity representing pores that

exclude TG (ε_{TG}) was measured from the elution time of TG, which was assumed to be totally excluded from those smaller pores. Hence, the mesopore porosity that is useful for size separation of smaller proteins and peptides (ε_{pp}) was calculated as the difference between the total and TG flow-through porosities, $\varepsilon_{pp} = \varepsilon_T - \varepsilon_{TG}$. ISEC experiments were performed with aqueous buffer as solvent.

4.2.4 Scanning Electron Microscopy

A section of monolithic polymer in a capillary was cut and placed on a sticky carbon foil, which was attached to a standard aluminum specimen stub. Monolithic columns were characterized by scanning electron microscopy (SEM, FEI Philips XL30 ESEM FEG, Hillsboro, OR). The morphologies of the monoliths were observed from the SEM images.

4.2.5 Safety Considerations

The PEGMEA and PEGDA monomers may act as sensitizers. Relative MSDS information for these reagents should be consulted, and precautions should be taken for handling them. Additionally, caution must be taken (i.e., wearing glasses and gloves), since high power UV radiation can cause severe burns to skin and eyes.

4.3 Results and Discussion

4.3.1 Flow Properties of Monolithic Columns

My previous work demonstrated the generation of mesopores within poly(PEGMEA-co-PEGDA) monoliths for size separation of proteins using high MW copolymers as porogens.[5] However, the size-exclusion selectivity for proteins was not very high, and a relatively high proportion of mesopores resulted in decreased permeability of the monolithic bed. For further optimization, I evaluated another option, the use of Brij

surfactants as porogenic solvents. In search of the best porogen, I found that Brij 58 P with MW of 1124 in a mixture with a long chain alcohol (such as 1-dodecanol) and hexanes as the porogen system could result in a good monolith. The use of lower molecular weight of Brij polymers (i.e., 362 and 683) usually resulted in transparent or translucent monolithic structures that did not allow flow, and Brij with a higher molecular weight of 4670 was difficult to dissolve in most organic solvents.

The flow resistance of monolithic columns is conveniently characterized by the column permeability, K, using Darcy's equation:[32]

$$K = \frac{Q\eta L}{\Delta p A}$$

Where Q is the flow rate, η is the viscosity of the fluid, L is the column length, Δp is the pressure drop along the length of the column, and A is the cross sectional area of the column. K can be estimated from monitoring the flow rate dependence on applied pressure.

Column permeability is usually controlled by the average size of the throughpores. Polymer monoliths having a large proportion of small pores always exhibit excessively low permeabilities due to the typical monomodal pore size distribution. Hence, permeability data can provide useful information relating to pore structure. As shown in Table 4.2, the polymerization mixtures contained 0.006 g DMPA, 0.6 g monomers (PEGMEA and PEGDA; 0.15:0.45) and 1.4 g porogenic solvent mixture (Brij 58 P, 1-dodecanol and hexanes). To investigate the influence of porogen composition on permeability, the weight fraction of one porogen was kept constant, while the weight fractions of the other two porogens were varied. The data for M1-M3 show that an increase in ratio of hexanes to dodecanol (0.3/0.8, 0.6/0.5, and 0.7/0.4, w/w) while keeping the Brij concentration

constant increased the permeability. However, an increase in ratio of Brij to hexanes (M3-M5; 0.3/0.7, 0.5/0.5, and 0.7/0.3) resulted in a decrease in permeability. Additionally, when the content of hexanes was kept constant, the permeabilities of the monoliths remained almost constant, even when changing the weight ratio of Brij 58 P to docecanol (M6, 0.5/0.2; M3, 0.3/0.4; and M7, 0.2/0.5). These data show that both Brij 58 P and dodecanol serve as microporogens to produce small pores, while hexanes produce macropores for good bulk flow properties. To investigate the role of Brij in generating mesopores, another column, M0, was also prepared without the addition of Brij (dodecanol/hexanes, 0.5/0.6) for reference. Comparing M2 to M0, the column permeability decreased by adding Brij 58 P to the porogenic mixture, which indicates that Brij may produce more mesopores.

4.3.2 Pore Properties of Monolithic Columns

Since the monolithic materials in this study were used in combination with liquids in LC, determination of their pore properties in the wet state was deemed to be more valuable than properties measured in the dry state with techniques such as mercury intrusion porosimetry. Inverse size exclusion chromatography (ISEC) was chosen as a convenient method to use, since it is based on liquid chromatography. Since the poly(PEGMEA-co-PEGDA) monoliths exhibit negligible interaction with proteins and peptides, the real analytes (proteins and peptides) could be used as probes to estimate pore size distributions.

Generation of mesopores within monolithic columns in this work was aimed at the separation of proteins and peptides smaller than TG (see Table 4.1). Therefore, ISEC could be used to determine porosities for the monoliths that were prepared. Changes in the ratios

of porogen components enabled fine-tuning of the pore size distribution. As shown in Table 4.2, the total porosity (ε_T) was determined according to the elution volume of uracil, and the porosity representing pores that permit passage of the largest protein (TG) through the monolith (ε_{TG}) was determined from the elution volume of TG. Therefore, the porosity that represents pores that are useful for size separation of the smaller proteins and peptides than TG (ε_{pp}) can be calculated as the difference between the total and TG porosities. Using this technique, I systematically investigated the relative porosities of the monoliths listed in Table 4.2. Monolithic columns M1, M2, M4 and M5 gave ε_{pp} values larger than 0.10, which could include micropores and small mesopores (below the diamter of TG, 17 nm). Permeabilities were greatly reduced by an increasing proportion of smaller pores in the monolith. Figure 4.1 shows SEM images of M-0 and M-2 monoliths prepared without Brij and with 0.3 g Brij in 1.4 g total porogens, respectively. The micrographs clearly show the effect of porogen composition on porosity. In M-0, globules are clumped together, however, individual globules are clearly visible. In M-2, the monolithic structure is more compact and the globules are fused together. The fused-globule morphology was found to be less permeable than the aggregated-globule morphology.

4.3.3 ISEC Curves of Monolithic Columns

ISEC curves are similar to SEC calibration curves. The slope of the SEC calibration curve provides information related to the practical pore size distribution. Figure 4.2 shows SEC calibration curves for poly(PEGMEA-co-PEGDA) monoliths prepared with and without Brij. The preparation of poly(PEGMEA-co-PEGDA) monoliths using low MW solvents (M0) often yields materials that are unable to separate proteins according to their molecular weights due to the steep slope for the MW range between STI and TG. The SEC

Table 4.2. Efficiency, resolution and flow permeability values of the poly(PEGMEA-co-PEGDA) monoliths.[a]

Monolith	1-Dodecanol	Hexanes	Brij 58 P	ε_T	ε_{TG}	ε_{pp}	Permeability[c] ($\times 10^{-15}$ $m^{2)}$ mean±SD[d]	Efficiency (plates) mean±SD[d]	Resolution (TG/BSA) mean±SD[d]
M0[b]	0.5	0.6	0	0.70	0.63	0.07	26.1±0.6	41300±800	0.2±0.1
M1	0.8	0.3	*0.3*	0.62	0.45	0.17	7.7±0.2	35100±700	1.0±0.1
M2	0.5	0.6	*0.3*	0.72	0.56	0.16	18.4±0.4	68400±1600	1.6±0.1
M3	*0.4*	*0.7*	*0.3*	0.76	0.67	0.09	24.2±0.5	43400±900	0.4±0.1
M4	*0.4*	0.5	0.5	0.64	0.53	0.11	9.8±0.3	53100±1300	0.7±0.1
M5	*0.4*	0.3	0.7	0.59	0.45	0.12	5.9±0.2	32400±700	0.8±0.1
M6	0.2	*0.7*	0.5	0.73	0.65	0.08	23.0±0.5	57600±1500	0.6±0.1
M7	0.5	*0.7*	0.2	0.71	0.62	0.09	19.4±0.5	54300±1400	0.6±0.1

[a]The polymerization mixture contained 30% (W/W) monomers (PEGMEA and PEGDA; 0.15:0.45) and 70% porogenic solvent (Brij 58, 1-dodecanol and hexanes), and the polymerization was carried out in 20 cm × 150 μm i.d. columns for 6 min.

[b]A reference polymer was polymerized without Brij. [c]Permeability data were caculated according to Darcy's law.[32]

[d]Calculations were based on 95% confidence level, n = 3.

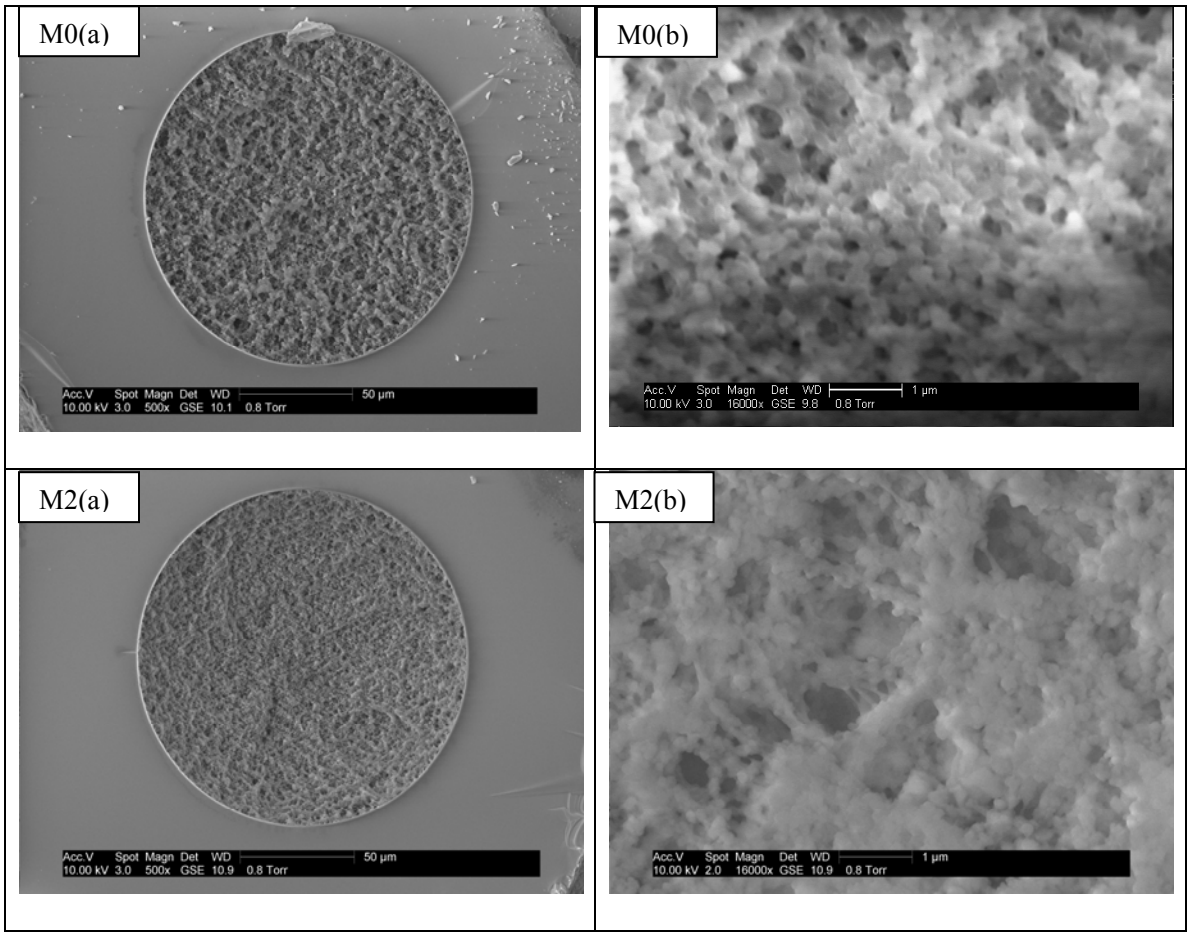

Figure 4.1. SEM images of M0 and M2 monoliths (see Table 4.2).

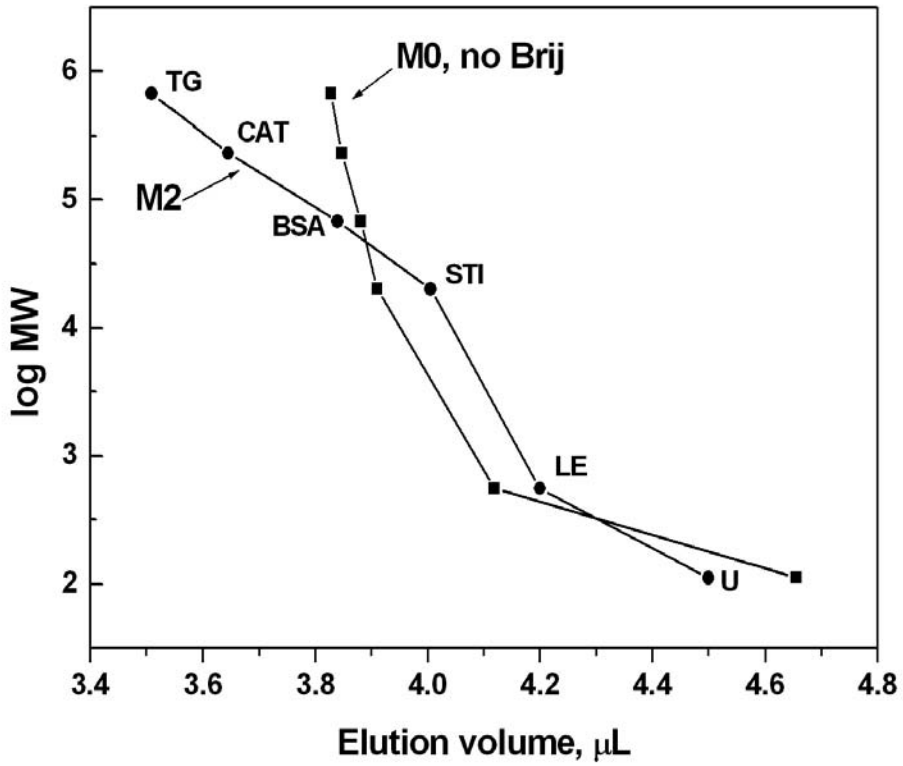

Figure 4.2. SEC calibration curves for proteins and peptides using an M2 column (23 cm × 150 μm i.d.). A reference sample (M0) polymerized without Brij at a 1-dodecanol/ hexanes ratio of 0.5:0.6 is also included (see Table 4.2). Only one measurement was made.

curves show that a monolith containing larger mesopores was obtained with porogenic mixtures that included Brij. The addition of even a small amount of Brij in the porogen mixture significantly improved the separation for proteins with molecular weights between STI and TG. Addtionally, proteins larger than STI (4.3 nm diameter) could not enter micropores (< 2 nm) or mesopores smaller than 4.3 nm. On the other hand, micropores were accessible to low MW peptides, such as LE. Hence, the difference between the elution volumes of STI and uracil can be considered to be the volume of micropores. Obviously, for this monolithic column, the micropore volume fraction from U to STI was decreased greatly, while the mesopore volume fraction in the range from STI to TG (7-17 nm) was increased, compared to the previous SEC monolith synthesized using a triblock copolymer.[5] It should be emphasized, that the pore structures of monolithic beds determined by ISEC in this way assumes negeligible interaction between the bed and proteins or peptides in an aqueous buffer without organic additives. Swelling or shrinking of the polymeric phase in any other media would alter its pore structure and change the pore size distribution.

4.3.4 SEC Separation of Proteins

A combination of the properties of monoliths, i.e., the large mesopore volume, with the high efficiency that small particles can generate would be optimal for SEC. Separation of BSA and TG was used for evaluation, since this pair represents an order of magnitude difference in MWs (i.e., 66 000 and 670 000, corresponding to hydrodynamic sizes of 6.7 and 15.7 nm). M2 gave the best resolution between TG and BSA due to a combination of large ε_{pp} and high efficiency. Other monolithic columns do not provide good resolution between TG and BSA because of either low ε_{pp} or low efficiency.

Figure 4.3 demonstrates the separation of a mixture of three proteins and one peptide using a 23 cm long poly(PEGMEA-co-PEGDA) monolithic column. Both the column efficiency for this short SEC column and its selectivity were good. Considering the relatively low back-pressure experienced for this SEC separation, the column length can be easily extended for more efficient separations. As discussed above, these monoliths possess a broad size exclusion separation range, evident from their SEC calibration curves. Compared to monoliths prepared using triblock copolymers, better permeability was obtained for even higher proportion of mesopores.

4.3.5 Effect of flow rate and column length

As shown in Figure 4.4, reducing the flow rate from 200 to 100 nL/min did not increase the resolution significantly because increased axial diffusion counteracted the more favorable mass transfer, leading to almost constant separation efficiency. Of course, a longer column improves the separation mainly by increasing the column efficiency, but at the expense of longer analysis time (Figure 4.5). The resolution between TG and BSA increased from 1.5 to 1.9 when the column length increased from 23 cm to 40 cm. This obeys the proportional relationship between resolution and square foot of column length.

4.4 Conclusions

Porous poly(PEGMEA-co-PEGDA) monoliths using a novel ternary porogenic solvent consisting of Brij 58 P, 1-dodecanol and hexanes have been synthesized. The resulting monoliths were suitable for SEC separation of proteins. The newly developed porogenic system containing Brij produced pore properties in poly(PEGMEA-co-PEGDA) monoliths that are more appropriate for SEC separation of proteins compared to monoliths produced by polymerization involving other polymeric porogens or low MW

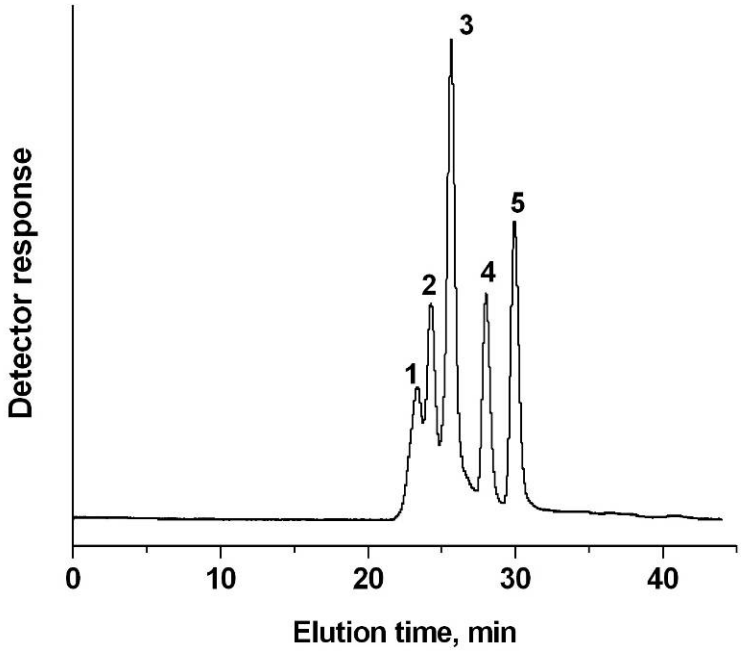

Figure 4.3. SEC separation of a protein mixture using a poly(PEGMEA-co-PEGDA) monolith (M2, see Table 4.2). Conditions: 23 cm × 150 μm i.d. monolithic column; 20 mM phosphate buffer (pH 7.0) containing 0.15 M NaCl, 0.15 μL/min; 60 nL injection volume; UV detection at 214 nm; Peak identifications: 1 TG, 2 CAT, 3 BSA, 4 LE, 5 U.

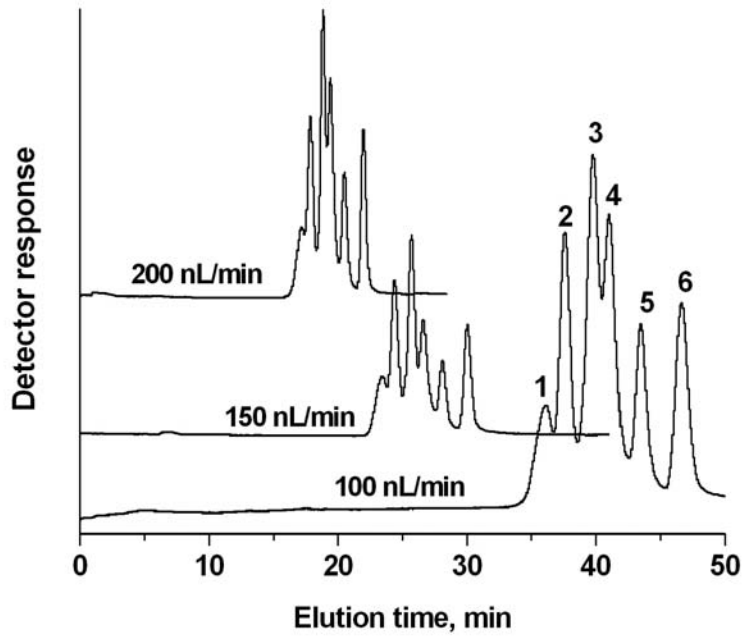

Figure 4.4. Influence of mobile phase flow rate on SEC resolution. Peak identifications: 1 TG, 2 CAT, 3 BSA, 4 STI, 5 LE, 6 U. Conditions as in Figure 4.3.

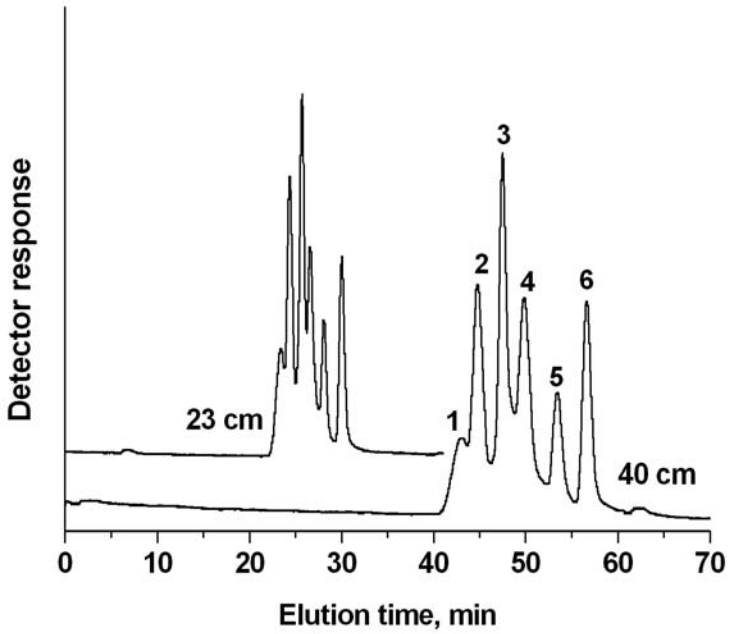

Figure 4.5. Influence of column length on SEC resolution. Peak identifications: 1 TG, 2 CAT, 3 BSA, 4 STI, 5 LE, 6 U. Conditions as in Figure 4.3.

organic solvents. The use of Brij 58 P produced a relatively large fraction of mesopores that resulted in improved SEC of proteins.

4.5 References

1. Hjertén, S.; Liao, J. L.; Zhang, R. *J. Chromatogr.* **1989**, *473*, 273-275.
2. Minakuchi, H.; Nakanishi, K.; Soga, N.; Ishizuka, N.; Tanaka, N. *Anal. Chem.* **1996**, *68*, 3498-3501.
3. Ishizuka, N.; Minakuchi, H.; Nakanishi K.; Soga N.; Tanaka N. *J High Resol. Chromatogr.* **1998**, *21*, 477-479.
4. Li, Y.; Zhang, J.; Xiang, R.; Yang, Y.; Horvath, C. *J. Sep. Sci.* **2004**, 27, 1467-1474.
5. Li, Y.; Tolley, H. D.; Lee, M. L. *Anal. Chem.* **2009**, *81*, 4406–4413.
6. Gu, B.; Li, Y.; Lee, M. L. *Anal. Chem.* **2007**, *79*, 5848-5855.
7. Li, Y.; Gu, B.; Tolley, H. D.; Lee, M. L. *J. Chromatogr. A* **2009***, 1216,* 5525-5532.
8. Hahn, R.; Podgomik, A.; Merhar, M.; Schallaun, E.; Jungbauer, A. *Anal. Chem.* **2001**, *73*, 5126-5132.
9. Xu, Z.; Yang, L.; Wang, Q. *J. Chromatogr. A* **2009**, *1216*, 3098–3106
10. Hemströem, P.; Nordborg, A.; Irgum, K.; Svec, F.; Fréchet, J. M. J. *J. Sep. Sci.* **2006**, *29*, 25-32.
11. Jiang, Z.; Reilly, J.; Everatt, B.; Smith, N. W. *J. Chromatogr. A* **2009**, *1216*, 2439-2448.
12. Svec, F.; Fréchet, J. M. J. *Biotechnol. Bioeng.* **1995**, *48*, 476-480.
13. Xie, S.; Svec, F.; Fréchet, J. M. J. *Biotechnol. Bioeng.* **1999**, *62*, 30-35.
14. Motokawa, M.; Kobayashi, H.; Ishizuka, N.; Minakushi, H.; Nakanishi, K.; Jinnai, H.; Hosoya, K.; Itegami, T.; Tanaka, N. *J. Chromatogr. A* **2002**, *961*, 53-63.

15. Kobayashi, H.; Tokuda, D.; Ichimaru, J.; Ikegami, T.; Miyabe, K.; Tanaka, N. *J. Chromatogr. A* **2006**, *1109*, 2-9.

16. Guiochon, G. *J. Chromatogr. A* **2006**, *1126*, 6-49.

17. Moravcová, D.; Jandera, P.; Urban, J.; Planeta, J. *J. Sep. Sci.* **2003**, *26*, 1005.

18. Guiochon, G. *J. Chromatogr. A* **2007**, *1168*, 101-168.

19. Lubda, D.; Lindner, W.; Quaglia, M.; von Hohenesche C. du Fresne; Unger, K. K. *J. Chromatogr. A* **2005**, *1083*, 14-22.

20. Al-Bokari, M.; Cherrak, D.; Guiochon, G. *J. Chromatogr. A* **2002**, *975*, 275-284.

21. Nakanishi, K.; Shikata, H.; Ishizuka, N.; Koheiya, N.; Soga, N. *J. High Resol. Chromatgr*. **2000**, *23*, 106-110.

22. Liao, J. -L.; Zhang, R.; Hjertén, S. *J. Chromatogr.* **1991**, 586, 21-26.

23. Marti, N.; Quattrini, F.; Butté, A.; Morbidelli, M. *Macromol. Mater. Eng.* **2005**, 290, 221-229.

24. Petro, M.; Svec, F.; Gitsov, I.; Fréchet, J. M. J. *Anal. Chem.* **1996**, *68*, 315-321.

25. Yau, W. W.; Kirkland, J. J.; Bly, D. D.; Stoklosa, H. J. *J. Chromatogr.* **1976**, *125*, 219-230.

26. Barth, H. G. *LC-GC Eur*. **2003**, *16*, 46-50.

27. Svec, F.; Fréchet, J. M. J. *Chem. Mater.* **1995**, *7*, 707-715.

28. Gu, B.; Armenta, J. M. Lee, M. L. *J. Chromatogr. A* **2005**, *1079*, 382-391.

29. Patterson, B. C. Surfactant micelles as templates in hydrogels, Ph.D. dissertation, Department of Chemistry, Florida State University, Tallahassee, FL, 2000.

30. Stout, R. W.; DeStefano, J. J. *J. Chromatogr.* **1985**, *326*, 63-78.

31. Uversky, V. N. *Biochemistry* **1993**, *32*, 13288-13298.

32. Darcy, H. In: *Physical Hydrology*; Freeze, R. A.; Back, W., Ed.; Hutchinson Ross: Stroudsburg, PA, 1983.

CHAPTER 5 CAPILLARY LIQUID CHROMATOGRAPHY OF HIGH DENSITY LIPOPROTEINS

5.1 Introduction

Lipoproteins are macromolecular complexes that contain both lipids and globular proteins. Non-polar lipids, such as triglycerides and cholesterol esters, are located in the core. Polar lipids, such as phospholipids and free cholesterol, and one or several proteins, the so-called apolipoproteins, are located on the surface. The primary function of lipoproteins is to transport triglycerides and cholesterol from sites of absorption and formation through the vascular and extravascular body fluids to sites of storage and usage.[1] Abnormal lipid transport processes are critical in etiology of several disease states such as coronary heart disease and atherosclerosis. According to density, human lipoproteins are classified into three major groups: high-density (HDLs, 5-12 nm), low-density (LDLs, 18-25 nm), and very low density lipoproteins (VLDLs, 30-80 nm).[2] LDL is the primary carrier of cholesterol through plasma, and is considered to be "bad cholesterol." A high LDL level is a positive risk factor for heart disease and atherosclerosis. HDL is the so-called "good cholesterol." The determination of HDL subpopulations provides more power to predict recurrent cardiovascular disease events than traditional risk factors.[3]

HDL is also a heterogeneous class of lipoprotein particles with subspecies that differ in apolipoprotein and lipid composition, size, density, and charge, and different subspecies appear to have different physiological functions.[4,5] Traditionally, HDL has been separated into major subclasses based on either density, size or apolipoprotein content (charge). Differences in these properties can be used as the basis for separation methods applied in purification strategies. For example, ultracentrifugation can separate HDL into

two main subclasses with approximate hydrated densities of 1.075 and 1.12 g/mL, which are labeled HDL_2 and HDL_3.[6] However, this technique takes a long time to perform and structural modifications of the lipoproteins may occur. HDL also separates into additional distinct subclasses of particles with different electrophoretic mobilities on nondenaturing polyacrylamide gradient gels.[7] Using segmented gradient gel electrophoresis (GGE) pioneered by Krauss,[8] Berkeley HeartLab breaks HDL into five distinct categories with different diameters.[9] Based on size, high performance size exclusion chromatography using two gel permeation columns in series was also applied for separation of HDL, and three major sizes of native HDL particles were detected.[10]

Besides the methods mentioned above, lipoprotein identification on the basis of apolipoprotein composition is also very important because diverse apolipoproteins exist within one lipoprotein and they serve different functions. Separation techniques based on charge, such as capillary electrophoresis (CE), isoelectric focusing (IEF), and ion exchange chromatography (IEC), could provide this type of information. CE has been reported to be a rapid and sensitive method for the determination of apo A-I in clinical samples, which reflects the level of HDL.[11] A method has been developed using CE to quantitate plasma levels of apo A-I and apo A-II in HDL samples.[12] Hu et al. foresaw the potential of CE-based methods to separate and determine the concentration of each class of lipoproteins simultaneously and to differentiate the isoforms of Lp (a).[13] Analytical IEF of HDL apolipoproteins provided evidence for multiple isoproteins in the apo A-I range, with nine different bands being detected instead of the usual four bands observed in normal objects.[14] Six distinct subpopulations of HDL were obtained by von Hodenberg et al. using preparative IEF, and the major difference between the subfractions was in the molar ratio of

apo A-I to apo A-II, ranging from 2.1 to 0.5.[15] IEF, which separated delipidated HDLs due to their different pI values, resulted in 8 peaks with corresponding pI values of 7.40, 6.92, 6.64, 5.48, 5.30, 5.18, 4.92 and 4.63.[16] In a later report by Farwig et al., 25 bands of HDL were characterized by a combination of high-accuracy pI measurements.[17] A survey analysis of 12 of these bands by MALDI mass spectrometry indicated that they were associated with the known HDL apolipoproteins. This technique was claimed to be an efficient method to characterize the complex mixture of apolipoproteins. Rapid isolation of urea-soluble apolipoproteins from delipidated human HDLs has been achieved using fast anion-exchange chromatography (AEC).[18] Here apo A-I and A-II were identified by comparing their chromatographic, electrophoretic and immunological behaviors with those of purified standards of each protein. In another interesting report,[19] delipidated HDL was fractionated by AEC using a continuous NaCl gradient of 0.06-0.13 M. The elution pattern had 3 main characteristics: a small peak at an NaCl concentration of 0.076, followed by a large peak, and finally a slowly eluting fraction which began at an NaCl molarity of 0.096. However, the 3 fractions isolated by AEC were not the same as those isolated by centrifugation (HDL_1, HDL_2 and HDL_3).

Compared to single-dimension methods, two-dimensional separation methods should provide greater resolution and more detailed sample information. A two-dimensional gel electrophoresis (2D-GE) system was developed to identify apo A-I-containing subclasses in HDL.[20] In the first dimension, separation by charge was measured by comparing particle mobilities to endogenous albumin (R_f); they classified particles as α (median $R_f = 1$), preα (median $R_f > 1$), and preβ (median R_f 0.3 to 0.8). This is also in accordance with the fact that 3 particles with charge differences were fractionated

by AEC.[19] In the second dimension, particles were differentiated according to their modal diameters. Twelve sub-populations were detected. Despite the high resolving power achieved, this technique was very labor-intensive and difficult to automate. Additional challenges in maintaining good reproducibility and quantitation have stimulated efforts to find alternative techniques.

Different separation techniques have been coupled together in various system combinations such as liquid chromatography-capillary electrophoresis (LC-CE) and capillary isoelectric focusing-liquid chromatography (CIEF-LC),[21,22] where separation by charge (i.e., CE or IEF) is one of the dimensions. Two-dimensional liquid chromatography (2D LC) is an excellent alternative because of its greater flexibility (different separation modes are available), speed, and ease of automation.[23,24] Recently, IEC based on charge separation has also been combined with selected LC modes, including reversed phase liquid chromatography (RPC) and size exclusion chromatography (SEC), i.e., IEC-RPC and IEC-SEC.[25] As mentioned above, the beauty of 2D-GE as a separation technique for HDL separation is the orthogonality of the two separation dimensions - separation by charge (isoelectric point, p*I*) in the first dimension and separation by size in the second dimension. For a chromatographic approach to provide comparable separation power, two modes must be selected that have different separation selectivities.[26] Coupling SEC and IEC as the first and second dimensions, respectively, has two appealing advantages. The first advantage is that the two modes have complementary selectivities that are similar to those of 2D-GE. IEC separation is roughly equivalent to IEF, and SEC provides separation according to molecular size. Therefore, the resolving power of the coupled modes is expected to approximate, even exceed, that of 2D-GE. The second advantage of this

approach is the solvent compatibility of the two modes. The elution solvents for IEC (aqueous buffers with varying concentrations of a neutral salt) are the right solvents for SEC.

Porous polymer monoliths have attracted significant attention as versatile, high-surface-area matrices useful for chromatography of large biomolecules, such as proteins and polynucleotides, as well as large particles such as viruses.[27] The first polymeric monolith was a soft polyacrylamide gel used as a continuous sorbent bed in LC in 1989.[28] In the early 1990s, Svec and coworkers introduced rigid macroporous monoliths obtained via a very simple "molding" process.[29] Typically, the polymerization of a monolith involves a mixture of monomers, porogens and free-radical initiator, which is triggered by heating or by UV irradiation. In the presence of porogens, a porous structure is formed as a result of phase separation initiated by precipitation of the polymer. The surface chemistry and porous properties of the monoliths can be tailored to suit a variety of applications by adjusting the composition of the initial monomer solution and the polymerization conditions.[30] The vast majority of polymeric monoliths are poly(styrene-co-divinylbenzene) (PSDVB) developed by Huber's group,[31] or polymethacrylate-based copolymers, such as poly(glycidyl methacrylate-co-ethylene dimethacrylate) (GMA-co-EDMA), which have been extensively exploited by Svec's group.[32] A new method of ring-opening metathesis polymerization (ROMP) was recently reported by Buchmeiser et al. for the preparation of polycyclooctene-based monoliths.[33] Recently, PEG-functionalized acrylic monomers have been used to reduce non-specific protein adsorption.[34,35] This has been especially meaningful for monolithic LC separation of lipoproteins, since lipoproteins are extremely "adherent" toward most column supports and

matrices. In addition, I should mention that most references concerning HDL separation by charge focus on delipidated HDL, since very hydrophobic lipids destroy the separation of lipoproteins through non-specific interactions. This is not a major problem in my case because I use PEG monoliths that exhibit the lowest non-specific adsorption of proteins.

Large monolithic columns are desirable for preparative-scale separations. However, due to the small sample volumes and low concentrations encountered in proteomics analysis, capillary monolithic columns for use in nano-LC have recently grown in interest.[34-36] The capillary format also provides two other advantages: first, immobilization of the monolith at the capillary wall eliminates the necessity of preparing a tiny retaining frit; second, direct on-line coupling of capillary LC to mass spectrometry becomes easier.[37]

In this chapter, a new capillary SEC method for size separation of native HDL particles from plasma using a packed capillary column was developed. Then, capillary SEC and capillary strong AEC of non-delipidated HDL were perfomed using the developed poly(polyethylene glycol methyl ether acrylate-co-polyethylene glycol diacrylate) [poly(PEGMEA-co-PEGDA)] and poly[2-(acryloyloxy)ethyl trimethlyammomium chloride-co-polyethylene glycol diacrylate] [poly(AETAC-co-PEGDA)] monoliths, respectively.

5.2 Experimental Section

5.2.1 Chemicals and Reagents

Sodium dodecyl sulfate (SDS), poly(vinyl alcohol) (PVA, MW 89,000-98,000), poly(propylene oxide)-block-poly(ethylene oxide)-block-poly(propylene oxide) (PPO-PEO-PPO, Mn 2,500), dimethylformamide and HPLC water (CHROMASOLV®) were purchased form Sigma-Aldrich (Milwaukee, WI). Phosphate and tris buffer solutions

with surfactant additives were prepared by adding SDS into buffer salt solutions. HPLC water was used for buffer and sample preparation, and all solutions were filtered through 0.22-μm membrane filters before use. The HDL solution standard (human plasma, 22.6 mg/mL) was from Calbiochem (San Diego, CA), which is described as HDL in 150 mM NaCl, 0.01% EDTA, pH 7.4 (Composition: 50% lipid, 50% protein). The high HDL2b fraction from a real blood sample was provided by Berkeley HeartLab (Alameda, CA). High molecular weight protein standards used for identifying 5 different subclasses of HDLs, including thyroglogulin, apoferritin, catalase, lactate dehydrogenase, and bovine serum albumin were purchased from Sigma-Aldrich. Table 5.1 provides a list of the characteristics of these proteins.

5.2.2 Column Preparation

The size exclusion monolithic poly(PEGMEA-co-PEGDA) column was prepared as described previously. DMPA (0.008 g, 1 wt % with respect to the monomers) was dissolved in 0.8 g of a mixture of PEGDA (40 wt %) and PEGMEA (60 wt %). A ternary porogen solvent (1.4 g) consisting of PPO-PEO-PPO copolymer (20 wt %), dimethylformamide (20 wt %), and ethyl ether (60 wt %) were admixed with the monomers. A small part of the polymerization mixture was removed using a 100 μL syringe for capillary preparation. A 25 cm × 75 μm i.d. silanized capillary was attached to the syringe inlet and filled with the polymerization mixture. Then the capillary was irradiated using a UV curing system as previously reported.[34] The bulk polymerization solution in the vial was also irradiated for easy disposal.

Additionally, several packed capillary columns were prepared and studied for SEC of HDL. The packing material was removed from a commercial BioSep-SEC-4000 guard

column purchased from Phenomenex (Torrance, CA) with the following specifications: hydrophilic bonded silica, 5 μm particle size, 500 Å pore size, 15,000-2,000,000 Daltons exclusion range for native proteins. A high-pressure packing system used to prepare columns for this study was described previously.38 The inner walls of 75 μm, 150 μm and 200 μm i.d. fused silica capillaries clad with polyimide (Polymicro Technologies, Phoenix, AZ) were coated with PVA using procedures published previously to reduce adsorption of proteins.39 Slurries of silica particles were made by mixing porous particles in 100 mM phosphate buffer solution (pH 7.0). Then the slurry was transferred to the packing reservoir. Liquid carbon dioxide from a compressed cylinder was used to drive the silica particle slurry into the capillary column. Both the column and the reservoir were placed in an ultrasonic bath (Branson Ultrasonic, Danbury, CT) during packing. The pressure was increased gradually from 900 psi to 2500 psi and kept constant at high pressure until the column was completely filled with packing material. After packing, high pressure was applied for at least a half hour before depressurizing slowly. Frits were sintered at the ends of the column using a resistive heating device (InnovaTech, Hertfordshire, UK) while water was flushed through the column to dissipate the heat. The flushing pressure should be the same as, or close to, the packing pressure. A poly(AETAC-co-PEGDA) monolith for strong AEC of HDL was also prepared as described in Chapter 2.

5.2.3 LC of High Density Liporotein

All LC experiments were carried out using an Eksigent Nano 2D LC system described in Chapter 3. The detection cell was a 3-nL ULT-UZ-N10 from LC Packings (Sunnyvale, CA). The column was connected to the detection cell using a zero dead volume P-720 union (Upchurch, Oak Harbor, WA), and the detection wavelength

Table 5.1. Five proteins used in this study.

Proteins	Abbreviation	MW (KD)[a]	p*I*[b]	Diameter (nm)[c]	Source[a]
Thyroglobulin	TG	670	4.6	~15.7	Porcine thyroid gland
Apoferritin	APF	444	5.2	~12.3	Horse spleen
Catalase	CAT	250	6.7	~10.9	Bovine liver
Lactate dehydrogenase	LDH	143	8.5	~8.9	Rabbit muscle
Albumin	BSA	66	4.9	~6.7	Bovine serum

[a]As specified by suppliers. [b]From Refs. 34 and 41. [c]Based on the Stokes' radius calculated from log (Rs) = 0.369 log (MW) – 0.254.[42]

volume P-720 union (Upchurch, Oak Harbor, WA), and the detection wavelength was 214 nm. Data acquisition and processing were accomplished using Eksigent v2.08 software.

After complete flushing, the capillary column was connected to the LC instrument and equilibrated with buffer. SEC separations of HDL were performed on the packed BioSep-SEC-4000 or the poly(PEGMEA-co-PEGDA) monolithic columns, and the AEC separation of HDL was performed on the poly(AETAC-co-PEGDA) monolithic column. The chromatographic conditions are given in the figure captions.

5.3 Results and Discussion

5.3.1 SEC Separation Using Packed BioSep-SEC-4000 Columns

Berkeley HeartLab divided HDL fractions into five subclasses according to size varying from 5 to 12 nm using density gradient electrophoresis. SEC should be a good alternative for resolving HDLs according to size. High molecular weight protein standards were used for identifying 5 different subclasses of HDLs, including thyroglogulin, apoferritin, catalase, lactate dehydrogenase, and bovine serum albumin (see Table 5.1). The size range of these five proteins is in accordance with that of HDLs (5-12 nm).

One of the difficulties of lipoprotein analysis by LC is the high propensity for the analytes to adsorb on the separation column, leading to peak broadening or even compound loss. Poly(vinyl alcohol) has been utilized as a coating material to diminish protein adsorption on the bare fused-silica capillary. At the beginning of my experiments, I investigated the use of PVA coating to reduce protein adsorption. As shown in Figure 5.1A, broad peaks and peak tailing resulted when using a bare capillary containing the packing material. However, when the capillary column was coated with PVA, lower adsorption of proteins and improved peak shapes were obtained (see Figures 5.1B and C). At the same

time, the influence of column diameter on protein resolution was investigated. Figure 5.1 shows the separations of high molecular weight proteins on columns with internal diameters of 75, 150, 250 μm. The BioSep-SEC-4000 capillary columns, however, separated only three major bands (peaks). The three peaks most likely belong to TG, coelution of APF, CAT and LDH, and to BSA. It was found that the packed capillary columns with 200 μm i.d. provided better resolution than the 75 μm i.d. and 150 μm i.d. packed capillary columns due to increased pore volume in the stationary phase.

HDL 2b from fresh human plasma sample (provided by Berkeley HeartLab) separated into at least three distinct peaks of HDL on the 150 μm i.d. BioSep-SEC-4000 column. As shown in Figure 5.2, the first peak, representing the largest apo A-I- containing species, eluted at the approximate position as TG and contained particles of ~670 KDa (~15.7 nm diameter). The second peak, which eluted at the approximate position as the coelution of APF, CAT and LDH, included particles of 143-444 KDa (~8.9-12.3 nm diameter). The third peak, which eluted at the approximate position as BSA, included HDL particles of 66 KDa in size (~6.7 nm diameter). Actually, the high intensity of the third peak is mostly attributable to the existence of the highly abundant albumin in the HDL sample from human plasma. I also believe that the large amount of albumin in the sample adheres to the wall of the detection cell and causes adsorption of the HDL components, resulting in decreased resolution of the second and the third peaks. These results showed that the PVA coating could not effectively suppress HDL adsorption on the capillary wall. Therefore, for accurate quantitative analysis, depletion of the highly abundant albumin from the HDL sample must be done before injecting the sample onto the column. Additionally, the small peaks after the main three peaks were probably from impurities in the sample, and

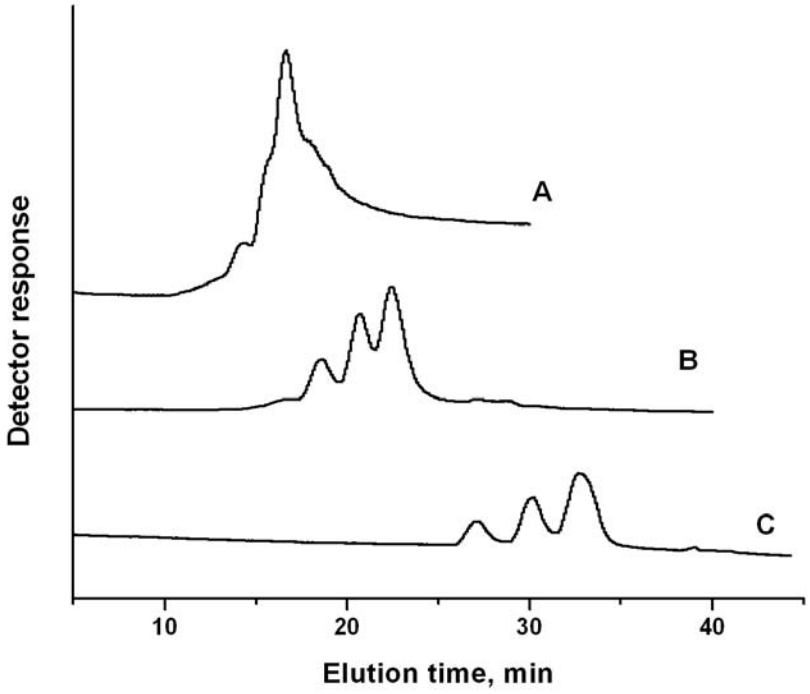

Figure 5.1. Separations of high MW protein standards using BioSep-SEC-4000 particle-packed SEC columns. Conditions: (A) 25 cm × 75 μm i.d. bare capillary, 0.06 μL/min, (B) 59 cm × 150 μm i.d. PVA-coated capillary, 0.3 μL/min, (C) 59 cm × 200 μm i.d. PVA-coated capillary; 20 mM phosphate containing 0.10 M NaCl mobile phase (0.3 μL/min); 60 nL injection volume; UV detection at 214 nm.

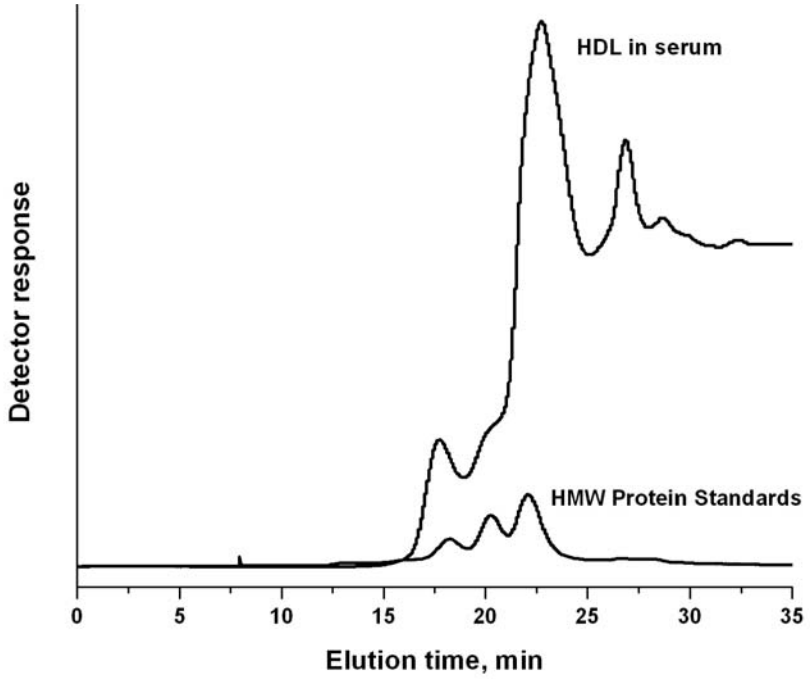

Figure 5.2. Separation of HDL using a BioSep-SEC-4000 particle-packed capillary SEC column. Conditions: 59 cm × 200 μm i.d. PVA-coated capillary; 20 mM phosphate containing 0.10 M NaCl, 0.4 μL/min; 60 nL injection volume; UV detection at 214 nm.

they did not belong to the HDL species.

In addition to their adhesiveness to column supports and matrices, HDL particles, once eluted off the columns, continued to adsorb strongly on the detection cell made from a bare silica capillary. To suppress such strong analyte-wall interaction, an anionic surfactant (SDS) was added to the running buffer to form complexes with the lipoproteins due to the presence of apolipoproteins on the surface. As a result, lipoproteins became negatively charged and adsorption was suppressed due to electrostatic repulsion. However, care had to be taken becasue too much SDS denatured the lipoproteins due to strong hydrophobic interactions between the alkyl chains and very hydrophobic liporoteins.

5.3.2 SEC Separation Using the Monolithic Column

Challenges in developing SEC polymer monolithic columns stem mainly from two aspects. First, a nonadsorptive monolith must be synthesized since SEC is a non-interactive chromatography mode. Second, the monolith must have appropriate pore size distribution for effective size exclusion of HDLs. The first issue was solved by the synthesis of a novel protein-nonadsorptive monolith (Figure 5.3). The monolith was based on the copolymerization of polyethylene glycol methyl ether acrylate (PEGMEA) and polyethylene glycol diacrylate (PEGDA). This monolith was found to resist the adsorption of proteins and HDLs. At present, the second requirement is the most challenging, since no precedent can be used for reference. After much investigation, surfactants were introduced as porogens to create mesopores of defined size within the polymeric matrix in chapters 3 and 4.

Using PPO-PEO-PPO, dimethylformamide and ethyl ether as porogens, the resulting monolith gave different retention for three proteins: BSA, catalase subunit and

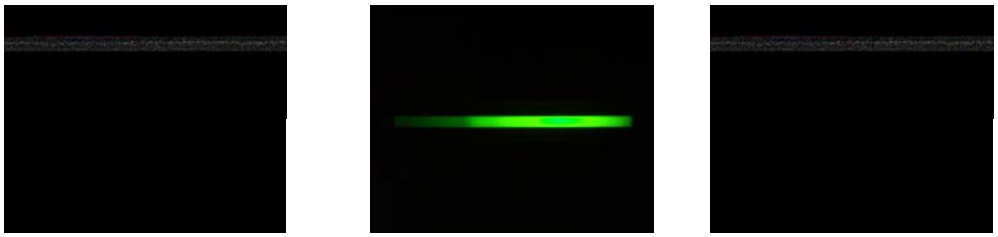

Figure 5.3. Low adsorption of proteins on a PEG monolith. (A) Background; (B) After loading with FITC-BSA; (C) After flushing with aqueous buffer.

α-lactalbumin (LCA) (Figure 5.4). This indicates that the pore size that provides SEC separation is mainly the small mesopores (below 7 nm), while the larger mesopores (7 – 50 nm) are not abundant enough for separation of larger proteins. However, the results are very promising, since this mesopore-forming method can produce an acceptable column back-pressure, even with a significant number of small mesopores.

SEC separation of the HDL standard from Calbiochem was also carried out using the same monolithic column, as shown in Figure 5.5. Similarly, at least four distinct peaks were identified. The first peak, representing the largest apo A-I-containing species, eluted in the BSA and CAT subunit fractions and included particles of 58-66 KDa (~5.9-6.7 nm diameter). The second peak, which eluted between the CAT subunit and LCA, included particles of 14-58 KDa (~4.3-5.7 nm diameter). The third peak, which eluted at the approximate position as LCA, included HDL particles of 14 KDa in size (~4.2 nm diameter). The peak after the main three peaks was probably an impurity in the sample, and it did not belong to the HDL species. The adsorption of HDL on the column matrix was reduced, but not completely eliminated, due to the use of PEG in the monolith. The components of the HDL standard from Calbiochem were different from the high HDL 2b sample provided by Berkeley HeartLab. My results showed that the particle sizes of the former are smaller than the latter. As shown in Figure 5.6, a separation using gradient gel electrophoresis indicates that most of the particle sizes in the HDL standard were 6.7-10.9 nm (MW 66-250 KDa). Further investigations are still needed to prove the usefulness of this monolithic SEC column for separation of native HDL. Of course, the other two SEC monoliths with improved exclusion range for HDL described in Chapters 3 and 4 should be investigated in the future.

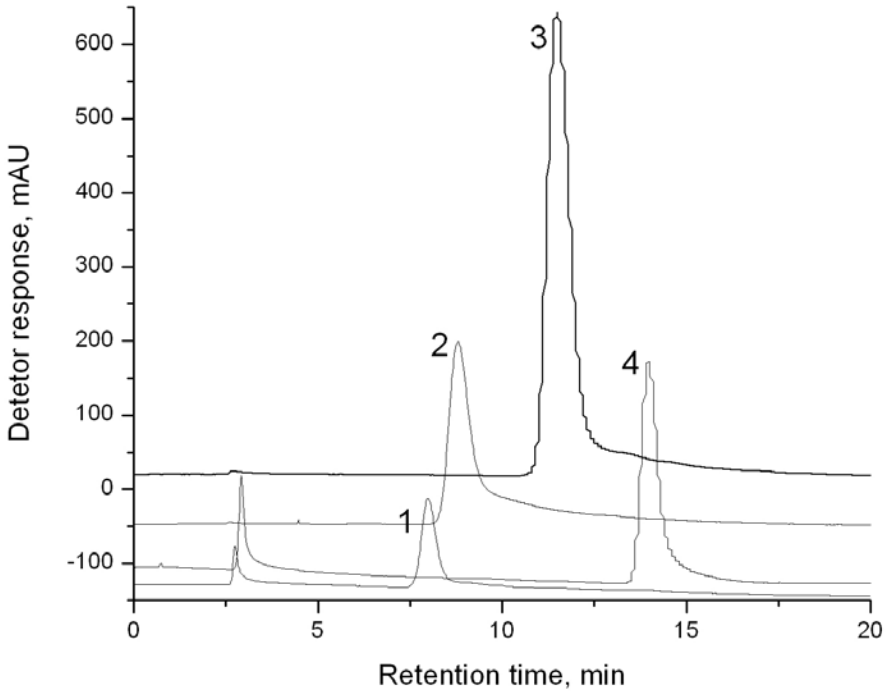

Figure 5.4. Chromatograms of individual proteins: (1) BSA (MW, 66,000), (2) Catalase subunit (MW, 58,100), (3) α-Lactalbumin (MW, 14,200), (4) Uracil (MW, 112). Conditions: 17 cm × 75 μm i.d. poly(PEGMEA-co-PEGDA) monolithic column, 10 mM phosphate (pH 7.0) containing 0.5 M NaCl, 80 nL/min, on-column UV detection at 214 nm.

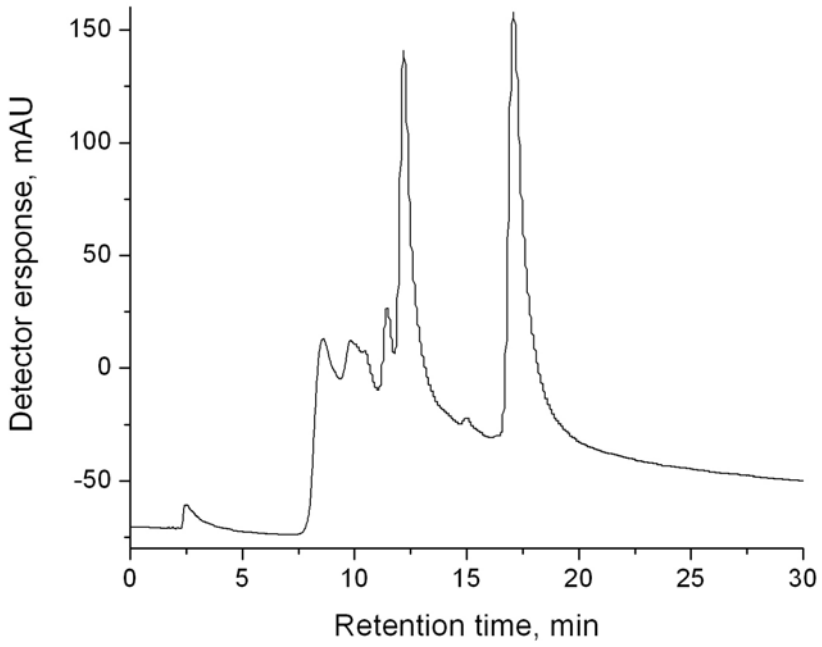

Figure 5.5. Chromatogram of an HDL standard. Conditions: the same as in Figure 5.4.

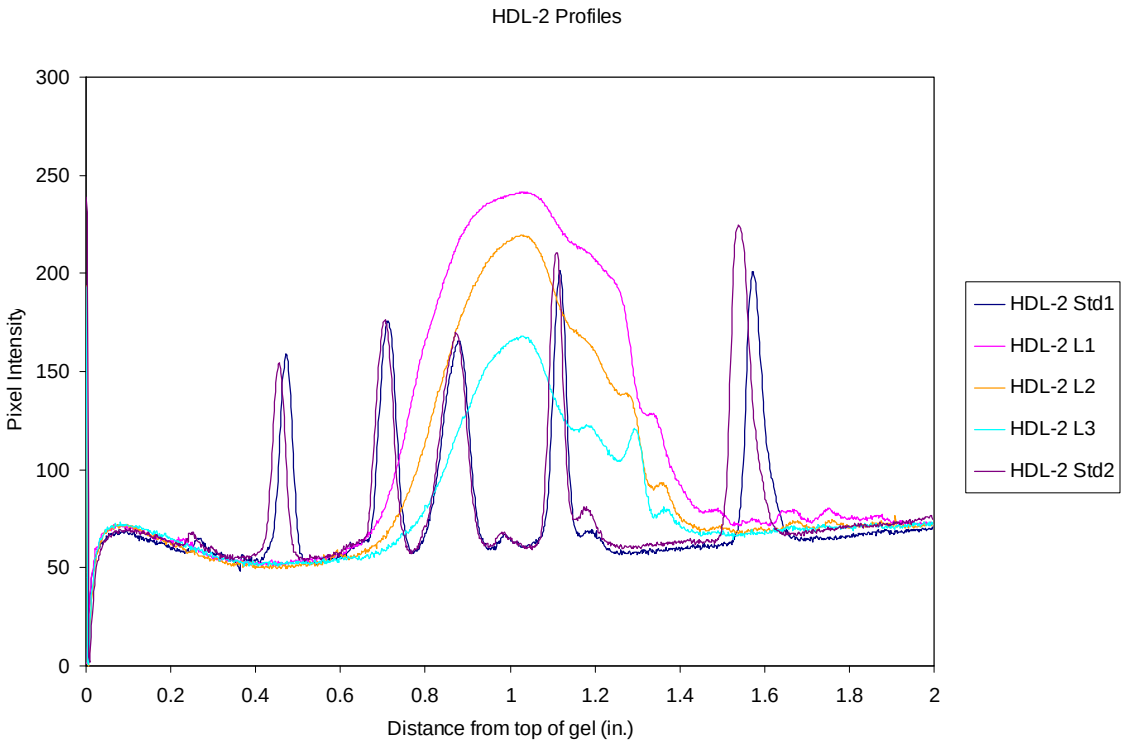

Figure 5.6. Separation of HDL standard using gradient gel electrophoresis (provided by Berkeley Heartlab).

5.3.3 Anion-exchange Chromatography of HDL

The apolipoproteins of HDL are comprised mainly of apo A-I and -II and apo C-I, and –III. Recent MALDI analysis of this mixture has shown that each of these apoliporoteins exists in different isoforms due to posttranslational modification.[40] Considering pI values smaller than 7 for most apolipoproteins in HDLs, an anion-exchange monolith in LC should resolve HDLs when operated in physiological buffer pHs (e.g., pH 7 to 8). The column was synthesized by copolymerizing AETAC and PEGDA. The resolution and column efficiency for protein standards were comparable to commercially available packed columns and other polymer monolithic columns. The separation of a native HDL standard was carried out using this column as shown in Figure 5.7. Here, native HDL was fractionated by AEC using a continuous NaCl gradient of 0.01-0.35 M. The elution pattern had 3 main characteristics: two sharp peaks at NaCl concentration of 0.01, followed by a large peak eluted at NaCl concentration of 0.12 M, and finally a slowly eluting fraction using an NaCl molarity of 0.17 to 0.25 M. Approximately 12 small peaks appeared, despite the fact that the resolution was destroyed due to the tailing of very hydrophobic and bulky lipids. The repeatable profiles indicate that these peaks may belong to apolipoproteins or other proteins in the sample.

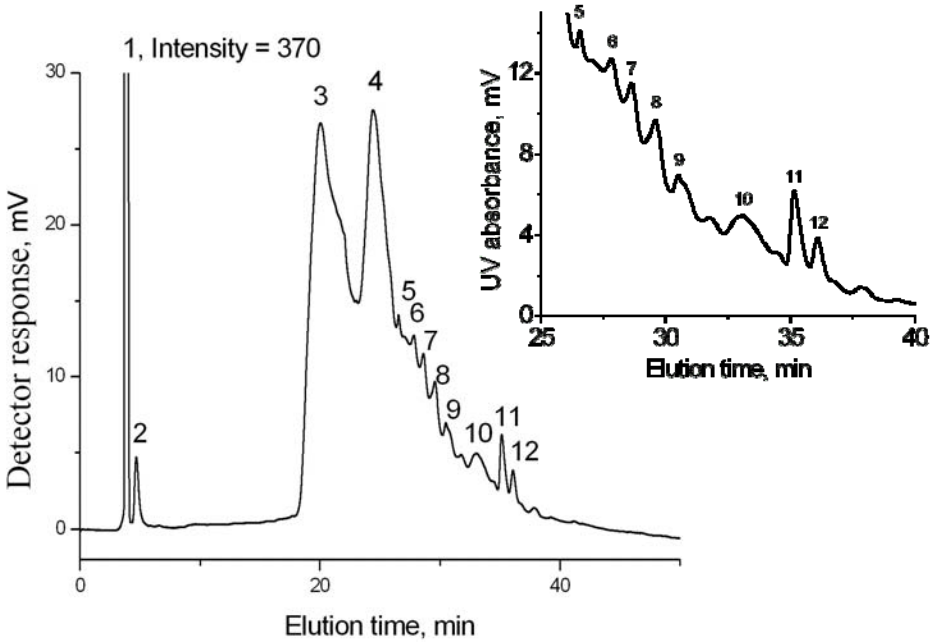

Figure 5.7. Strong anion-exchange chromatography of HDLs. Conditions: 16 cm × 75 μm i.d. poly(AETAC-co-PEGDA) monolithic column; buffer A: 10 mM Tris (pH 8.0), buffer B: buffer A plus 1.0 M NaCl, 2 min isocratic elution of 1% B, followed by a linear AB gradient (0.7 % B/min) to 35% B and 2 min isocratic elution of 50% B; UV detection at 214 nm.

5.4 Conclusions and Perspective

In this chapter, I developed a new capillary SEC method for size separation of native HDL particles from plasma using a capillary packed with BioSep-SEC-4000 particles, Three major sizes of HDL particles were separated. Additionally, capillary SEC and capillary strong AEC of non-delipidated HDL were accomplished using the poly(PEGMEA-co-PEGDA) and poly(AETAC-co-PEGDA) monoliths. According to my findings, the fractions separated by size were not the same as those separated by charge. The subfractions obtained using SEC were dependent on the lipid content, while those obtained using AEC were dependent on the protein content. These new LC methods using packed or monolithic stationary phases have the following advantages: (1) rapid separation of HDLs, (2) easy automation of instrument operation and data analysis, and (3) easy preparation of LC columns that could be reused without regeneration.

In order to relate my findings using AEC to known subclass separations by size or density, a second dimension based on particle size is needed. My suggestion is that SEC using the optimized monolithic column should be applied to HDL samples provided by BL. Again, the results should be compared directly with GGE analyses of the same samples by Berkeley HeartLab in terms of resolution, recovery, robustness, stability, reproducibility, and time. Additionally, future samples should be selected by BHL, designed to validate our IEC methods for charge separation by comparison to the IEF results published by Asztalos[33] et al. Coupling of two-dimensional monolithic IEC-SEC would be the final goal.

5.5 References

1. Rifai, N.; Bachorik, P. S.; Albers, J. J. In *Textbook of Clinical Chemistry*; Burtis, C. A.; Ashwood, E. R.; Tietz, N. W. Eds.; Saunders: New York, 2000, 809-861.

2. Rifai, N.; Warnick, G. R.; Dominiczak, M. H. *Handbook of Lipoprotein Testing: Apolipoproteins and Lipoproteins in Human Plasma*; American Association for Clinical Chemistry Inc.: Washington, DC, 2000; Chapter 1.
3. Asztalos, B. F.; Collins, D.; Cupples, A.; Demissie, S.; Horvath, K. V.; Bloomfield, H. E.; Robins, S. J.; Schaefer, E. J. *Arterioscler Thromb Vasc Biol* **2005**, *25*, 2185-2189.
4. Mowri, H. O.; Patsch, W.; Smith, L. C.; Gotto, A. M.; Patsch, J. R. *J. Lipid Res.* **1992**, *33*, 1269-1279.
5. Von Eckardstein, A.; Huang, Y.; Assmann, G. *Curr. Opin. Lipidol.* **1994**, *5*, 404-416.
6. Kremer, J. M.; Havekes, L. *Clin. Chim. Acta.* **1981**, *109*, 21-29.
7. Blanche, P. J.; Gong, E. L.; Forte, T. M. *Biochim. Biophys. Acta* **1981**, *665*, 408-419.
8. Krauss, R. M., Burke, D. J. *J. Lipid. Res.* **1982**, *23*, 97-104.
9. Warnick, G. R.; McNamara, J. R.; Clendenen, F.; Landolt, C. C. *Clin. Lab Med.* **2006**, *26*, 803-846.
10. Nanjee, M. N.; Brinton, E. A. *Clin. Chem.* **2000**, *46*, 207-223.
11. Liebich, H. M.; Lehmann, R.; Weiler, A. E.; Grübler, G.; Voelter, W. *J. Chromatogr. A* **1995**, *717*, 25-31.
12. Cruzado, I. D.; Song, S.; Crouse, S. F.; O'Brien, B. C.; Macfarlane, R. D. *Anal. Biochem.* **1996**, *243*, 100-109.
13. Hu, A.Z.; Cruzado, I. D.; Macfarlane, R. D. *Am. Lab.* **1996**, *28*, 18N-18P.
14. Franceschini, G.; Sirtori, C. R.; Capurso, A.; Weisgraber, K. H.; Mahley, R. W. *J. Clin. Invest.* **1980,** *66*, 892-900
15. von Hodenberg, E.; Heinen, S.; Howell, K. E.; Luley, C.; Kübler, W.; Bond, H. M. *Biochim. Biophys. Acta* **1991**, *1086*, 173-184.

16. Knipping, G.; Steyrer, E.; Holasek, A. *Int. J. Biochem.* **1984**, *16*, 1149-1154.

17. Farwig, Z. N.; Campbell, A. V.; Macfarlane, R. D. *Anal. Chem.* **2003**, *75*, 3823-3830.

18. Mezdour, H.; Clavery, V.; Kora, I.; Koffigan, M.; Barkia, A.; Fruchart, J. C. *J. Chromatogr.* **1987**, *414*, 35-45.

19. Rubenstein B. *Atherosclerosis*, **1979**, *33*, 415-423.

20. Asztalos, B. F.; Sloop, C. H.; Wong, L.; Roheim, P. S. *Biochimica et Biophysica Acta* **1993**, *1169*, 291-300.

21. Optiek, G. J.; Jorgenson, J. W.; Anderegg, R. J. *Anal. Chem.* **1997**, *69*, 2283-2291.

22. Tong, W.; Link, A.; Eng. J. K.; Yates, J. R. III. *Anal. Chem.***1999**, *71*, 2270-2278.

23. Wolters, D. A.; Washburn, M. P.; Yates, J. R. III *Anal. Chem.* **2001**, *73*, 5683-5690.

24. Gilar, M.; Olivova, P.; Daly, A. E.; Gebler, J. C. *Anal. Chem.* **2005**, *77*, 6426-6434.

25. Moore, A. W.; Larmann, J. P.; Lemmo, A. V.; Jorgenson, J. W. *Methods Enzymol.* **1996**, *270*, 401-419.

26. Giddings, J. C. *J. High Resolut. Chromatogr. Commun.* **1987**, *10*, 319-323.

27. Peterka, M.; Glover, D.; Kramberger, P.; Banjac, M.; Podgornik, A.; Barut, M.; Štrancar, A. *Bioprocess. J.* **2005**, *March/April*, 1-6.

28. Hjertén, S.; Liao, J. L.; Zhang, R. *J. Chromatogr.* **1989**, *473*, 273-275.

29. Svec, F.; Fréchet, J. M. J. *Anal. Chem.* **1992**, 64, 820-822.

30. Yu, C.; Xu, M. C.; Svec, F.; Fréchet, J. M. J. *J. Polym. Sci., Part A: Polym. Chem.* **2002**, *40*, 755-769.

31. Premstaller, A.; Oberacher, H.; Huber, C. G. *Anal. Chem.* **2000**, *72*, 4386-4393.

32. Švec, F.; Fréchet, J. M. J. *J. Chromatogr. A* **1995**, *702*, 89-95.

33. Lubbad, S.; Buchmeiser, M. R. *Macromol. Rapid Commun.* **2002**, *23*, 617-621.

34. Gu, B.; Armenta, J. M.; Lee, M. L. *J. Chromatogr. A* **2005**, *1079*, 382-391.

35. Li, Y.; Gu, B.; Tolley, H. D., Lee, M. L. *J. Chromatogr. A* **2009**, *1216*, 5525–5532.

36. Barroso, B.; Lubda, D.; Bischoff, R. *J. Proteome Res.* **2003**, *2*, 633-642.

37. Tomer, K. B.; Moseley, M. A.; Deterding, L. J.; Parker, C. E. *Mass spectrom. Rev.* **1994**, *13*, 431-457.

38. Wu, N.; Collins, D.C.; Lippert, J. A.; Xiang, Y.; Lee, M. L. *J. Microcolumn Sep.* **2000**, *12*, 462-469.

39. Clarke, N. J.; Tomlinson, A. J.; Schomburg, G.; Naylor, S. *Anal. Chem*. **1997**, *69*, 2786-2792.

40. Bondarenko, P. V.; Farwig, Z. N.; McNeal, C. J.; Macfarlane, R. D. *Int. J. Mass. Spectrom. Ion Processes* **2002**, *219*, 671-680.

41. Stout, R. W.; DeStefano, J. J. *J. Chromatogr.* **1985**, *326*, 63-78.

42. Uversky, V. N. *Biochemistry* **1993**, *32*, 13288-13298.

CHAPTER 6 FUTURE DIRECTIONS

6.1 Investigation of New Meso-porogens for Developing Monoliths for Size Exclusion Chromatography (SEC) of Proteins

Challenges in developing SEC polymer monolithic columns stem mainly from two aspects. First, a non-adsorptive monolith must be synthesized. Second, the monolith must have appropriate pore size distribution for effective size exclusion of HDL. The first issue was solved by synthesizing a novel non-adsorptive monolith containing significant polyethylene glycol (PEG) functionality. This monolith was based on copolymerization of polyethylene glycol methyl ether acrylate (PEGMEA) and polyethylene glycol diacrylate (PEGDA).[1]

At present, the second requirement has been the most challenging, since no precedent can be used for reference. After much investigation, surfactants were introduced as porogens to create mesopores of defined size within the polymeric matrix.[2,3] Two types of surfactants have been investigated and found effective in producing mesopores. The resulting monoliths showed SEC separation in the range from bovine serum albumin (BSA, 66 000) to thryglobulin (TG, 670 000).

The first surfactant porogen is a tri-block copolymer, poly(propylene oxide)-poly(ethylene oxide)-poly(propylene oxide) (PPO-PEO-PPO) or PEO-PPO-PEO having molecular weights (MWs) ranging from 2 700 to 5 800. I mainly investigated the influence of the porogen copolymer on the separation properties of the monolith by changing its MW or proportion in the porogenic system. The effect of monomer composition on the separation properties was also investigated. In addition, the influence

of monolithic column diameter and length on resolution, and the influence of flow rate on resolution have been investigated. To use a copolymer with MW of 8 400, a new porogenic system was employed to create a homogeneous monolith with low pressure drop. However, this method did not lead to further increased resolution or increased mesopore volume.

Compared to the spherical packing material with well-defined 15 000-2 000 000 exclusion range, the new SEC monolithic column demonstrated an extended lower separation range from 112 to 670 000, but less resolution in the range from 66 000 to 670 000. The pore size distribution was examined using a well-defined MW range series of proteins and peptides by inverse size-exclusion chromatography (ISEC). From these data, an optimized monolith should have a micropore (< 2 nm) porosity of 11.9% and a mesopore porosity of 8.5% in the range from 2.8 to 15.7 nm, which would provide good size-exclusion separation of peptides and proteins. However, the mesopore porosity in the range from 7 to 17 nm so far has been only 3.8%, which provides poor separation of TG and BSA. Of course, a long column or reduced flow rate would improve the separation by increasing the column efficiency, but at the expense of long analysis time. Additionally, if the current pore size range could be shifted to the larger mesopores (7-17 nm), the separation of larger proteins would be possible.

Another porogen surfactant, Brij, proved to be effective in creating larger mesopores in the poly(PEGMEA-co-PEGDA) matrix. Similarly, compared to the tri-block copolymer, a different porogenic system was applied to create a homogeneous monolith with relatively low pressure drop. Chapter 4 describes the separation of TG, catalase and BSA on a 23 cm × 150 μm i.d. monolithic column synthesized using Brij 58 P. Obviously, for this monolithic column, the micropore volume fraction was decreased greatly (< 5.0%),

while the mesopore volume fraction in the range from BSA to TG (7-17 nm) was increased to 9.7%, compared to 3.8% for the SEC monolith synthesized using PEO-PPO-PEO. Combining two SEC monolithic columns with different exclusion ranges in series is expected to provide further improved resolution and an extended separation range.

A micelle templating mechanism has been described for the use of surfactants in producing micropores or mesopores in a hydrogel matrix, such as polyacryamide and poly(2-hydroxyethylmethacrylate).[4] Although this hypothesis cannot be verified at this stage of my studies, differences in molecular weight separation ranges between monoliths prepared with PEO-PPO-PEO or Brij and their monolith counterparts prepared without these porogens were observed to be consistent with the creation of approximately 7-17 nm pores. Based on these findings, a series of surfactants with different micellar diameters are expected to produce the desired pore diameters for SEC of biomolecules. Table 6.1 lists some surfactants previously used for templating polyacrylamide and poly(2-hydroxyethyl methacrylate). For example, the small micelle-forming surfactants (such as SDS and DTAB) may be applied to produce micropores within the poly(PEGMEA- co-PEGDA) matrix for SEC separation of peptides or small proteins. Larger micelle-forming surfactants (such as Brij and Tween) should be useful in producing mesopores for SEC separation of proteins. Figure 6.1 gives the chemical structures of the proposed surfactants (Pluoronic, Brij and Tween) for synthesizing new monoliths. Of course, other factors, such as the compostion of monomers, the proportion of monomers in the polymerization mixture, and the composition of porogenic system, will influence the porous properties of the monoliths.

Table 6.1. Physical micelle parameters of some surfactants used for templating polyacrylamide and poly(2-hydroxyethyl methacrylate).[11]

Surfactant	Type	Average molecular weight	Aggregation number	CMC (mM)	Micelle shape	Micelle radius (nm)
Sodium dodecylsulfate (SDS)	Anionic	289	64	8.16×10^{-3} (25^{o}C)	Elliptical	2.1
Dodecyltrimethylammonium (DTAB)	Cationic	228	53	1.56×10^{-2} (25^{o}C)	Spherical	1.8
Tetradecyltrimethylammonium (TTAB)	Cationic	256	71	3.5×10^{-3} (30^{o}C)	Spherical	2.1
Cetyltrimethylammonium (CTAB)	Cationic	284	91	9.8×10^{-4} (35^{o}C)	Spherical	2.3
Pluoronic 25R4	Neutral	3600	-	5×10^{-1} (49^{o}C) (wt %)	-	6.7
Pluoronic F127	Neutral	12600	-	5×10^{-3} (42^{o}C) 7×10^{-1} (15^{o}C) （wt %）	Spherical	9.0
Brij 30	Neutral	362	20-40	4.0×10^{-5}	Spherical	2.6
Brij 56	Neutral	683	70	1.25×10^{-2} (25^{o}C) (wt %)	-	4.0

Brij 58	Neutral	1122	-	$3.9\text{-}13\times10^{-6}$ (25^{o}C)	-	7.0
Brij 35	Neutral	1200	-	6.0×10^{-5} (25^{o}C)	-	7.2
Brij 700	Neutral	4670	-	-	-	26.4
Tween 20	Neutral	1228	-	6.0×10^{-5} (25^{o}C)	-	7.5
Tween 40	Neutral	1277	-	2.7×10^{-5}(20-25^{o}C)	-	-
Tween 80	Neutral	1310	60	1.2×10^{-5} (25^{o}C)	-	-

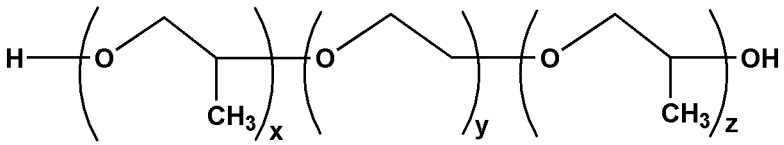

Pluoronic

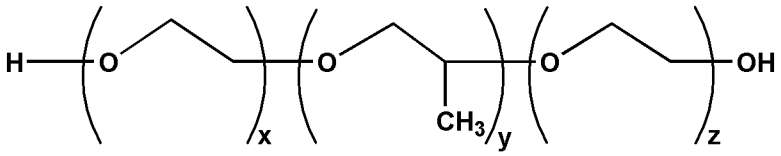

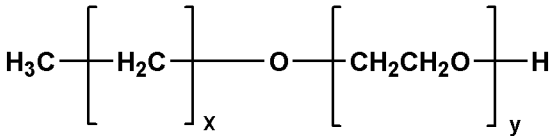

Brij

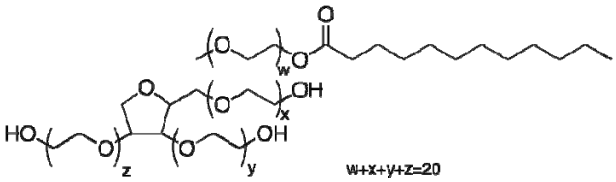

Tween 20

Figure 6.1. Chemical structures of the proposed surfactants for synthesizing new monoliths.

The hard template technique using particles such as silica is the most popular strategy for synthesizing a mesoporous polymer. The monolith porosity is dictated by the size of the spherical silica particle templates.[5,6] In addition to tailoring the pore size, this method offers the ability to influence the surface characteristics of the finished polymer by employing silica beads with specific surface chemistry. However, these silica beads are not biocompatible and it is diffcult to remove the templates for generating well-ordered mesopores without destroying the monolithic structure.

Recently, the use of dendrimers for generation of uniform mesopore structures has been investigated in a methacrylate-based monolith.[7] Dendrimers represent an exciting class of macromolecule templates. Unlike classical polymers, dendrimers have a high degree of molecular uniformity, narrow molecular weight distribution, specific size and shape characteristics, and a highly-functionalized terminal surface. Most importantly, they have the same dimensions as biomolecules ranging from approximately 1 to over 10 nm. For example, polyamidoamine dendrimers are manufactured by a divergent repetitive growth technique and are typically based on an ethylenediamine core with repeating tertiary amine/amide branching units. Theoretically, the macromolecules can be incorporated in the non-adsorptive poly(PEGMEA-co-PEGDA) by free-radical initiated polymerization. The removal of solvent and dendrimers produces a continuous rod of polymer with uniform porosity and dendrimer-influenced surface characteristics.

6.2 Further Improvement in Anion-exchange Monolithic Columns

The weak anion-exchange monolith obtained from copolymerization of 2-(diethylamino)ethyl methacrylate (DEAEMA) and PEGDA only gave 48% monomer conversion. This is likely due to poor copolymerization resulting from unfavorable

monomer reactivity ratio between methacrylate monomer and acrylate crosslinker. It was found that acrylate is much more reactive than methacrylate and their reactivity ratios are quite different from unity.[8] Such low monomer conversion resulted in a relatively low dynamic binding capacity (24 mg/mL), refered to chapter 2. A copolymer of 2-(diethylamino)ethyl acrylate (replacing DEAEMA) and PEGDA is expected to give higher monomer conversion so that more functionalities are incorporated, which will provide improved binding capacity and separation efficiency (Figure 6.2). Obviously, functional monomers with low hydrocarbon content incorporated in the monolithic backbone will decrease its hydrophobicity.[9] Elimination of a methyl group from the monomer is also expected to decrease the hydrophobicity of the monolith.

Although current ion-exchange monoliths developed have provided highly efficient separations, further effort is still needed for decreasing the back pressure to achieve fast analysis. Obviously, this can be achieved by increasing the content of large pores, since the average through-pore size usually controls the column permeability.[10] Decreasing the content of crosslinker in the polymerization mixture, increasing the ratio of poor solvent to good solvent in the porogenic system, or increasing the ratio of porogens to monomers are the most common approaches to accomplishing this. Changing the type of porogen can also be effective. However, large surface area mainly from small pores is still required for chromatographic application. Therefore, a compromise must be found between these two requirements.

6.3 Prepareation of Other Types of Polymer Monoliths Using PEGDA as Crosslinker

As noted in Chapter 2, the design of new ion-exchange monoliths has followed

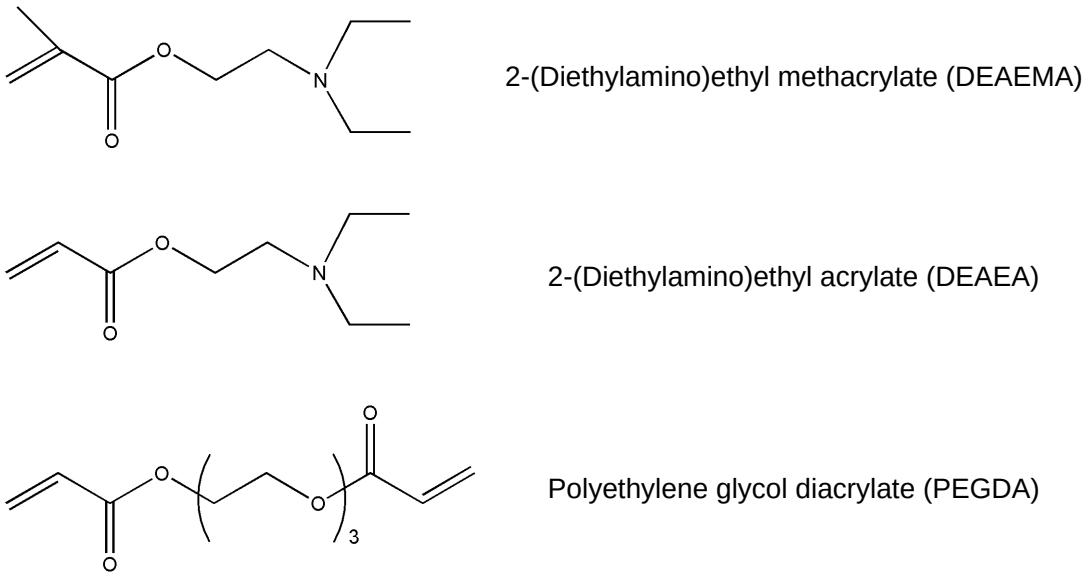

Figure 6.2. Monomers involved in synthesizing weak anion-exchange monoliths.

two strategies: (1) use of a new crosslinker, PEGDA, for formation of the monolithic stationary phase with the lowest non-specific adsorption, and (2) inclusion of functional monomers that simultaneously provide functionalities with high selectivity. Low non-specific adsorption and high selectivity are two very important features of a stationary phase for protein chromatography. Further monolith development must continue to focus on both of these properties.

New momomers containing various functional groups (see Figure 6.3) for chromatographic retention mechanisms should be explored. For example, 2-carboxyethyl acrylate contains a weak cation-exchange group, the carboxymethyl group, which provides selectivity for protein separations. 2-Cyanoethyl acrylate contains a cyano group that can retain small polar molecules. A poly(2-cyanoethyl acrylate-co-PEGDA) is expected to have low hydrophobicity for rapid elution of hydrophobic analytes, significantly less retention than C18, excellent retention of strongly basic analytes, and be compatible with highly aqueous organic phases. Phenyl groups provide selectivity through π-π interactions and phenyl LC columns provide superior separations of hetero-aromatic compounds and other pi acceptors in the reversed-phase mode. Such a monolith may be obtained by copolymerization of poly(ethylene glycol) phenyl ether acrylate and PEGDA. Incorporation of PEG units in the monomer should help to reduce non-specific adsorption.

6.4 Two-dimensional LC of High Density Lipoproteins

It is proposed that a size exclusion column be used for the first dimension and an anion (or cation) exchange column for be used the second dimension in a two-dimensional LC configuration. SEC selection is based on size and shape of a solute with respect to stationary phase pore size. SEC typically produces low peak capacity and relatively wide

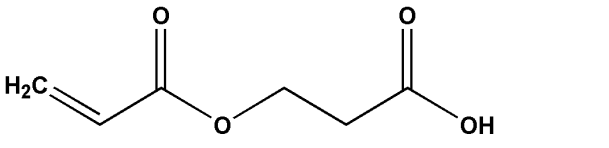

2-Carboxyethyl acrylate

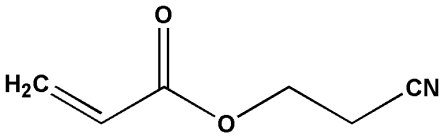

2-Cyanoethyl acrylate

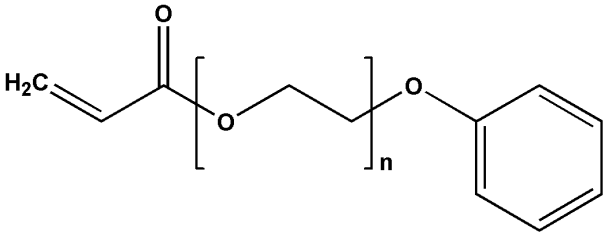

Poly(ethylene glycol) phenyl ether acrylate

Figure 6.3. Chemical structures of proposed monomers.

peak widths. In comparison, ion-exchange chromatography produces a relatively large peak capacity and is based on charge-charge interactions between the proteins in the sample and the charges immobilized on the stationary phase surface. A combination of SEC and IE meets the requirement of orthogonality, which means that the separation mechanisms of the individual dimensions are totally different. If an SEC peak contained multiple components of similar size but different surface charge, then the components would be separated by the ion-exchange column.

Eluent compatibility is an important issue for successful 2D separation. In principle, the eluent from the first dimension should be miscible with the sample solvent in the second dimension. An aqueous buffer with or without salt should be used for both SEC and IEC of lipoproteins, so eluent compatibility is not a problem. However, when transferring from the first to the second column, the sample volume must be minimized to reduce any interference of the sample or salt solution with the subsequent gradient elution. This would be the first attempt to combine SEC in the first dimension and IEC in the second dimension for 2D LC separation.

6.5 References

1. Gu, B.; Armenta, J. M.; Lee, M. L. *J. Chromatogr. A* **2005**, *1079*, 382-391.
2. Li. Y.; Tolley, H. D.; Lee, M. L. *Anal. Chem.* **2009**, *81*, 4406–4413.
3. Li, Y.; Lee, M. L. in preparation.
4. Patterson, B. C. Surfactant micelles as templates in hydrogels, Ph.D. dissertation, Department of Chemistry, Florida State University, Tallahassee, FL, 2000.
5. Johnson, S. A.; Ollivier, P. J.; Mallouk, T. E. *Science* **1999**, *283*, 963.

6. Jeong, U. Y.; Ryu, D. Y.; Kim, J. K.; Kim, D. H.; Russell, T. P.; Hawker, C. J. *Adv. Mater.* **2003**, *15*, 1247
7. Doneanu, A.; Chirica, G. S.; Remcho, V. T. *J. Sep. Sci.* **2002**, *25*, 1252-1256.
8. Zou, Y.; Lin, D.; Dai, L.; Zhang, J.; Pan, R. *Polymer* **1997**, *38*, 3947-3950.
9. Gu, B.; Li, Y.; Lee, M. L. *Anal. Chem.* **2007**, *79*, 5848-5855.
10. Kobayashi, H.; Tokuda, D.; Ichimaru, J.; Ikegami, T.; Miyabe, K.; Tanaka, N. *J. Chromatogr.* A **2006**, *1109*, 2-9.
11. http://www.sigmaaldrich.com/etc/medialib/docs/Sigma/Instructions/detergent_selection_table.pdf.